Appendix A: Ethics approvals

MRC
SOUTH AFRICA
The Medical Research Council

Ethics Committee for Research on Animals (ECRA)

PO Box 19001, Tygerberg, 7505, Cape Town, South Africa
off Hindle Road, Brentwood Park, Driftsands
Tel +27 (0)21 955 1900, Fax +27 (0)21 955 1330
E-mail: gieliana.fourie@mrc.ac.za
Http://www.sahealthinfo.org/Modules/ethics/ethics.htm

17 April 2007

Prof Jan Verschoor
Dept. of Biochemistry
UNIVERSITY OF PRETORIA

Dear Prof Verschoor

YOUR REVISED APPLICATION TO THE ECRA : REF. 06/07 "Polymeric nano-drug delivery system for Tuberculoses (TB) drugs".

The ECRA Committee received your revised application and it has been approved.

You may start with your experiment now.

May I remind you that you are required to submit a brief progress report on the progress of this study at six monthly intervals so the ECRA can be kept informed of the progress you are making and of any problems you may encounter.

Your progress report dates : November 2007 and May 2008.
We will remind you by letter.

Kind regards.

PROF D DU TOIT
Chairperson : ECRA Committee

Colorado State University
Knowledge to Go Places

Research Integrity & Compliance Review Office
Office of the Vice President for Research
321 General Services Building - Campus Delivery 2011 Fort Collins, CO
TEL: (970) 491-1553
FAX: (970) 491-2293

NOTICE OF APPROVAL FOR ANIMAL RESEARCH

Animal Welfare Assurance Number: A3572-01

DATE:	June 03, 2011	
TO:	Lenaerts, Anne, MIP - Microbiology Section	
	Hoover, Edward, MIP - Pathology Section, Woolhiser, Lisa, MIP - Microbiology Section	
FROM:	Moseley, Bill, , CSU IACUC	
PROTOCOL TITLE:	Polymeric nano-drug delivery system for tuberculosis (TB) drugs	
FUNDING SOURCE:	Council for Scientific and Industrial Research	
PROTOCOL NUMBER:	10-1862A	
APPROVAL PERIOD:	Approval Date: June 03, 2011	Expiration Date: June 15, 2013

Colorado State University's Institutional Animal Care and Use Committee (IACUC) has completed its review of the protocol titled "Polymeric nano-drug delivery system for tuberculosis (TB) drugs." In accordance with federal and state requirements on the care and use of animals and policies established by Colorado State University, the committee has approved this protocol. If the committee is placing any special conditions on approval, notes will be included at the bottom of this letter with additional requirements or instructions. This protocol will need to undergo annual review and approval prior to June 02, 2012.

If you would like to involve additional personnel or change any aspects of the protocol in the future, please submit an Amendment Request to the Institutional Animal Care and Use Committee for review via eProtocol https://csu.keyusa.net.

Good luck in your research endeavors.

Sincerely,

Colorado State University
Knowledge to Go Places

Research Integrity & Compliance Review Office
Office of the Vice President for Research
321 General Services Building - Campus Delivery 2011 Fort Collins, CO
TEL: (970) 491-1553
FAX: (970) 491-2293

Moseley, Bill

Appendix B: Publications and conference proceedings

B1: First authorship- Manuscript submitted to the International Journal of Pharmaceutics

"*In vivo/in vitro* pharmacokinetic and pharmacodynamic study of spray-dried poly(DL-lactic-*co*-glycolic) acid nanoparticles encapsulating rifampicin and isoniazid"

B2: Co- First authorship

"*In vivo* uptake and acute immune response to orally administered chitosan and PEG coated PLGA nanoparticles"

B3: Second authorship

"*In vivo* evaluation of the biodistribution and safety of PLGA nanoparticles as drug delivery systems"

B4: Second authorship

"Effects of protein-binding on the biodistribution of PEGylated PLGA nanoparticles post oral administration"

B5: Conference proceedings- CSIR Conference 2010~ General science, engineering & technology

"*In vitro* characterisation of PLGA nanoparticles encapsulating rifampicin and isoniazid - Towards IVIVC"

In vivo/in vitro pharmacokinetic and pharmacodynamic study of spray-dried poly-(DL-lactic-*co*-glycolic) acid nanoparticles encapsulating rifampicin and isoniazid

Booysen, L.L.I.J.[a,b], Kalombo, L.[a], Brooks, E.[c], Hansen, R. [d], Gilliland J. [c], Gruppo, V. [c], Lungenhofen, P. [d], Semete-Makokotlela, B.[a], Swai, H.S.[a], du Plessis, L.H.[e]*, Kotze, A.F.[b], Lenaerts, A.[c]

[a] *Council for Scientific and Industrial Research, Pretoria, 0001, South Africa*
[b] *Department of Pharmaceutics, North-West University, Potchefstroom Campus, Potchefstroom, 2520, South Africa*
[c]*Department of Microbiology, Immunology and Pathology, Colorado State University, Fort Collins, CO, 80523-4629, USA*
[d]*Department of Pharmacology, CSU Animal Cancer Centre, Fort Collins, CO, 80523-4629, USA*
[e] *Unit for Drug Research and Development, North-West University, Potchefstroom Campus, Potchefstroom, 2520, South Africa*

Abstract

Poly-(DL-lactic-co-glycolic acid (PLGA) nanoparticles were prepared by a double emulsion solvent evaporation spray drying technique an coated with polyethylene glycol (PEG 1% v/v) The PLGA nanoparticles had a small size (229± 7.6 to 382± 23.9 nm), uniform size distribution and positive zeta potential (+12.45± 4.53 mV). *In vitro/ in vivo* assays were performed to evaluate the pharmacokinetic (PK) and pharmacodynamic (PD) performance of these nanoparticles following nanoencapsulation of the anti-TB drugs rifampicin (RIF) and isoniazid (INH). The results demonstrated the potential for the reduction in protein binding of these drugs by protection in the polymer core. Furthermore, *in vitro* efficacy was demonstrated using *Mycobacterium tuberculosis (M.tb.)* (strain $H_{37}Rv$). Sustained drug release over 7 days were observed for these drugs following once-off oral administration in mice with subsequent drug distribution of up to 10 days in the liver and lungs for RIF and INH, respectively. It was concluded by these studies combined with our previous reports that spray-dried PLGA nanoparticles demonstrate potential for the improvement of TB chemotherapy by nanoencapsulation of anti-TB drugs.

Keywords: PLGA nanoparticles; *in vitro*; *in vivo*; pharmacokinetic; pharmacodynamic; rifampicin; isoniazid

*Corresponding author. Tel: (018) 299 4246 Fax: (018) 299 2248
Email address: Lissinda.DuPlessis@nwu.ac.za

1. Introduction

The World Health Organization (WHO) reported in 2011 that the TB incident cases have fallen since 2006 (WHO 2011). However, because 8.8 million new TB incident cases in were reported in 2010, the TB burden is still considered a global crisis. In 2010, approximately 10 million children were orphaned as a result of parent deaths caused by TB (WHO 2011). South Africa currently ranks third of the 22 high burden countries in terms of TB incident cases per 100 000 population. Limitations exist in TB chemotherapy such as non-localised delivery of drugs, high dose and dose frequency as well as the adverse side effects that the therapy presents. To address these challenges various groups have reported the encapsulation of antituberculosis drugs where slow release, improved intracellular delivery and high drug loading parameters can be achieved by nanoencapsulation (Ahmad *et al*. 2006;Ahmad *et al*. 2008;Azarmi *et al*. 2008;Kisich *et al*. 2007). Furthermore, nanoencapsulation of drugs in a biodegradable polymer has been reported to minimize first pass metabolism via protection of the drug in the core of the polymeric shell (Couvreur and Vauthier 2006). Physico-chemical properties of nanoparticles such as size, surface charge, hydrophobicity and polymer composition all contribute toward protein binding, biodistribution, cellular uptake and immune response. PLGA is a biodegradable and biocompatible polymer widely used in pharmaceutical applications (Jain 2000). Liposomal drug carrier technology also has numerous advantages in drug delivery and have demonstrated improved efficacy in cancer chemotherapy (Ledet and Mandal 2012). However, a few drawbacks exists for this system such as leakage of the drug, limited shelf-life, instability *in vivo*, difficulties in optimization of the surface structure and limitation to the parenteral use only (Epstein *et al*. 2008).

This report aims to evaluate the *in vitro/in vivo* properties of spray-dried PLGA nanoparticles for the purpose of sustained drug delivery and distribution of the anti-TB drugs RIF and INH. Our previous reports have demonstrated the protein binding, biodistribution, macrophage uptake and immune response to these nanoparticles in the absence of encapsulated drug (Semete *et al*. 2010a, 2010b, 2012). This report will show the potential of the nanoparticles in TB chemotherapy, by demonstrating *in vitro* efficacy and sustained drug release and drug distribution *in vivo* following once-off oral dosing. RIF and INH was selected based on the fact that they are two of the four first-line drugs in TB chemotherapy and the most widely investigated (Benator *et al*. 2002; Brooks and Orme 1998;Dhillon and Mitchison 1992; Ellard 1999;Grosset and Leventis 1983; Gurumurthy *et al*. 1999; Maggi *et al*. 1966; Panchagnula and Agrawal 2004; Pape *et al*. 1993; Takayama *et al*. 1972).

2. Materials and methods

2.1 Nanoparticle preparation

Nanoparticles were prepared with poly-(DL)-Lactic-*co*-Glycolic Acid (PLGA) 50:50 (Mw: 45000-75000) using a modified double emulsion solvent evaporation spray-drying technique (Kalombo 2008) as described in (Semete *et al*. 2012). The most important variation in the formulation is the encapsulation of drug. RIF was added in the oil phase with the polymer and INH was added in the aqueous phase. For PEG coating, a 40 ml mixture was prepared consisting of 5 ml of 1% v/v PEG, 10 ml of 5% lactose, 15 ml of 1 % v/v PVA and 10 ml of 0.3 % chitosan during the second emulsion step. The first w/o emulsion was then dispersed in this mixture and emulsified. The second w/o/w emulsion was then spray dried.

2.2 Particle characterization

Particle size and size distribution of PLGA and zinc oxide (ZnO) particles as well as polystyrene beads were measured by Dynamic Laser Scattering (DLS), also referred to as Photon Correlation Spectroscopy (PCS), using a Malvern Zetasizer Nano ZS (Malvern Instruments Ltd, UK). Nanoparticles (1-3 mg) were suspended in filtered water (0.2 μm filter), then vortexed and/or sonicated for a few minutes. The zeta potential was also determined using the same instrument. Surface morphology of PLGA nanoparticles was analysed via scanning electron microscopy (LEO 1525 Field Emission Scanning Electron Microscope). Preparation of the samples for scanning electron microscopy analysis was done by means of the gold sputtering technique. The nanoparticles were fixed to the aluminium sample stubs with double sided carbon tape and sputter coating with gold was applied for viewing by scanning electron microscopy. The percentage encapsulation efficiency (%EE) of the drugs was determined by UV-spectrophotometer readings of the supernatant following centrifugation of a representative sample of nanoparticles.

2.3 *In vitro* protein binding assays

The nanoparticle protein binding was analysed using an adapted method as described previously for protein adsorption to polymer nanoparticles (Stolnik *et al*. 2001). The adapted method is described in previous work (Semete *et al*. 2012). To determine the percentage protein binding of the unencapsulated (free) drugs as positive controls, equilibrium dialysis was used. Free RIF and INH controls were prepared in the same ratios with human plasma as the nanoparticle formulations and placed in the sample chamber of an equilibrium dialysis device with buffer chamber containing PBS (pH 7.4). Diffusion against a concentration gradient was facilitated on an orbital shaker at 100 rpm for 4 hours at room temperature. The samples in both chambers were analysed using UV-spectrophotometry at 330 nm for RIF and 262 nm for INH. The samples collected from the sample

and buffer chambers were analysed to determine the percentage of unbound drug. Percentage unbound drug was calculated as illustrated in Equation. 1.1.

$$(\frac{drugPBS}{drugPlasma} x100) = \%unbound$$

$$\%bound = 100\% - \%unbound \qquad \text{Eqn 1}$$

2.4 Animals used in assays

For the *in vivo* experiments specific pathogen-free, immunocompetent female Balb/C mice 6-8 weeks old were acquired from Charles River Laboratories, Wilmington, MA. The mice weighed 18-23g and were housed under standard environment conditions at ambient temperature of 25°C, and supplied with food and water *ad libitum*. Ethics approval was obtained for this study from the Colorado State University's Institutional Animal Care and Use Committee (IACUC), Fort Collins, CA.

2.5 Culture of *Mycobacterium tuberculosis (M.tb)*

M.tb (strain H37Rv, Trudeau Institute, Saranac Lake, NY) was grown in 50 ml of 7H9 broth (Difco) containing oleic acid-albumin-dextrose-catalase (OADC) enrichment (7H9-OADC) and 0.05% Tween 80. The cultures were incubated at 37°C with rotary agitation, grown to mid-exponential phase (optical density at 600 nm [OD_{600}] of approximately 0.6 to 0.8, at 14 to 21 days), and harvested by centrifugation. The cell pellets were resuspended in a small amount of the enriched 7H9-OADC medium containing 10% sterile glycerol, transferred to cryogenic vials, and stored at -70°C as starter stocks for further use. To prepare stock for an experiment, starter stock was added to 50 ml 7H9-OADC containing 0.1% Tween 80 and incubated at 37°C with agitation. The starter culture was grown to an OD_{600} of 0.3 to 0.5 and then diluted to an OD_{600} of approximately 0.1 by using 7H9-OADC containing 0.1% Tween 80 (resulting in ~3 x 10^5 CFU per well). OD600 readings were measured spectrophotometrically (BioRad Benchmark Plus).

2.6 *In vitro* MIC/MBC of nanoencapsulated RIF and INH

To determine whether nanoparticle drug release over time was sufficient to inhibit and/or result in significant killing of H_{37}Rv *M.tb* MIC/MBC analysis of nanoencapsulated RIF and INH were performed. The microdilution method was employed to determine the MIC of nanoencapsulated drugs over time. Briefly, washed nanoparticles, i.e. nanoparticle formulations in which the free drug was removed was suspended in deionized water and ten serial dilutions (1:2) were prepared and added to 96-well microtitre plates. Nanoparticle dilution range was 32µg/ml to 0.125µg/ml. Standard dilutions of free drugs were also included (RIF 0.96-0.00375 µg/ml and INH 0.48-0.001875 µg/ml) based on the known MIC of each drug. The difference in the concentration ranges of the free- and

nanoencapsulated drugs was because preliminary results showed that no inhibition was observed for nanoencapsulated drugs at similar ranges as free-drug. This suggested that insufficient drug release occurred to reach MIC concentrations. The concentrations were increased and MIC profiles were compared to the free-drug MIC profiles. The negative controls contained no drug. In addition, blank (drug-free) nanoparticles were added as a control to determine whether the PLGA nanoparticles had an inhibitory effect on *M.tb*. *M.tb* was added at 5 x 10^4 CFU per well and incubated. OD_{600} readings were measured every 2 to 3 days until day 18. The MBC assay was conducted similarly to the MIC assays with the major variant being the concentration of the inoculants. For the MBC assay a concentration of 1 x 10^6 CFU per well was used. OD_{600} readings were measured every 1-2 days up to day 18 and confirmed by visual inspection.

2.7 *In vivo* bioavailability studies for PLGA nanoparticles encapsulating RIF and INH

To evaluate the bioavailability of nanoencapsulated drugs versus free (unencapsulated) drug using *M.tb* is indicator strain a published method for the rapid assessment of the oral bioavailability of experimental compounds against *M.tb* was used (Gruppo *et al*. 2006).

The animals were dosed at 60 mg/kg for RIF (free and encapsulated) and INH 150 mg/kg (free and encapsulated) via oral gavage. Blood samples were collected via cardiac puncture per time point per drug, at 2hr, 8hr, 1 day, 2 days, 3 days, and 7 days for nanoparticle-encapsulated drug and at 2hr, 8hr, 1 day, and 2 days, for free drugs. Blood was collected aseptically in serum separator tubes and centrifuged to collect serum. Serum was stored at -70°C and used within one week.

For the assay, serum samples were prepared as two-fold dilutions using the sera of naïve (untreated) mice as diluents. The dilutions ranged from 10% to 0.312%. The serum was then added in 10 µl aliquots to 96- well plates with 10% serum of drug-treated mice as starting point in the top well. The reason for the maximum concentration of 10% was due to the fact that higher serum concentrations demonstrated growth inhibition of *M.tb*. Free-drug standards were included on the same 96-well microtitre plate in threefold dilutions ranging from 30µg/ml to 0.51ng/ml, in the presence of- and without serum. The inclusion of wells with and without serum for drug standards was to determine whether serum protein binding to drugs had any effect on the assay results. The free drugs in the standard lanes were diluted with 100 % DMSO to avoid possible solubility problems with a resultant 2% DMSO as final concentration. The *M.tb* stock was added to the 96-well plates at 2 x 10^5 CFU per well in a volume of 50 µl 7H9 medium. The final volume was adjusted to 100 µl. The plates were subsequently sealed in plastic bags for containment and incubated at 37°C. OD_{600} readings were measured every 3-4 days until day 14. Results were confirmed with visual inspection. Inhibition of bacterial growth in this bioassay would indicate whether there are sufficiently high concentrations of

bioactive product in the bloodstream. Wells were scored as positive (drug containing) when the OD_{600} values were less than 50% of the OD_{600} value of the untreated control wells. An estimation of serum drug levels (in µg per ml serum) was obtained by using the MIC data from the standard drug lanes.

2.8 *In vivo* drug release and drug distribution

Orally administered RIF (60mg/kg, free and encapsulated) and INH (150mg/kg free and encapsulated) were evaluated over 10 days and compared to free drug. Samples of plasma (via terminal bleed) and tissues of the animals dosed with free-drug and nanoparticles were collected. Blood samples were collected into plasma separator tubes and centrifuged to collect plasma. Plasma supernatant (200 µl) was immediately frozen at -80°C. The tissues, i.e. lungs, liver (caudate and left lobe), spleen and kidneys was snap frozen in liquid nitrogen in cryovials and stored at -80 °C. Tissues samples were only collected for day 1, 3, 7 and 10. Plasma and tissue samples were analysed via LCMS-MS analysis (API-3200, Applied Biosystems). Non-compartmental pharmacokinetic analysis was used for plasma samples.

2.9 Statistical analysis

Statistical analyses of results were performed by use of the Student's T test in Microsoft Excel 2010. Results are presented as mean± standard deviation of the means (SD). The significance level was set at $p \leq 0.05$. Non-compartmental analysis was used to calculate the PK parameters for anti-TB drugs in mouse plasma. All values below the lower limit of quantitation (LLOQ) were not included in the calculations. The equations for the PK parameters in Table 3 were programmed in Microsoft Excel 2010 and calculated accordingly.

3. Results and discussion

3.1 Nanoparticle characterization

A particle size range of 220 nm to 380 nm with a polydispersity index of 0.2-0.4 was obtained for these formulations. A zeta potential of +12.45± 4.53 mV for the nanoparticles were observed. The size range and zeta potential were comparable to our previous studies (Semete *et al.* 2010, 2012). It was observed that the zeta potential was not significantly affected by presence or absence of poloxamer coating or drug encapsulation. Lactose was included in the formulation for surface modification as well as the mucoadhesive polysaccharide chitosan. The inclusion of chitosan which is a positively charged ligand has been reported to enhance uptake through the gastrointestinal tract (Cui *et al*. 2006;Takeuchi *et al*. 2005). The %EE for RIF and INH were 68.48± 2.09 % and 55.2± 2.29%, respectively. Nanoparticle characterization is an important consideration since chemical and physical properties of these particles determine its PK and biodistribution (Li and Huang 2008).

Furthermore, considering the limited pore size of the epithelium wall, this is the primary delivery barrier for nanoparticles and therefore particles size plays an important role in nanoparticle biodistribution. The particle size of the nanoparticles used in this study were not below 100nm, but were still within a size range (229± 7.6 to 382± 23.9nm) to promote longer circulation for the surface-modified particles. Although particles with neutral zeta potential have longer blood circulation times than charged particles, the positive zeta potential of the particles evaluated was still adequate to prolong circulation. The %EE observed was satisfactory (55.2- 68.48 %).

3.2 *In vitro* protein binding

The positive controls for RIF and INH protein binding resulted in values for plasma protein binding at 20-40 % for INH and 70-90 % for RIF as depicted in Table 1. This corresponds to the findings of Woo *et al* (1996) of 70-80 % protein binding for RIF and 20 % for INH (Woo *et al*. 1996). However, differences in protein binding were observed for the different plasma to drug ratios as indicated in Table 1. Protein concentrations and percentage protein bound was calculated using the equation for the linear regression of the standard curve for the Bradford reagent.

Table 1 Protein binding for nanoparticle formulations with varying ratios of plasma: nanoparticle suspension, 10:90, 20:80 and 40:60. Results are presented as mean± SD (n=3). * indicates statistical significant differences p≤0.05 compared to the control.

Formulations	**10:90**	**20:80**	**40:60**
Control RIF [1]	71.12± 0.78	79.47± 1.60	90.00± 1.38
Control INH[1]	43.37± 6.6	29.96± 10.90	23.00± 5.2
PLGA-INH	*23.95± 6.60	18.83± 7.50	15.40± 5.50
1% PEG-INH	*10.16± 4.32	*16.87± 2.11	*12.92± 2.15
PLGA-RIF	*19.80± 4.30	*13.15± 5.81	*15.07± 3.40
1%PEG-RIF	*18.94± 3.7	*14.40± 4.60	*15.80± 2.00

[1] *% protein bound was calculated as indicated in Eqn 1.*

Protein binding of drug-free nanoparticles has been reported in previous work (Semete *et al.* 2012). For PLGA-RIF, 23.95% ± 6.6 protein binding was observed compared to 71.12% ± 0.78 for free RIF. This observation demonstrates a significant decrease in protein binding. To further substantiate the findings, the same formulation was coated with 1% PEG. A 57% decrease in protein binding was observed when PLGA-RIF nanoparticles were coated with 1% PEG (10.16% ± 4.32) compared to unencapsulated (free) RIF. Based on these results, it can be suggested that nanoencapsulation could

minimize exposure of the drugs to plasma proteins. Thus more unbound drug would reach the site of action with potential for possible dosage adjustment. Furthermore, a slight decrease in percentage protein binding was observed for PLGA-RIF formulation from 10 %, 20 % and 40 % v/v plasma, but this was found to not be statistically significant. In addition, for PLGA-RIF formulations coated with 1 % PEG, no significant difference was observed at the different plasma concentrations either. RIF has been reported to have a low volume of distribution of approximately 1.44L/kg (Nawaz, 1988) but is still pharmacologically effective despite the high percentage protein binding. As previously mentioned, INH has a very low protein binding (20-30 %). However, when comparing encapsulated INH with unencapsulated (free) INH, a significant difference ($p \leq 0.01$) was observed. Free INH at 10% v/v plasma had a protein binding of 43.4 % ± 6.6 which was significantly decreased to 19.80 % ± 4.3 following nanoencapsulation. Comparison of the uncoated and coated PLGA-INH formulation resulted in no significant difference in protein binding. In addition, the effect of plasma content for these INH formulations was also evaluated. It was observed that incubation of the nanoparticle suspensions with 20 and 40% v/v plasma content had no significant effect on the protein binding compared to 10% v/v plasma content. For the same reason, surface-modified nanoencapsulated INH was evaluated. The effect of surface modification became evident in the drug-free nanoparticles, where drug presence could have no effect. This, however, was dependant on plasma concentration. At 40% plasma content nanoparticle protein binding was decreased by 6% for 1% PEG coated particles. Therefore, protein binding evaluation of nanoparticles encapsulating INH would not have a significant effect on PK and biodistribution of INH.

Figure 1 illustrates SDS-PAGE gel images for PLGA encapsulating RIF and INH, respectively. Since albumin is the major binding plasma protein for most neutral or acidic drugs (Woo *et al*. 1996), binding of albumin and binding of whole plasma is considered synonymous. The protein fragments with the strongest intensity appear in the marker range of 70 kDa in both images. This molecular weight range is reported to be plasma albumin (Carter *et al*. 1989). In Figure 1, the uncoated PLGA-RIF formulations demonstrated the greatest intensity of the albumin fragment, much lower intensities observed for the formulation coated with 1% PEG. A similar result was observed for the INH formulation. The difference observed at different ratios can be interpreted as being a function of the different concentrations of the bound protein, in this case albumin. The observations discussed cannot be directly compared to Table 1, since these data reflect denatured proteins and not absolute protein concentrations as summarized in Table 1 since gel analysis is not quantitative. Other plasma proteins associated with these nanoparticles to a lesser extent were the apolipoproteins (Mw 28, 34 and 43 kDA), and possibly cholesteryl ester transfer protein (Mw 53 kDA) as reported in a previous study (Cedervall *et al*. 2007).

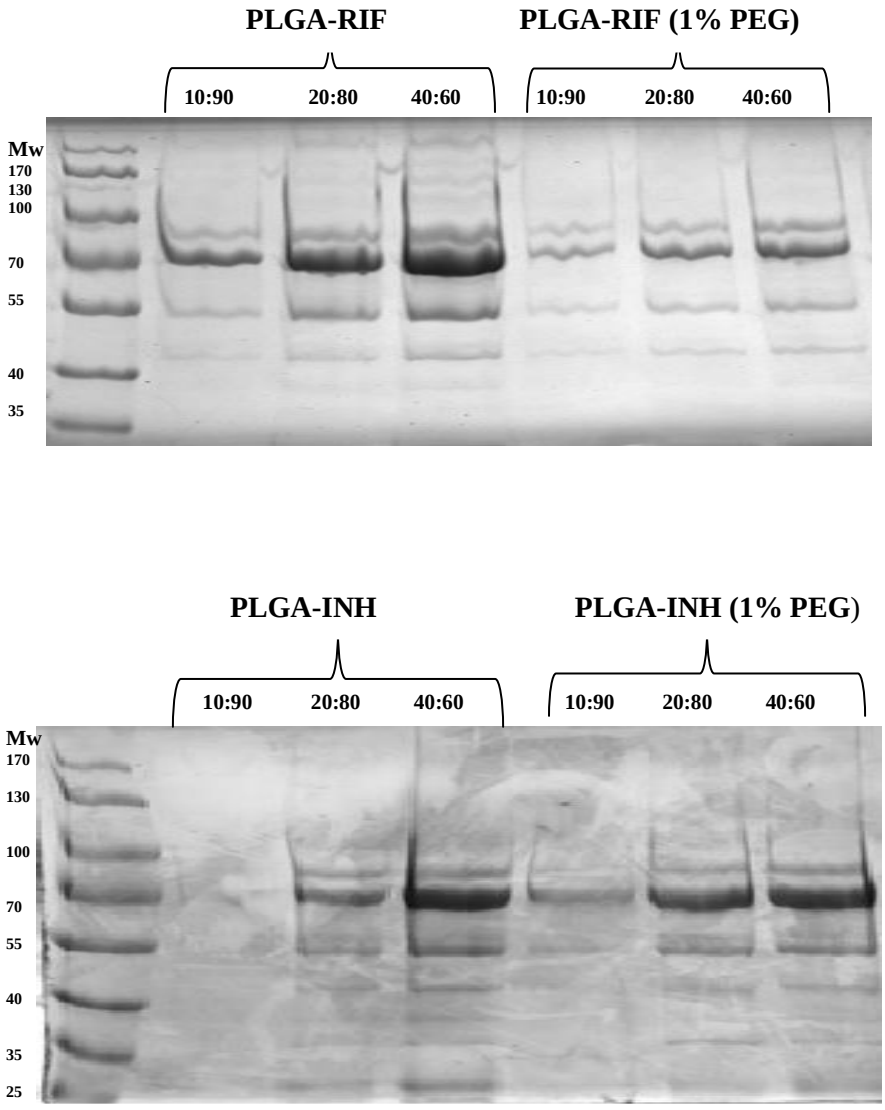

Figure 1 SDS-PAGE gel images of PLGA-RIF and PLGA-INH coated with and without PEG. The image depicts the band intensities of the different proteins bound to the nanoparticles. Albumin with Mw 70 kDa demonstrated the strongest band intensity. The strongest intensity was observed for the PLGA-RIF formulation at 40:60 suspensions.

3.3 *In vitro* MIC/MBC assays

For the OD_{600} readings measured on day 6 of the study, the free drug control wells appeared active with some inhibition observed. No inhibitory activity was observed for any of the nanoparticle formulations. On day 8 variations were observed among the six free-INH replicates (average OD_{600} reading 0.0780 ± 0.00026 and 0.1722 ± 0.1595 for 0.12µg/ml and 0.03µg/ml control wells, respectively). For INH-NP, three of the 6 replicates demonstrated MIC of 16ug/ml, but there were large variations in OD_{600} observed for both the control (no drug) wells and the nanoparticles wells. Free RIF MIC concentration was observed at 0.12ug/ml. No variation was observed among the six

replicates. RIF-NP's demonstrated MIC concentrations between 32 and 16ug/mL, though some variation was observed among replicates.

Figure 2 illustrates the MIC profile of INH (free and nanoencapsulated) at observed MIC's. Concentrations selected for graphical representation demonstrated growth inhibition over time based on OD_{600} readings. For free INH, concentration below 0.03 µg/ml demonstrated OD_{600} readings comparable to untreated controls. No inhibition for nanoparticles at concentrations below 16µg/ml was observed. Since the MIC observed for nanoencapsulated drug is dependent on the drug being released from the nanoparticle and the MIC profile observed was comparable to that of the free drug at MIC 0.03µg/ml, it may suggest that the amount of drug released from the nanoparticles at 16µg/ml was ~0.03 µg/ml INH. The increase in OD_{600} observed at day 18 was due to decrease in well volume as a result of the wells drying out. This could suggest that continued MIC could have been observed past the day 18 time point as a result of sustained release of INH from the nanoparticles.

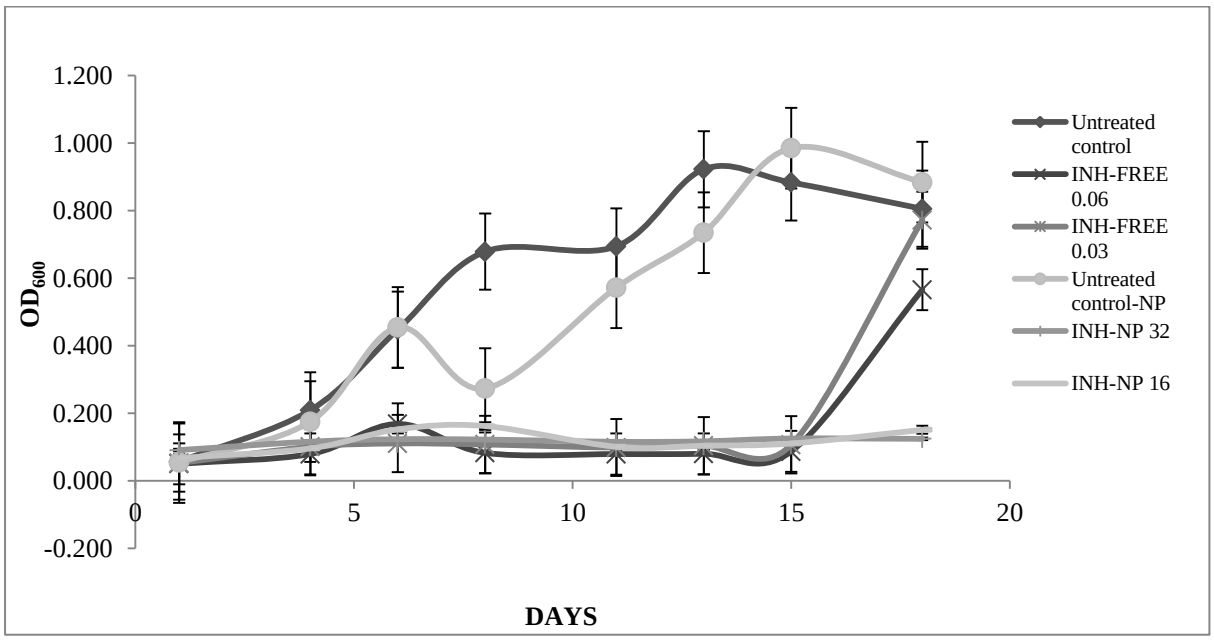

Figure 2 MIC profile for INH- free and nanoencapsulated compared against untreated controls. Values calculated as mean± SD, n=6. Drug concentrations are in µg/ml.

RIF demonstrated similar results (Figure 3). The MIC for RIF is 0.06µg/ml and a similar trend was observed for RIF-NP at 8µg/ml, suggesting that MIC drug concentrations were released from the nanoparticle formulations at this concentration. RIF-NP at 32µg/ml demonstrated an MIC profile similar to that of RIF-FREE at 0.12, 0.48 and 0.96µg/ml.

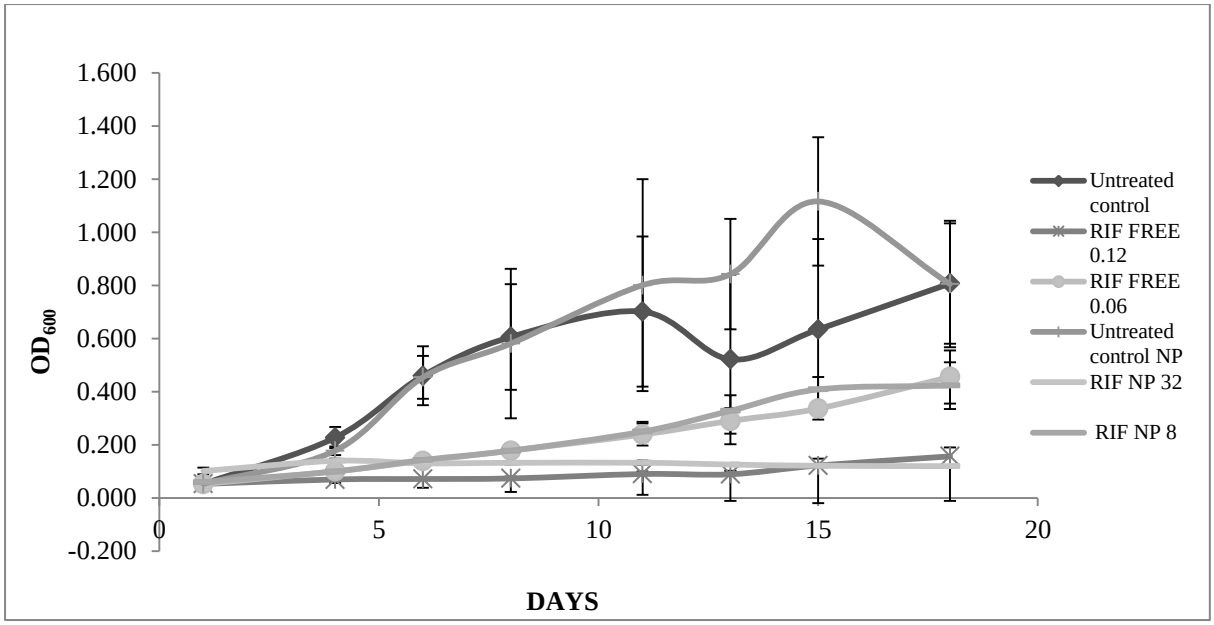

Figure 3 MIC profile for RIF- free and nanoencapsulated compared against untreated controls. Values calculated as mean± SD, n=6. Drug concentrations are in µg/ml.

The MIC profiles for RIF-nanoparticle formulations at 8µg/ml were comparable to the free-drug controls at MIC for RIF as observed in this study (0.06µg/ml). Similarly, INH nanoparticle formulations (16µg/ml) demonstrated MIC profiles comparable to free-drug MIC profiles at MIC for INH (0.03µg/ml). Thus, at the nanoparticle concentrations used sufficient drug was released to facilitate growth inhibition over time *in vitro*. Therefore, based on these *in vitro* assays, nanoparticle-based RIF and INH chemotherapy forms a sound basis for a reduction in dosing frequency and also offers the possibility of reducing the drug dosage. Confirming these findings with *in vivo* efficacy assays would be the focus for future work.

Figure 4 A and B summarizes the MBC for INH following plating of MIC samples over 18 days. The untreated controls indicate where 100% bacterial growth is still present (100 % line). Below 50% and 1% lines was where 50 % and 99 % bacterial killing was expected based on decrease in cfu's. Free-INH (Figure 4 A) exhibited 99 % killing at 0.12µg/ml which equals four times the MIC of INH with 100% killing at higher concentrations. Figure 4 B demonstrated that at 30µg/ml INH-NP, 99% bacterial killing could be achieved.

that at 16µg/ml, nanoencapsulated RIF elicited 99% bacterial killing. For free-RIF Figure 5 B, 99% killing was achieved at 0.05µg/ml with 100% killing observed at higher concentrations.

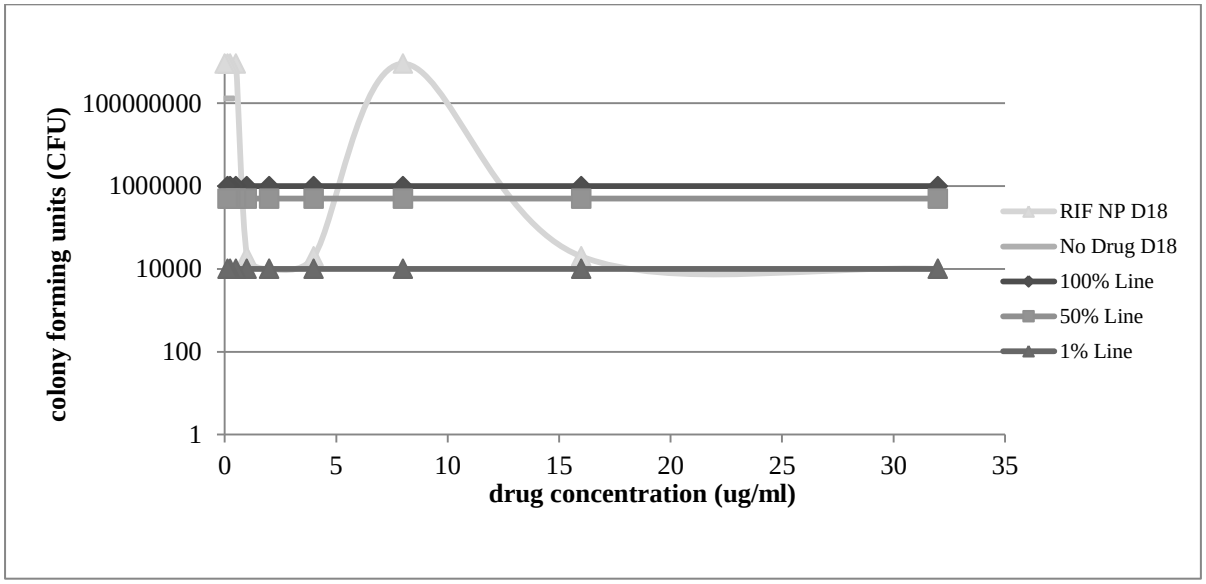

A

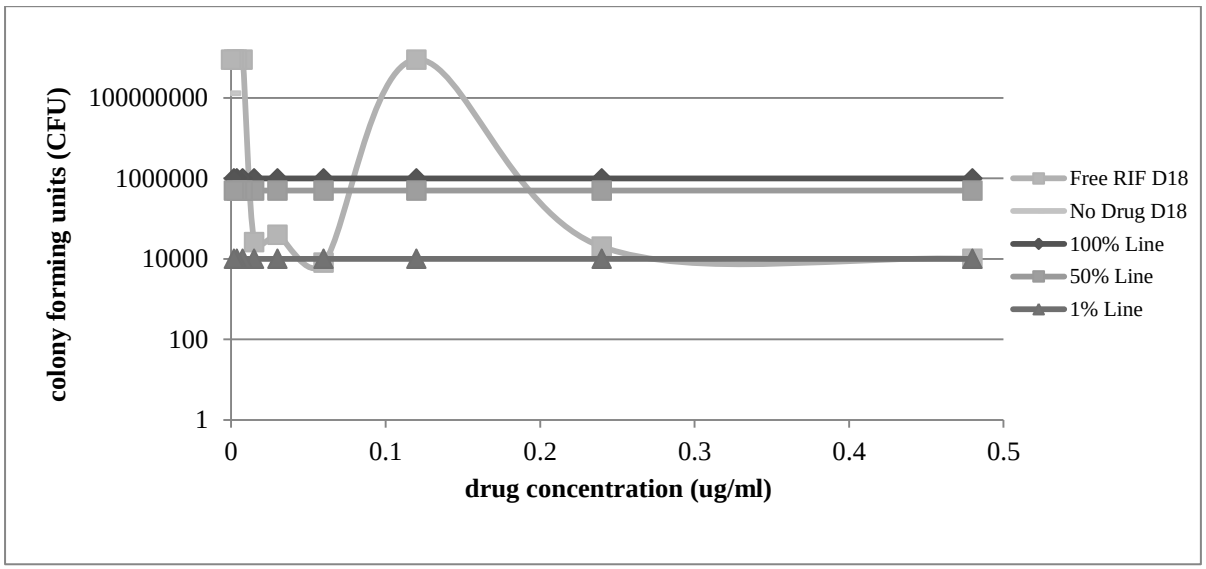

B

Figure 5 A-MBC profile for free-RIF and B- MBC profile for nanoencapsulated RIF at day 18 of MBC analysis. The decrease in colony forming units (cfu) are depicted as the 100 % line (no bacterial killing), 50 % line (50 % killing) and 1 % line (99 % killing).

3.4 *In vivo* bioavailability assays

Drug levels in the mouse serum were estimated by multiplying the dilution factor by the MIC value of the drug in the absence of serum. The dilution factor (DF) represents the last dilution step of the serum samples in which drug activity was still observed in the bioassay. Bioavailability of the two

drugs were rated according to the dilution factor and by correlating the standard drug concentrations used in the assay with the OD_{600} reading obtained for the different wells as shown in Table 5.6. Rating of bioavailability: Low: at a DF of 1:10 and 1:20, Medium: DF is 1:40 or 1:80, High: if DF is 1:160 or 1:320. The MIC is based on the lowest concentration at which growth inhibition was observed.

Table 2 Determination of MIC levels of both free and encapsulated INH and RIF in mouse treated serum over 7 days.

Drug formulation	MIC (no serum)	MIC (10% serum)	Drug dose (mg/kg)	Dosing route	Approximate drug level (µg/ml) in serum after:					
					2hr	8hr	1 day	2 days	3 days	7 days
INH-NP	0.041	0.041	150	Oral gavage	>13.12	3.28	BD	0.41	0.41	BD
INH-Free	0.041	0.041	150	Oral gavage	>13.12	0.41	BD	BD	NA	NA
RIF-NP	0.041	0.041	60	Oral gavage	>13.12	>13.12	3.28	0.41	0.41	BD
RIF-Free	0.041	0.041	60	Oral gavage	>13.12	>13.12	>13.12	0.82	NA	NA

BD, below detection limit of the bioassay. The detection limit is 10x the MIC_{90} of the tested compound in the presence of serum (due to the restriction of using a maximum of 10% serum in the M.tb. NA: not analysed.

As expected, both free- nanoencapsulated drugs were bioavailable, based on OD_{600} readings and visual inspection of the microtitre plates. For free-INH, growth inhibition was only observed up to the 8-hour time point indicating the rapid elimination and/or distribution of the free drug. Free-RIF drug levels were observed up to two days in serum and these levels were sufficiently high to exhibit growth inhibition. For both nanoencapsulated formulations of RIF and INH, growth inhibition was observed up to the day 3 time point. This observation suggested at sufficient drug was released into the bloodstream from the nanoparticles to exhibit growth inhibition of *M.tb*. The standard compounds were used to determine approximate drug levels depicted in Table 1.2. As observed in Table 1.2 drug levels at the 2-hour and 8-hour time points for INH and RIF, respectively were high and the sera were not diluted to enough using the described method (dilution was up to 1:320). These drug levels were observed at >13.2 µg/ml. The method described for this study was designed to analyse experimental drugs and since bioavailability for these bioactive drugs are already known, the dilutions used may not have been optimal. However, the aim was to determine the bioavailability of the drugs following release from nanoparticles and this was confirmed. The fact that MIC was the same for all four formulations with and without serum indicates that no significant protein binding occurred. Based on free drug controls for both RIF and INH, the MIC was calculated at 0.041µg/ml. Therefore, at 10 times the MIC, 0.41 µg/ml serum concentrations were required to exhibit inhibition. As indicated in

Table 1.2, approximate drug levels for encapsulated drug were at 10 times MIC and inhibition was observed.

Although this was considered as a positive result in terms of bioavailability, the data could not be extrapolated to *in vivo* efficacy since the serum drug levels need to be sufficient at the disease sites where *M.tb* resides and this can only be confirmed by *in vivo* efficacy assays.

3.5 *In vivo* drug release and drug distribution

Detection and quantification of nanoencapsulated RIF up to 7 days in plasma versus only 2 days for free RIF were observed (Figure 6 A). This data provided a clear distinction between nanoencapsulated versus free drug plasma concentrations at the same dose. Furthermore, the observed plasma drug levels up to 7 days were above the MIC determined in the *in vitro* studies to be 0.06µg/ml. Sustained drug release was maintained for up to 7 days at drug levels exceeding 0.2µg/ml (Figure 6 B). This may be extrapolated to indicate that at the conventional dose, drug levels can be maintained above the MIC for INH which is 0.03µg/ml.

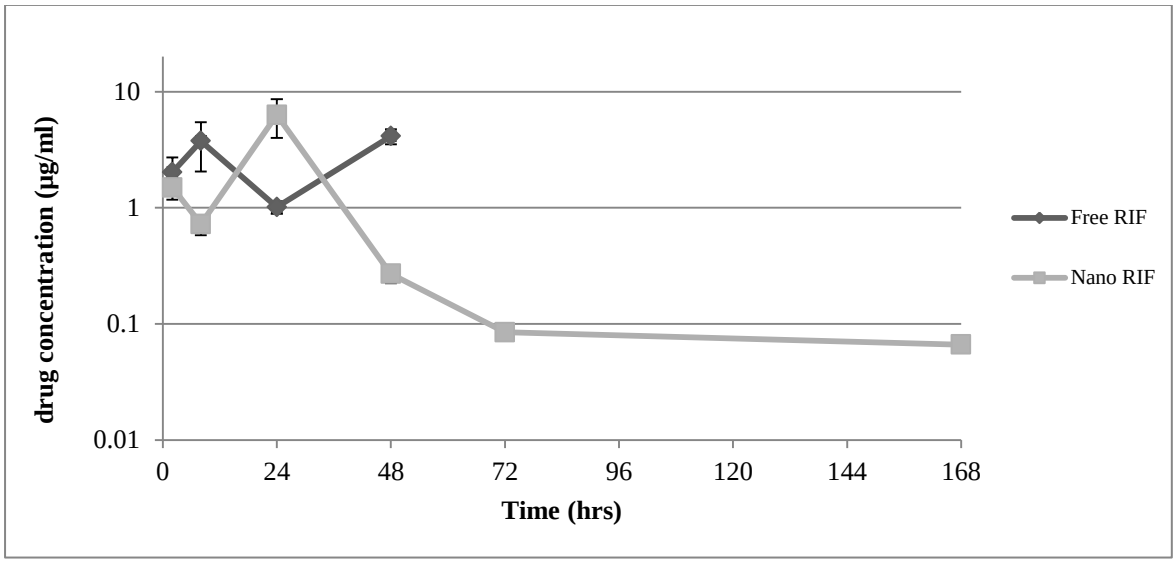

A

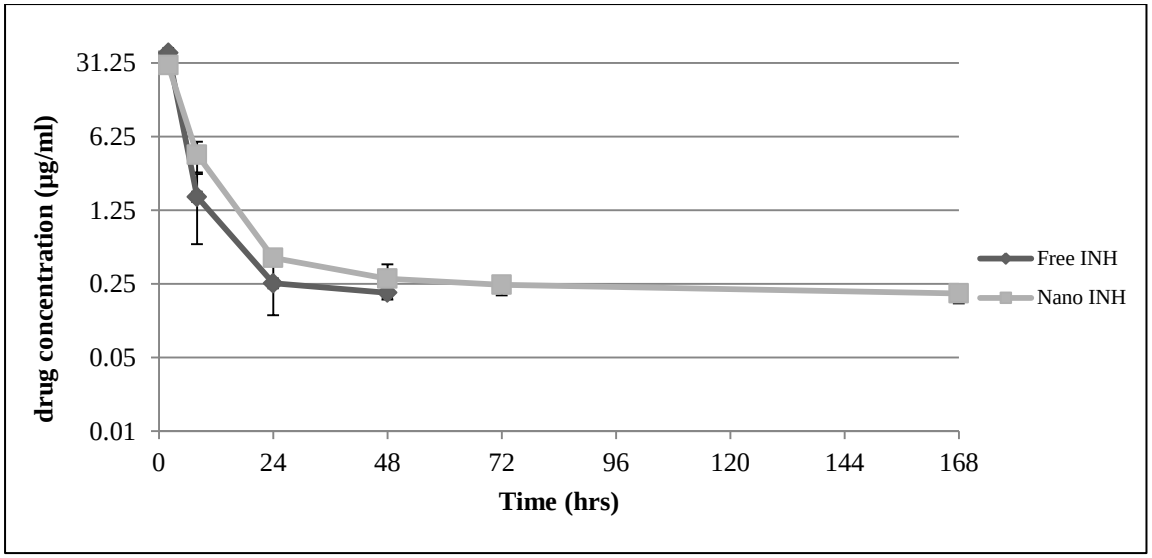

B

Figure 6 Plasma-concentration versus time profiles for free and encapsulated RIF (A) and INH (B) plotted on a logarithmic scale for legibility of the graph. Plasma drug concentrations are depicted as mean± SD.

Various pharmacokinetic parameters were evaluated to determine the differences, if any, between free versus nanoencapsulated anti-tuberculosis drugs. Table 3 summarizes the PK analysis. INH reached C_{max} at 2 hours and RIF-free only reached C_{max} at the 8-hour time point. RIF-free demonstrated a larger AUC which was significantly higher ($p \leq 0.05$) than what was observed for INH. For RIF-NP and INH-NP, plasma drug levels were detected up to 7 days of analysis. The half-life of these drug formulations were significantly longer ($p \leq 0.05$) compared to free drug at 3.85 and 5.77 hours, respectively.

It has been reported that near zero-order release kinetics and modification and improvement of pharmacokinetic parameters such as tissue distribution profile are achieved through nanoparticulate drug delivery (Couvreur & Vauthier 2006). Other advantages include improved bioavailability and decreased toxicity due to high loading efficiency which results in lower doses administered. These factors all culminate in an increase in patient compliance to treatment (Kingsley *et al*. 2006). INH and RIF nanoparticles maintained controlled drug release over seven days and free drugs only three days, which provided a clear distinction between nanoparticulate drug release versus free drug. The $AUC_{0\rightarrow\infty}$ values for these release profiles suggested improved absorption compared to what has been previously reported (Ahmad *et al*. 2006;McIlleron *et al*. 2006) and therefore, improved bioavailability which supports the hypothesis. Based on these results, INH and RIF nanoparticles demonstrated potential for reduction in dosing frequencies.

In one of our previous reports, nanoparticles were observed to localize in different areas of the organs evaluated and it was expected that the drugs would be released at these sites (Semete *et al*. 2010b). Of the organs harvested, only the organs of interest, namely lungs, liver, kidney and spleen were evaluated. Figure 7 illustrates tissue distribution of free and nanoencapsulated drugs. Figure 7 A depicts liver distribution of free and encapsulated RIF and INH. For RIF, drug levels were observed up to 10 days for nanoencapsulated and 7 days for free drug. RIF is primarily metabolized by the liver and the increased dose may be as a result of drug accumulation in the liver (Budha *et al*. 2008). INH was not quantifiable at the conventional dose in the liver. At 7 days, low levels were observed for free INH and only 2 out of 3 mice evaluated had detectable nanoencapsulated INH, with one being below lower limit of detection (LLOD) and one significantly higher ($p \leq 0.05$), which is the reason for the high standard deviation. Free drug was observed between 2 days and 7 days, but the levels at 7 days were below the LLOQ.

Drug levels for RIF were detected in the lungs up to 48 hours. According to literature RIF attains lung concentration equal to or more than serum levels (Budha *et al.* 2008). Therefore, RIF would be expected to be present for a longer period as was observed in plasma, but this was not the case as demonstrated in Figure 7 B. INH demonstrated similar accumulation in the lung, comparable to liver accumulation of RIF. Significantly higher levels were observed for free versus encapsulated RIF at 24 hours ($p \leq 0.05$) in the spleen (Figure 7 C). No INH levels were observed in the spleen. In Figure 7 D only free RIF was observed at 48 hours in the kidneys. INH was only detected on the 7-day time point in the kidneys.

Table 3 Plasma drug analysis for free-and nanoencapsulated RIF and INH.

Drug	$AUC_{0\rightarrow t}$ (ug/mL * min)	$k_{el}(\lambda)$ (min^{-1})	$AUC_{0\rightarrow\infty}$ (ng/mL * min)	$t_{1/2}\lambda$ (hr)	C_{max} (ng/mL)	T_{max} (min)	CL (mL/min)	$AUMC_{0\rightarrow t}$ (ng/mL * min^2)	MRT (min)	$V_{ss\ (L)}$
RIF-F	1057	0.0600	1126175.8	0.183	55666.67	480	1.08	15565339	14.7	0.016
RIF-NP	408	0.0000	498497.7	3.85	50200	120	2.80	5479347	13.4	0.016
INH-F	145	0.0400	149686.3	1.283	38700	120	20.1	738410.7	5.1	0.1
INH-NP	363	0.0000	503099.3	5.775	29733	120	8.2	6452101	17.8	0.1

Drug-F- unencapsulated (free) drug; Drug-NP- nanoencapsulated drug; $AUC_{0\rightarrow t}$: area under the concentration-time curve for time 0 to time t; k_{el} (λ): terminal elimination rate constant; $AUC_{0\rightarrow\infty}$: area under the concentration-time curve for time 0 to infinity (∞); $t_{1/2}\lambda$: terminal half life; CL: systemic clearance; C_{max}: maximum concentration; T_{max}: time of maximum concentration (C_{max}); $AUMC_{0\text{-}t}$: area under the first moment curve; MRT: mean residence time; V_{ss}: volume of distribution at steady state.

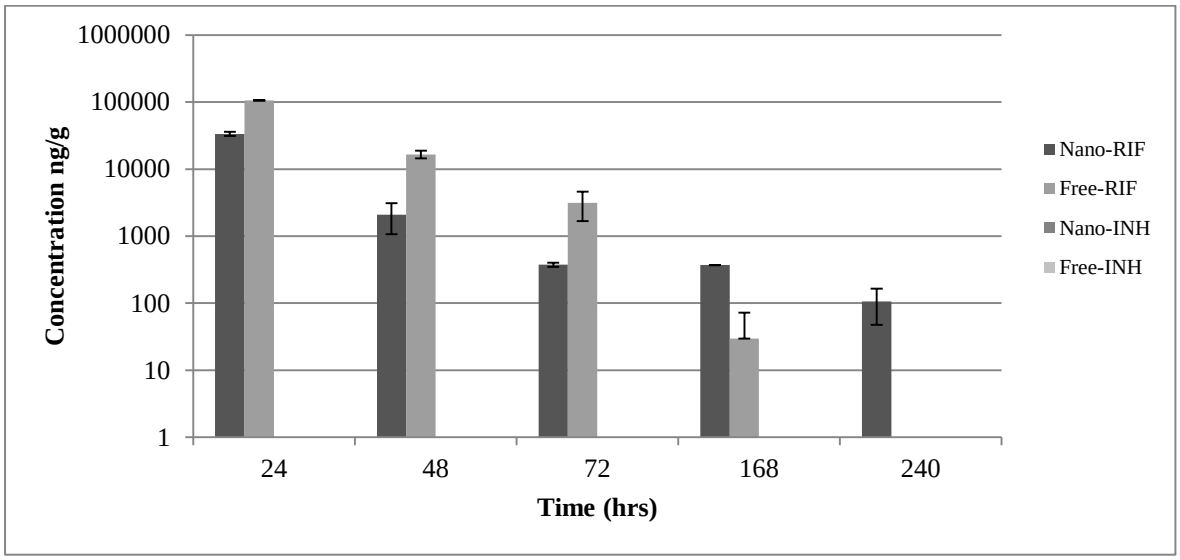
1000000
100000
10000
1000
100
10
1
Concentration ng/g
24
48
72
168
240
Time (hrs)
Nano-RIF
Free-RIF
Nano-INH
Free-INH

A

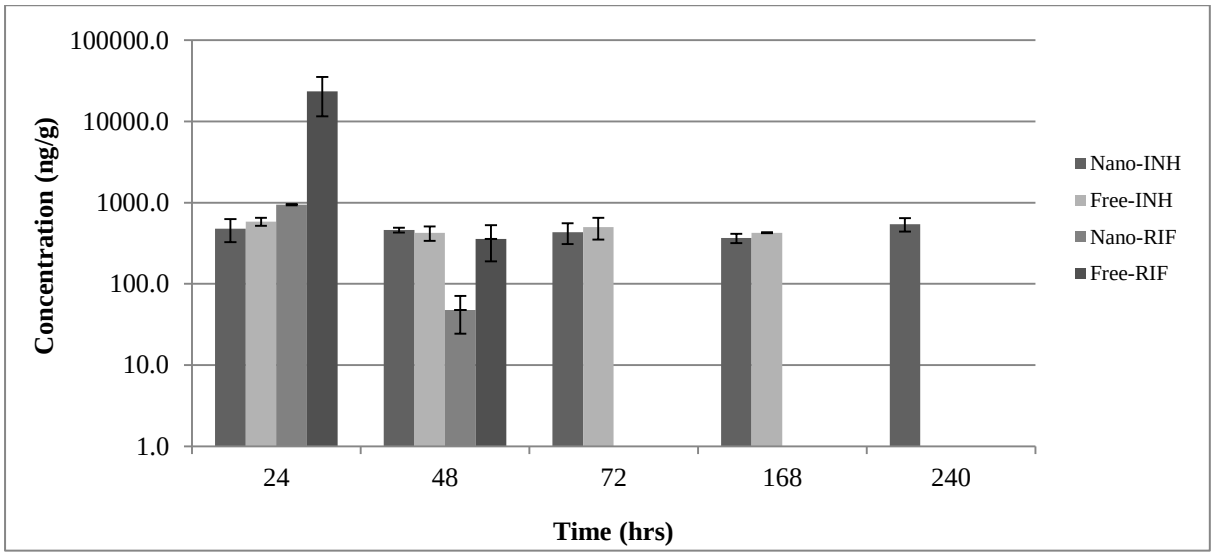
100000.0
10000.0
1000.0
100.0
10.0
1.0
Concentration (ng/g)
24
48
72
168
240
Time (hrs)
Nano-INH
Free-INH
Nano-RIF
Free-RIF

B

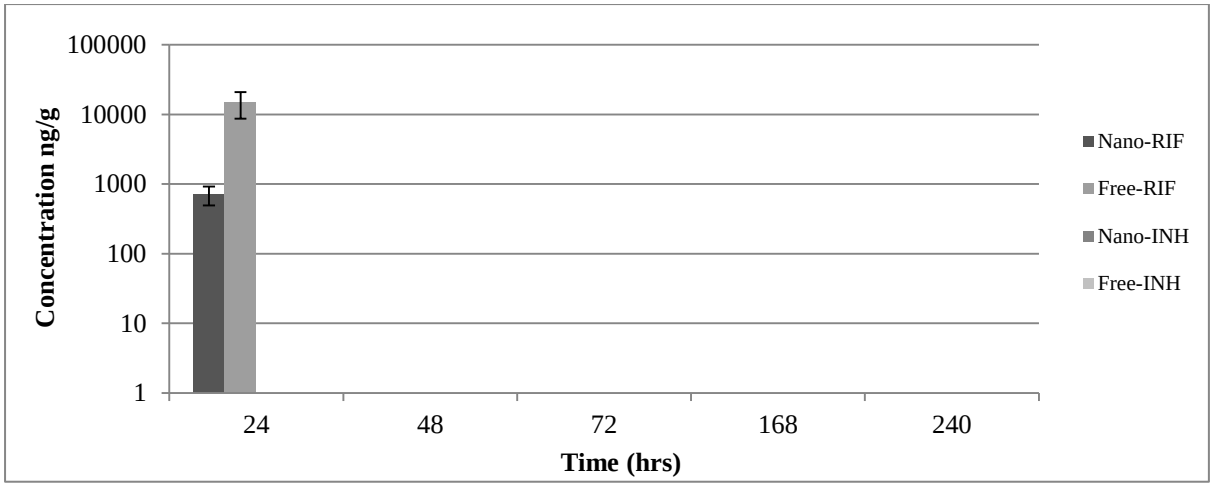

C

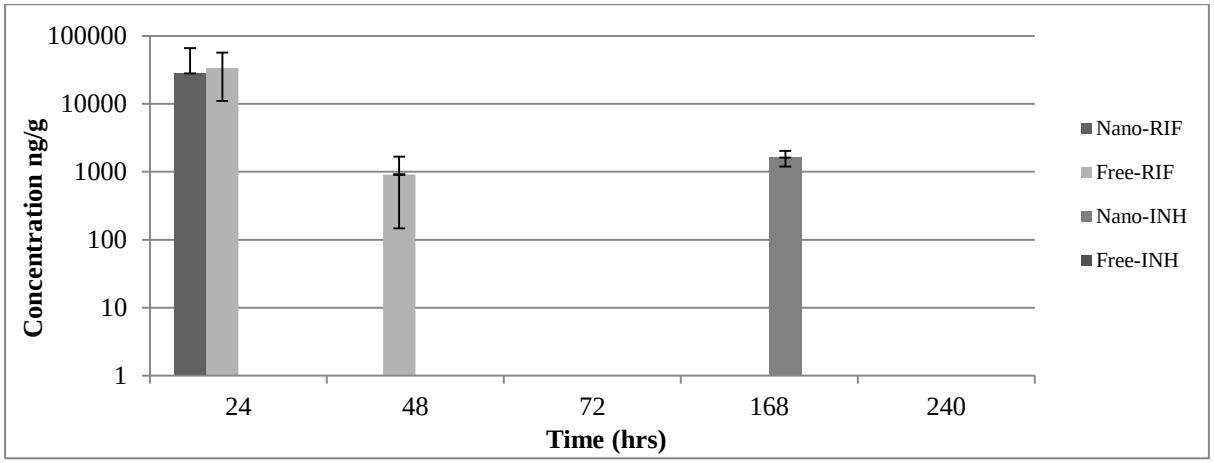

D

Figure 7 Summary of drug distributions of free- and nanoencapsulated RIF and INH in (A) the liver, (B) lungs (C) spleen and (D) kidneys. Mean± SD is shown in the graphs.

Subsequent to entering the vascular system, drugs are distributed to various tissues and body fluids, i.e. extravascular fluid. The differences in tissue distribution exist for different drugs and this is largely attributed to differential tissue affinity, blood flow to tissues, the drugs ability to cross biological membranes and also the drugs' physicochemical properties, i.e. lipophilicity and extent of ionization (Budha *et al.* 2008). RIF drug levels encapsulated in nanoparticles was observed up to 10 days in the liver. Since RIF accumulates and is metabolized by the liver due to first pass metabolism, this was an expected result. The presence of free-RIF was unexpected since clearance within 24 hours was expected. RIF drug levels encapsulated in nanoparticles were observed in the lungs up to two days and in the spleen and kidneys up to 24 hours. RIF is readily distributed into lung parenchyma and kidneys (Budha *et al.* 2008), which explains the high drug concentrations in the kidneys at 24 hours, but the low drug concentrations in the lungs cannot be explained. INH nanoparticles were

observed up to 10 days in the lungs which suggests drug accumulation in the lungs. No INH drug levels encapsulated in nanoparticles were observed in the liver and spleen. INH drug levels encapsulated in nanoparticles were observed in the kidneys only at the seven days' time point with no drug concentrations observed at earlier time points. Only 5-30% of INH is excreted in urine, this may be why earlier drug concentrations in the kidneys were not detected. Considering the low V_{ss} values calculated for all the drugs in Table 1.3, it may be assumed that the drugs were residing largely within the vascular space since volume of distribution relates the amount of drug in the body to plasma drug levels. Larger V_{ss} may have resulted in higher drug levels in the tissues.

4. Conclusion

The data demonstrates that PEG-coated nanoparticles reduced protein binding compared to uncoated particles in the presence of encapsulated drug compared to free drug. Along with size and surface charge, protein binding has been reported to be a key factor influencing biodistribution (Aggarwal *et al*. 2009). Spray-dried PLGA nanoparticle formulations encapsulating anti-tuberculosis drugs demonstrated promising pharmacodynamic properties, *in vitro.* Furthermore, pharmacokinetic data generated resulted in a 7-day sustained release profile for RIF and INH with subsequent drug distribution of these drugs for up to 10 days in the liver and lungs, respectively. Overall, this spray-dried formulation demonstrated promising PK/PD data for use in TB chemotherapy, but further studies are warranted.

References

Aggarwal, P., Hall, J.B., McLeland, C.B., Dobrovolskaia, M.A., & McNeil, S.E. 2009. Nanoparticle interaction with plasma proteins as it relates to particle biodistribution, biocompatibility and therapeutic efficacy. *Adv. Drug Deliv. Rev.* 61[6],428-437.

Ahmad, Z., Pandey, R., Sharma, S., & Khuller, G.K. 2008. Novel chemotherapy for tuberculosis: chemotherapeutic potential of econazole- and moxifloxacin-loaded PLG nanoparticles. *Int. J. Ant. Agents* 31[2],142-146.

Ahmad, Z., Pandey, R., Sharma, S., & Khuller, G.K. 2006. Pharmacokinetic and pharmacodynamic behaviour of antitubercular drugs encapsulated in alginate nanoparticles at two doses. *Int. J. Ant. Agents* 27[5],409-416.

Azarmi, S., Roa, W.H., & Löbenberg, R. 2008. Targeted delivery of nanoparticles for the treatment of lung diseases. *Adv. Drug Deliv. Rev.* 60[8],863-875.

Benator, D., Bhattacharya, M., Bozeman, L., Burman, W., Cantazaro, A., Chaisson, R., Gordin, F., Horsburgh, C.R., Horton, J., Khan, A., Lahart, C., Metchock, B., Pachucki, C., Stanton, L., Vernon, A., Villarino, M.E., Wang, Y.C., Weiner, M., & Weis, S. 2002. Rifapentine and isoniazid once a week versus rifampicin and isoniazid twice a week for treatment of drug-susceptible pulmonary tuberculosis in HIV-negative patients: a randomised clinical trial. *The Lancet* 360[9332],528-534.

Brooks, J.V. & Orme, I.M. 1998. Evaluation of Once-Weekly Therapy for Tuberculosis Using Isoniazid plus Rifamycins in the Mouse Aerosol Infection Model. *Antimicrob. Agents Chemother.* 42[11],3047-3048.

Budha, N.R., Lee, R.E., & Meibohm, B. 2008. Biopharmaceutics, Pharmacokinetics and Pharmacodynamics of Antituberculosis Drugs. *Curr. Med. Chem.* 15[8].809-825.

Carter, D.C., He, X.M., Munson, S.H., Twigg, P.D., Gernert, K.M., Broom, M.B., & Miller, T.Y. 1989. Three-dimensional structure of human serum albumin. *Science* 244[4909], 1195-1198.

Cedervall, T., Lynch, I., Foy, M., Berggård, T., Donnelly, S., Cagney, G., Linse, S., & Dawson, K. 2007. Detailed Identification of Plasma Proteins Adsorbed on Copolymer Nanoparticles. *Angewandte Chemie* 119[30], 5856-5858.

Couvreur, P. & Vauthier, C. 2006. Nanotechnology: Intelligent design to treat complex disease. *Pharm. Res.* 23, (7) 1417-1450.

Cui, F., Qian, F., & Yin, C. 2006. Preparation and characterization of mucoadhesive polymer-coated nanoparticles. *Int. J. Pharm.* 316, 154-161.

Dhillon, J. & Mitchison, D.A. 1992. Activity in vitro of rifabutin, FCE 22807, rifapentine, and rifampin against Mycobacterium microti and M. tuberculosis and their penetration into mouse peritoneal macrophages. *Am. J. Respir. Crit. Care Med.* 145[1], 212-214.

Ellard, G.A. 1999. The evaluation of rifampicin bioavailabilities of fixed-dose combinations of anti-tuberculosis drugs: procedures for ensuring laboratory proficiency. *Int. J. Tuberc. Lung Dis.* 3[11s3], S322-S324.

Epstein, H., Gutman, D., Cohen-Sela, E., Haber, E., Elmalak, O., Koroukhov, N., Danenberg, H., & Golomb, G. 2008. Preparation of alendronate liposomes for enhanced stability and bioactivity: *In vitro* and *in vivo* Characterization. *The AAPS Journal*, 10[4], 505-515.

Grosset, J. & Leventis, S. 1983. Adverse effects of Rifampicin. *Rev. Infect. Dis.* 5[3], S440-S450.

Gruppo, V., Johnson, C.M., Marietta, K.S., Scherman, H., Zink, E.E., Crick, D.C., Adams, L.B., Orme, I.M., & Lenaerts, A.J. 2006. Rapid Microbiologic and Pharmacologic Evaluation of Experimental Compounds against Mycobacterium tuberculosis. *Antimicrob. Agents Chemother.* 50[4], 1245-1250.

Gurumurthy, P., Ramachandran, G., Vijayalakshmi, S., Hemanth Kumar, A.K., Venkatesan, P., Chandrasekaran, V., Vjayasekaran, V., Kumaraswami, V., & Prabhakar, R. 1999. Bioavailability of rifampicin, isoniazid and pyrazinamide in a triple drug formulation: comparison of plasma and urine kinetics. *Int. J. Tuberc. Lung Dis.* 3, 119-125.

Italia, J.L., Bhatt, D.K., Bhardwaj, V., Tikoo, K., & Kumar, M.N.V. 2007. PLGA nanoparticles for oral delivery of cyclosporine: Nephrotoxicity and pharmacokinetic studies in comparison to Sandimmune Neoral®. *J. Controlled Release* 119[2], 197-206.

Jain, R.A. 2000. The manufacturing techniques of various drug loaded biodegradable poly(lactide-co-glycolide) (PLGA) devices. *Biomaterials*, 21[23], 2475-2490.

Kalombo, L. 2008, *Nanoparticle carriers for Drug Administration*, 2469965 (patent).

Kingsley, J., Dou, H., Morehead, J., Rabinow, B., Gendelman, H., & Destache, C. 2006. Nanotechnology: A Focus on Nanoparticles as a Drug Delivery System. *J. Neuroimmune Pharmacol.* 1[3], 340-350.

Kisich, K.O., Gelperina, S., Higgins, M.P., Wilson, S., Shipulo, E., Oganesyan, E., & Heifets, L. 2007. Encapsulation of moxifloxacin within poly(butyl cyanoacrylate) nanoparticles enhances efficacy against intracellular Mycobacterium tuberculosis. *Int. J. Pharm.* 345[1-2], 154-162.

Ledet, G. & Mandal, T.K. 2012. Nanomedicine: Emerging Therapeutics for the 21st Century. *US Pharm.* 37[3], 7-11.

Li, S.D. & Huang, L. 2008. Pharmacokinetics and Biodistribution of Nanoparticles. *Mol. Pharm.* 5[4], 496-504.

Maggi, N., Pasqualucci, C.R., Ballotta, R., & Sensi, P. 1966. Rifampicin: a new orally active rifamycin. *Chemotherapy* 11[5], 285-292.

McIlleron, H., Wash, P., Burger, A., Norman, J., Folb, P.I., & Smith, P. 2006. Determinants of Rifampin, Isoniazid, Pyrazinamide, and Ethambutol Pharmacokinetics in a Cohort of Tuberculosis Patients. *Antimicrob. Agents Chemother*. 50[4], 1170-1177.

Panchagnula, R. & Agrawal, S. 2004. Biopharmaceutic and pharmacokinetic aspects of variable bioavailability of rifampicin. *Int. J. Pharm.* 271, 1-4.

Pape, J.W., Jean, S.S., Ho, J.L., Hafner, A., & Johnson, W.D. 1993. Effect of isoniazid prophylaxis on incidence of active tuberculosis and progression of HIV infection. *The Lancet*, 342[8866], 268-272.

Semete, B., Booysen, L.I.J., Kalombo, L., Venter, J.D., Katata, L., Ramalapa, B., Verschoor, J.A., & Swai, H. 2010a. *In vivo* uptake and acute immune response to orally administered chitosan and PEG coated PLGA nanoparticles. *Toxicol. Appl. Pharmacol.* 249[2], 158-165.

Semete, B., Booysen, L., Kalombo, L., Ramalapa, B., Hayeshi, R., & Swai, H.S. 2012. Effects of protein binding on the biodistribution of PEGylated PLGA nanoparticles post oral administration. *Int. J. Pharm.* 424[1-2], 115-120.

Semete, B., Booysen, L., Lemmer, Y., Kalombo, L., Katata, L., Verschoor, J., & Swai, H.S. 2010b. In vivo evaluation of the biodistribution and safety of PLGA nanoparticles as drug delivery systems. *Nanomed Nanotech. Biol. Med.* 6[5], 662-671.

Slack, S. M. & Horbett, T. A. 1995, "The Vroman Effect," *In Proteins at Interfaces II*, Washington, DC: American Chemical Society, pp. 112-128.

Stolnik, S., Daudali, B., Arien, A., Whetstone, J., Heald, C.R., Garnett, M.C., Davis, S.S., & Illum, L. 2001. The effect of surface coverage and conformation of poly(ethylene oxide) (PEO) chains of poloxamer 407 on the biological fate of model colloidal drug carriers. *Biochim. Biophys. Act.* 1514[2], 261-279.

Takayama, K., Wang, L., & David, H.L. 1972. Effect of isoniazid on the in vivo mycolic acid synthesis, cell growth, and viability of *Mycobacterium tuberculosis*. *Antimicrob. Agents Chemother.* 2[1], 29-35.

Takeuchi, H., Matsui, Y., Sugihara, H., Yamamoto, H., Kawashima, Y., & Thongborisute, J. 2005. Novel mucoadhesion tests for polymers and polymer-coated particles to design optimal mucoadhesive drug delivery systems. *Adv. Drug Deliv. Rev.* 57, 1583-1594.

World Health Organization (WHO). 2011, *2011 Global TB Report*.

Woo, J., Cheung, W., Chan, R., Chan, S., Cheng, A., & Chan, K. 1996. In Vitro Protein Binding Characteristics of Isoniazid, Rifampicin, and Pyrazinamide to Whole Plasma, Albumin, and [alpha]-1-Acid Glycoprotein. *Clin. Biochem.* 29[2], 175-177.

Toxicology and Applied Pharmacology 249 (2010) 158–165

Contents lists available at ScienceDirect

Toxicology and Applied Pharmacology

journal homepage: www.elsevier.com/locate/ytaap

In vivo uptake and acute immune response to orally administered chitosan and PEG coated PLGA nanoparticles

B. Semete [a,*,1], L.I.J. Booysen [a,b,1], L. Kalombo [a], J.D. Venter [c], L. Katata [a], B. Ramalapa [a], J.A. Verschoor [d], H. Swai [a]

[a] Council for Scientific and Industrial Research, Polymers and Composites, P O Box 395 Pretoria, 0001, South Africa
[b] Department of Pharmaceutics, North-West University, Potchefstroom Campus, Potchefstroom, 2520, South Africa
[c] South African Medical Research Council, TB laboratory, Pretoria, 0001, South Africa
[d] Department of Biochemistry, University of Pretoria, Pretoria, 0001, South Africa

ARTICLE INFO

Article history:
Received 2 June 2010
Revised 31 August 2010
Accepted 3 September 2010
Available online 17 September 2010

Keywords:
PLGA nanoparticles
Inflammation
Cytokines

ABSTRACT

Nanoparticulate drug delivery systems offer great promise in addressing challenges of drug toxicity, poor bioavailability and non-specificity for a number of drugs. Much progress has been reported for nano drug delivery systems for intravenous administration, however very little is known about the effects of orally administered nanoparticles. Furthermore, the development of nanoparticulate systems necessitates a thorough understanding of the biological response post exposure. This study aimed to elucidate the *in vivo* uptake of chitosan and polyethylene glycol (PEG) coated Poly, DL, lactic-*co*-glycolic Acid (PLGA) nanoparticles and the immunological response within 24 h of oral and peritoneal administration. These PLGA nanoparticles were administered orally and peritoneally to female Balb/C mice, they were taken up by macrophages of the peritoneum. When these particles were fluorescently labelled, intracellular localisation was observed. The expression of pro-inflammatory cytokines IL-2, IL-6, IL-12p70 and TNF-α in plasma and peritoneal lavage was found to remain at low concentration in PLGA nanoparticles treated mice as well as ZnO nanoparticles during the 24 hour period. However, these were significantly increased in lipopolysaccharide (LPS) treated mice. Of these pro-inflammatory cytokines, IL-6 and IL-12p70 were produced at the highest concentration in the positive control group. The anti-inflammatory cytokines IL-10 and chemokines INF-γ, IL-4, IL-5 remained at normal levels in PLGA treated mice. IL-10 and INF-γ were significantly increased in LPS treated mice. MCP-1 was found to be significantly produced in all groups in the first hours, except the saline treated mice. These results provide the first report to detail the induction of cytokine production by PLGA nanoparticles engineered for oral applications.

Introduction

Nanoparticles have to date been extensively used for various applications including drug delivery (Liversidge and Cundy, 1995; Duncan, 2005), tissue engineering (Langer, 2000) and imaging (Bruchez, 2005). Their physiochemical properties including their small size and large surface area have led to these advances. In drug delivery, they have been reported to significantly improve the bioavailability of drugs and minimise drug toxicity (Bawarski et al., 2008; Farokhzad and Langer, 2006; Langer, 2000), thus leading to more efficient therapies.

In drug delivery, the nano size range of particles is the 'holy grail' of efficient drug delivery, facilitating efficient uptake of the drugs via various uptake mechanisms (Jones et al., 2003). Intracellular uptake of the drugs is not very efficient with conventional formulations, albeit its necessity, primarily for drugs against intracellular microorganism. This shortfall is addressed by nanoparticulate drug delivery systems, where increased intracellular concentrations of drugs are observed when the drugs were nanoencapsulated (Kisich et al., 2007). The first cellular targets for nanoparticles are macrophages and dendritic cells (DC), which are professional antigen presenting cells that are at the fore front of the body's defence system. After engulfing foreign material, they mature to become active antigen presenting cells expressing specific maturation markers such as CD11c and MOMA-2 and others (Noti and Reinemann, 1995). In addition, when these cells are activated, they produce cytokines such as interleukin (IL)-1, IL-6, IL-8, IL-10, IL-18 and tumor necrosis factor alpha (TNF-α) and chemokines that attract other inflammatory cells to the site of inflammation (Anderson et al., 2008).

Since nanoparticles are foreign, their uptake may result in the release of the pro-inflammatory cytokines (Chang, 2010; Lee et al., 2009). The immunogenicity of synthetic polymers highly depended

* Corresponding author. Fax: +27 12 841 3553.
E-mail address: Bsemete@csir.co.za (B. Semete).
[1] These authors contributed equally to this work.

0041-008X/$ – see front matter © 2010 Elsevier Inc. All rights reserved.
doi:10.1016/j.taap.2010.09.002

on their size, shape, composition, surfactant properties, electrical charge and on the inherent ability of the host to recognise them. Furthermore, the oxidative potential of nanoparticles is another important parameter for evaluating their inflammatory or immunological responses. Synthetic polymers used in biological applications, such a drug delivery and tissue engineering, must therefore be biocompatible and biodegradable, i.e. their introduction into the body must not provoke a hazardous reaction (Kim et al., 2007; Rihova, 2002). Various groups are thus proposing studies that will measure the cell viability, inflammatory effects and biomedical effects of nanomaterials (Kim et al., 2007).

In this study we investigated the *in vivo* uptake of chitosan and polyethylene glycol (PEG) coated PLGA (referred to in this manuscript as PLGA nanoparticles) nanoparticles post oral administration. These particles are currently being explored for delivery of various compounds including antibiotics for the treatment of tuberculosis (TB). Furthermore, we analysed the *in vivo* immunological response to the uptake of these particles. This is the first study to analyse the uptake of PLGA nanoparticles *in vivo* and in conjunction evaluate the subsequent immune reaction by analysing the concentration profile of the secreted pro- and anti-inflammatory cytokines.

Materials and methods

Preparation of PLGA particles

Poly, DL, lactic-*co*-glycolic Acid (PLGA) 50:50 (Mw: 45,000–75,000), nanoparticles were prepared using a modified double emulsion solvent evaporation technique (Lamprecht et al., 1999). An aqueous phosphate buffer solution (PBS) pH 7.4 was emulsified for a short period with a solution of 100 mg PLGA dissolved in 8 ml of ethyl acetate (EA), by means of a high speed homogeniser (Silverson L4R) with a speed varying between 3000 and 5000 rpm. This water-in-oil (w/o) emulsion obtained was transferred into a specific volume of an aqueous solution of 1% w/v of the polyvinyl alcohol (PVA) (Mw: 13,000–23,000, partially hydrolysed (87–89%)) as a stabiliser. The mixture was further emulsified for 5 min by homogenisation at 5000 or 8000 rpm. These methods were carried out aseptically using a laminar airflow chamber. The double emulsion (w/o/w) obtained was directly fed into a bench top Buchi mini-spray dryer (Model B-290) and spray dried at a temperature ranging between 95 and 110 degrees Celsius (°C), with an atomizing pressure varying between 6 and 7 bars.

1% PEG was used in the formulation as an excipient to increase the *in vivo* residence time of nanoparticles in the blood stream (Torchilin and Trubetskoy, 1995). In order to enhance the uptake in the gastrointestinal tract, a mucoadhesive and positively charged ligand, chitosan was added in the formulation as recommended in previous reports (Cui et al., 2006; Takeuchi et al., 2005). 3% (volume/volume) chitosan was added to the formulation. Rhodamine 6G (Sigma, South Africa) labelled PLGA nanoparticles were prepared using the same method, where Rhodamine 6G was added in the aqueous phase of the emulsion.

Particle characterisation

Particle size, zeta potential and composition. Particle size and size distribution of PLGA and ZnO particles as well as polystyrene beads were measured by Dynamic Laser Scattering (DLS) or Photon Correlation Spectroscopy (PCS) using a Malvern Zetasizer Nano ZS (Malvern Instruments Ltd., UK). For each sample 1–3 mg of nanoparticles were suspended in filtered water (0.2 μm filter), then vortexed and/or sonicated for a few minutes. Each sample was measured in triplicate. The zeta potential was also determined using the same instrument. Surface morphology of PLGA nanoparticles was studied by scanning electron microscopy (LEO 1525 Field Emission SEM). The chitosan content in the PLGA particles was characterised via Fourier Transformed Infrared (FT-IR) using the PerkinElmer Spectrum 100 FT-IR Spectrometer.

Test for pyrogens in the particles. The PryoDetect System supplied by Biotest AG (Germany) was used for the analysis of pyrogen content in the PLGA, polystyrene and ZnO nanoparticles, according to the manufactures' instructions. Briefly, the particles were mixed with sterile cryo blood (provided with the kit) in a cell culture plate in triplicate and kept in a CO_2 incubator at 37 °C for 24 h. The test detects for IL-1B produced by blood monocytes in the presence of pyrogens. For the detection of IL-1B, the nanoparticle–blood mixture was transferred into an ELISA microplate coated with antibody specific for IL-1B and incubated for 2 h, then washed. IL-1B molecules present in the supernatant would then bind to the immobilised antibody. A horseradish peroxidase (HRP) labelled anti-human polyclonal antibody specific for IL-1B was added and incubated for 1 h and thereafter washed. A substrate provided with the kit was added and incubated at room temperature for 20 min resulting in a colour reaction and a stop solution added thereafter. The plate was then analysed at 450 nm on the BIO-TEK ELx800 plate reader. The standard curve was generated using a different concentration of the endotoxin standard provided with the kit. The data was analysed using the Combistats software programme and presented in Endotoxin Units per ml (EU/ml).

Animals. Unchallenged, healthy Balb/C male mice weighing 20–25 g were selected and housed under standard environment conditions at ambient temperature of 25 °C, and supplied with food and water *ad libitum*. Ethics approval was obtained from this study from the MRC Ethics Committee for Research on Animals (ECRA), Tygerberg, Cape Town, South Africa.

In vivo particle uptake. To evaluate particle uptake, saline was administered via the oral and intraperitoneal (i.p) routes respectively to mice as a negative control (Group 1) and 4% Brewers thioglycolate broth as a positive control (Group 2). A volume of 0.2 ml of 20 mg/ml Rhodamine 6G labelled nanoparticles was administered via the oral route once daily over five days (Group 3) and another group via the intraperitoneal route once only over the period of five days (Group 4). PLGA nanoparticles that were not fluorescently labelled were also administered at the same concentration to another group in a similar manner (Group 5).

This specific dose of PLGA was selected as it corresponds to the concentration of PLGA particles used in our research group for the administration of PLGA encapsulated anti-TB drugs, at a drug dose

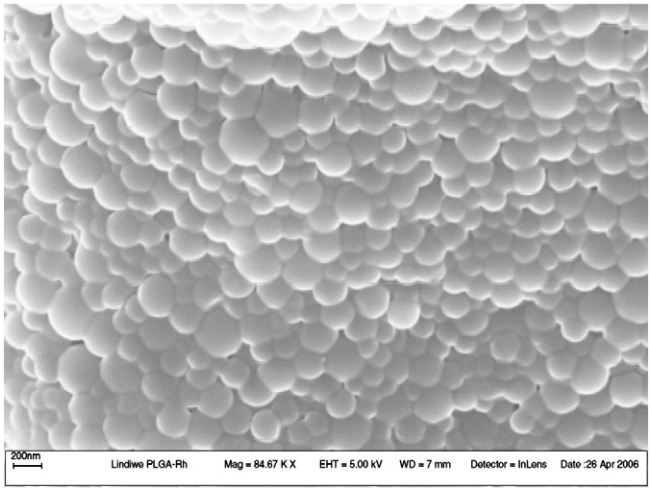

Fig. 1. SEM image of Rhodamine labelled PLGA nanoparticles.

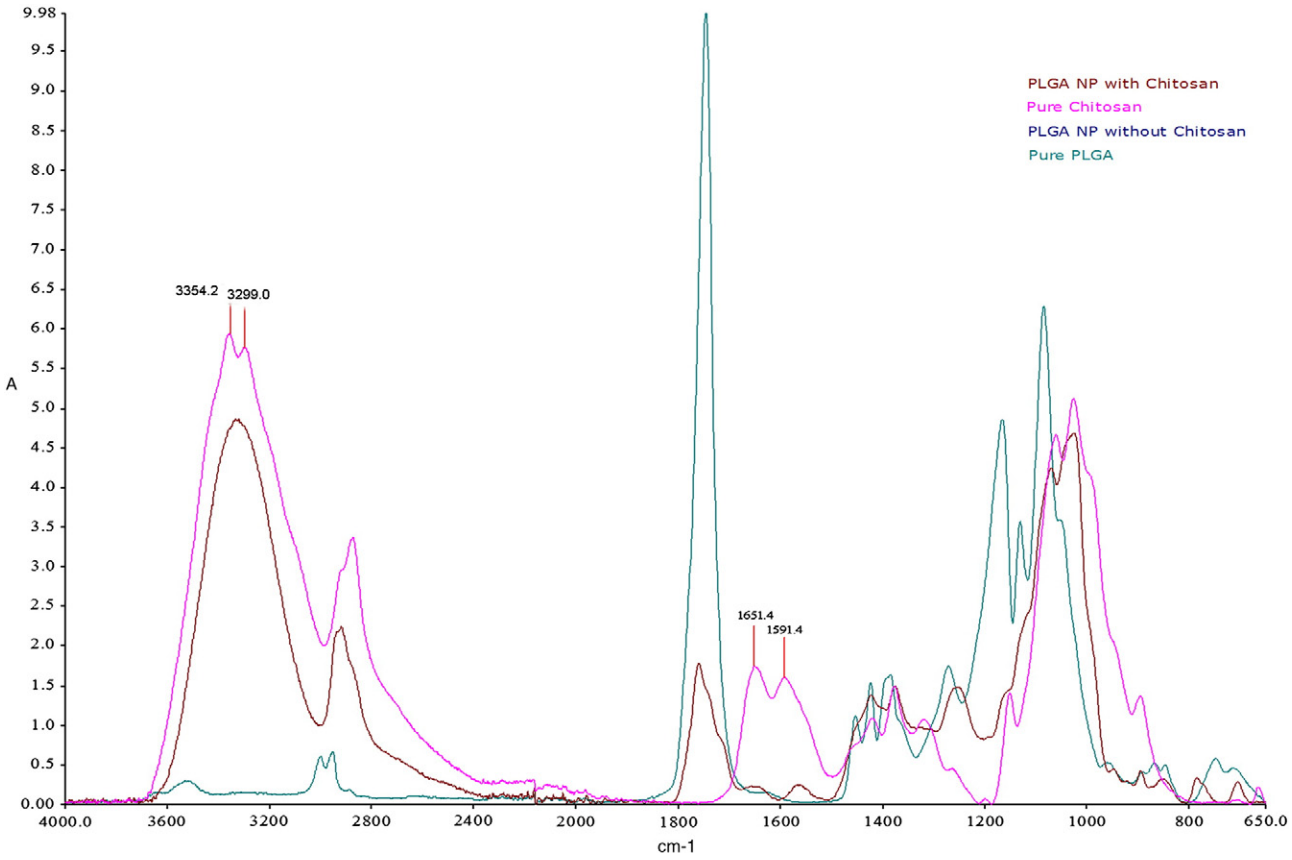

Fig. 2. FT-IR image of PLGA, chitosan and chitosan coated PLGA nanoparticles. The area under the curve for the peaks at 3354.2 and 3299.0 cm^{-1} as they are characteristic of the OH stretch was utilised for quantification of the chitosan content in the nanoparticles. The peaks at 1651.4 and 1591.4 cm^{-1} indicate the un-reacted NH bending of pure chitosan. A = absorbance.

which has proven to be efficacious (unpublished data). Thus, since this work forms part of that study, we maintained the same dose. Fluorescein-5-isothiocyanate (FITC) labelled polystyrene beads (0.2 μm, Sigma South Africa) were used as a control for uptake because they have a homogenous size distribution and they are well studied (Brown et al., 2001).

Peritoneal exudate cells (PECS) were collected from Balb/C mice subsequent to intraperitoneal or oral administration of the particles. Mice were sacrificed via cervical dislocation, and the PECS harvested by lavaging the peritoneal cavity with RPMI media. The harvested cells were counted using a haemocytometer and viability analysed via Trypan blue exclusion. The cells (1×10^6 cell/well) were cultured on 6-well plates in RPMI 1640 with 1% non-essential amino acid, 1% glutamine, 10% foetal bovine serum (FBS), Penicillin, (100 U/ml) and Streptomycin (100 μg/ml) for 2–3 h.

Fluorescently labelled monoclonal anti-mouse antibodies specific for phagocytic macrophages and dendritic cells, CD11c-Phycoerythrin (PE), and MOMA-FITC supplied by Beckman Coulter™ were utilised for the distinction of macrophage cells from the rest of the PECS population. The cells were incubated with the antibodies for 1 h. Extracellular particles and excess antibodies were washed off. The uptake of the particle by macrophages was analysed via fluorescence activated cell sorting (FACS) on the Beckman Coulter™ FC-500. Experiments were conducted in triplicate and repeated twice.

Cytokine production assay. To determine the acute immune response to nanoparticle exposure, particles were orally administered to mice. The supernatants from the peritoneal lavage as well as plasma were collected at 1, 2, 6, 8 and 24 h after exposure and utilised for determination of cytokine content. Lipopolysacharride (LPS, derived from *Salmonella enterica* serotype enteridis, was purchased from Sigma Aldrich, South Africa) at 20 mg/kg was used as a positive control of an inflammatory response due to its known ability to activate antigen presenting cells (Lee et al., 2009). Polystyrene beads that were not fluorescently labelled and of a similar size range to PLGA nanoparticles were used as a negative control. PLGA nanoparticles in a suspension of 20 mg/ml were administered in a volume of 0.2 ml. The same concentration was used for polystyrene beads. Spherical Zinc Oxide nanoparticles (ZnO nanopowder was supplied by Sigma Aldrich South Africa with an average particle size of 100 nm and a range of 50–150 nm) which have been reported to result in *in vitro* toxicity in cell lines (Lee et al., 2009) were included to represent metal based nanoparticles. Although the ZnO nanoparticle size was provided by the supplier, it was also analysed via DLS using the Malvern Zetasizer Nano ZS (Malvern Instruments Ltd., UK). Using ZnO nanoparticles would provide a comparison of biodegradable and biocompatible polymer based (PLGA) nanoparticles and metal based nanoparticles. ZnO nanoparticles were administered at 4 mg/0.2 ml saline (i.e. 20 mg/ml). The Mouse TH1/TH2 Kit (BD Biosciences) was utilised on the BD FACSarray™ for the detection of IL-4, IL-2, TNF-α and Interferon γ (INF-γ). IL-5, IL-6, IL-10, monocyte chemotactic protein (MCP-1) and IL-12p70 were analysed via the Mouse Inflammation Kit from BD Biosciences (Morgan et al., 2004). Cytokine concentrations were determined by the reference standard curves based on standards that were supplied with the kits. The cytokine data were analysed using the FCAP array™ v1.0 software and expressed as picograms per millilitre (pg/ml) of the mean of the triplicate and repeats.

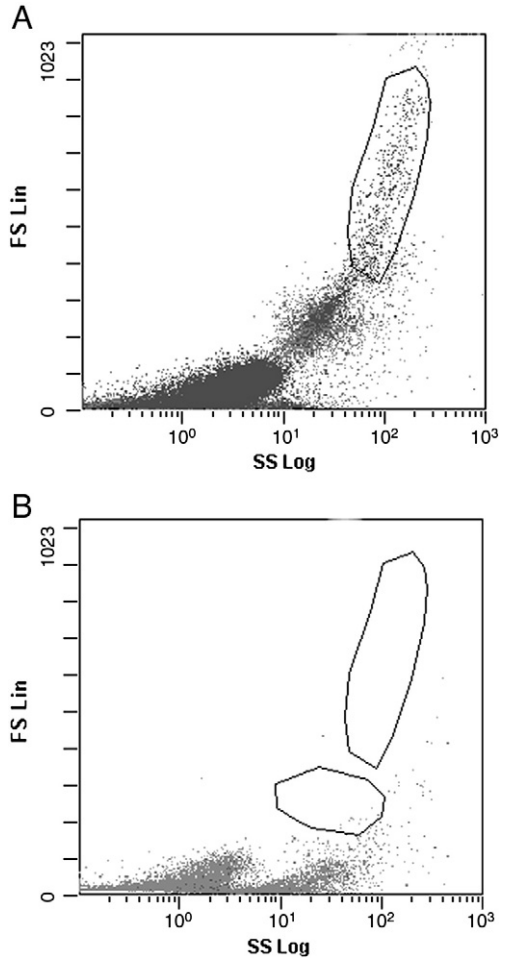

Fig. 3. FS/SS plot of peritoneal exudate cells after FACS analysis. The x-axis indicates the side scatter and the y-axis indicates the forward scatter. A = peritoneal exudate cells subsequent to thioglycolate administration to mice. B = peritoneal exudate cells subsequent to saline administration to mice.

Results

Particle characterisation

Various parameters were optimized to obtain an average particle size for PLGA ranging between 250 and 350 nm and an average polydispersity index (PDI) of 0.2. The use of a stabiliser, i.e. PVA, led to well distributed and uniform PLGA nanoparticles with an average size around 300 nm, characterised by a very smooth surface as depicted by the SEM image in Fig. 1. The particles had a zeta potential of −11 mV. It has been reported that small size (less than 500 nm) and a spherical shape give rise to an enhanced efficiency of cell internalization (Jani, 1990) and that spherical particles possess the right curvature allowing attachment onto the cells (Trewyn et al., 2008). It is generally accepted that spherical particles offer maximum volume for drug incorporation.

Based on the area under the curve from the peak at 3354.2 and 3299.0 cm^{-1} generated from the FT-IR image of the particles as depicted in Fig. 2, coating with chitosan was efficient, with approximately 2.8% chitosan on the surface of the particles from the initial 3% which was added in the formulation. 1% PEG was included in the preparation of PLGA nanoparticles. Since PEG has a similar composition to PVA which is also in the formulation, characterisation thereof would not be accurate. It was thus presupposed based on the loss chitosan in the formulation that the particles were coated with 0.9% PEG. ZnO nanoparticles presented with an average size of 110 nm with a range of 50–150 nm. Polystyrene beads had an average size of 200 nm, with a PDI of 0.1.

Pyrogen test of the particles

The PLGA particles presented with average EU/ml of 0.38 ± 0.18 at 0.5 mg/ml, 0.58 ± 0.12 at 2× dilution and 0.90 ± 0.11 at 4× dilution. ZnO nanoparticles presented with average EU/ml of 0.398 ± 0.08 at 0.5 mg/ml, at 2× dilution 0.247 ± 0.11 and at 4× dilution 0.258 ± 0.09. Polystyrene beads at 0.5 ml/ml had an average EU/ml of 0.4 ± 0.15, at 2× dilution 0.27 ± 0.21 and at 4× dilution 0.21 ± 0.18. Based on the pyrogen test data no pyrogens were present in either of the particles analysed since the average EU/ml detected was below the contaminant limit concentration (CLC) of 2.63 EU/ml as per the protocol provided with the kit. This kit detects for both Gram negative and positive bacteria components as well as yeast and moulds. Thus, it can be said based on these results that the particles were free of any these contaminants.

In vivo particle uptake

Various studies have been reported where particle uptake was observed *in vitro* (Yoshida et al., 2006; Kisich et al., 2007). However, this specific study presents data illustrating *in vivo* particle uptake, by macrophage cells of the peritoneal exudates cells. Initially macrophages were characterised from the subpopulation of PECS as indicated in Fig. 3A using thioglycolate broth induced macrophage proliferation as a positive control. Anti-CD11c and MOMA-2 antibodies were used to characterise these cells. In general macrophages are large in size and also granular, thus they were detected in the higher populations of the forward and side scatter as observed in Fig. 3A. In the saline treated group no activated macrophages were detected in the gated channel as depicted in Fig. 3B.

When FITC labelled polystyrene beads were administered intraperitoneally and orally to mice and the peritoneal exudate cells analysed for particle uptake, an increase in fluorescence intensity in the gated channel for macrophages was observed as indicated in Fig. 4. This result complements data from Olivier et al. (2004) where the *in vitro* uptake of polystyrene beads was observed. The high forward scattering (FS) indicates the large size of the cells and the increase in the FL3 indicates the intensity of the fluorescent label, FITC. Thus, indicating that the macrophage cell population has taken up the fluorescent beads.

The analysis of PECS subsequent to intraperitoneal and oral administration of PLGA nanoparticles indicated that peritoneal macrophages did take up the particle as indicated in Fig. 5 compared

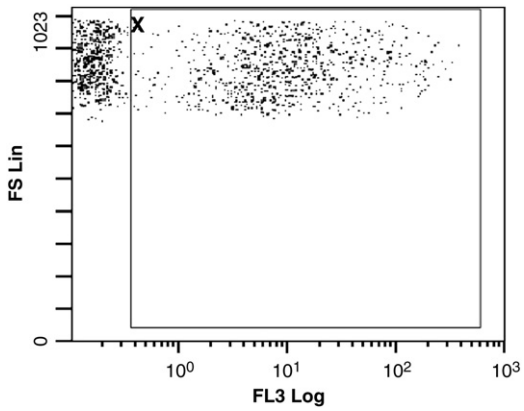

Fig. 4. FACS data of PECS subsequent to administration of polystyrene beads to mice. The x-axis indicates the fluorescent label for FITC and the y-axis indicates the forward scatter.

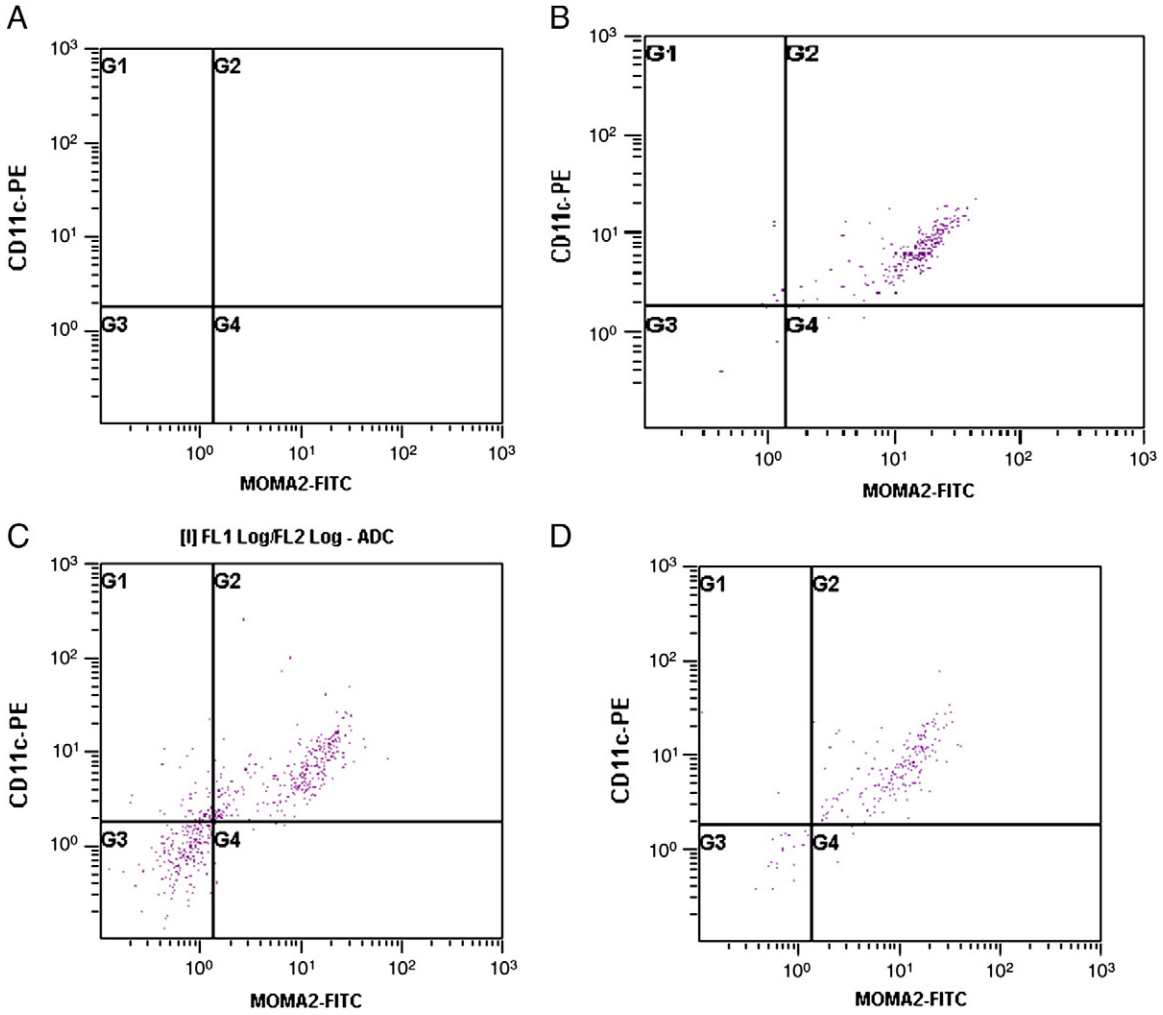

Fig. 5. Uptake of PLGA nanoparticles measured by FACS. A = negative control, where mice were treated with saline only. B = indicates positive control where mice were treated with thioglycolate. C = indicates macrophage cells subsequent to intraperitoneal administration and D = indicates post oral administration of PLGA particles.

to the negative control. A positive signal for both anti-CD11c and anti MOMA-2 was observed in the G2 quadrants of the positive control and the experimental group.

To further confirm that uptake of the particles by macrophages of the peritoneal did occur and that the macrophage population detected did not merely consist of activated monocytes that had not phagocytosed the nanoparticles, Rhodamine 6G labelled particles were administered intraperitoneally to mice. The detection was specific for the Rhodamine 6G fluorescence at excitation 525 nm and emission 555 nm, as depicted in Fig. 6 FS indicates the large cells and FL3 indicates the Rhodamine 6G fluorescence intensity. Thus similar to the FITC labelled polystyrene beads, these results illustrate that macrophages (high FS) have taken up the Rhodamine 6G labelled PLGA particles as indicated by the increase in FL3.

From this data, it can be suggested that PLGA particles are taken up *in vivo* by macrophages, and thus intracellular delivery can be achieved. The markers used, i.e. anti-CD11c and MOMA-2 allowed for the detection of macrophages within a population of peritoneal exudate cells. These markers thus represent phagocytotic macrophages which will thus function as antigen presenting cells. This hypothesis was further determined by analysing the cytokine production profile in PLGA treated mice. The particle uptake was further indicated by a population of macrophages that were positive for the Rhodamine 6G labelled particles. Although uptake of particles by macrophages has previously been reported (Ahsan et al., 2002; Olivier et al., 2004), much of the research has been conducted *in vitro.* With this approach, we were able to illustrate that subsequent to intraperitoneal and oral administration of PLGA nanoparticles of the reported size range, particle uptake by the macrophages of the peritoneum was observed. In our previous study (Semete et al., 2010)

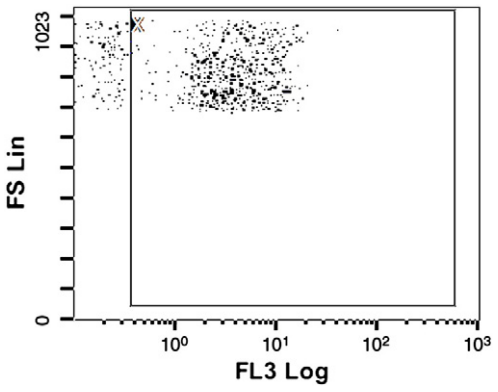

Fig. 6. Uptake of Rhodamine 6G labelled particles analysed by FACS. Data of PECS subsequent to i.p administration of Rhodamine 6G labelled nanoparticles to mice. The x-axis indicates the fluorescent label for Rhodamine and the y-axis indicates the forward scatter.

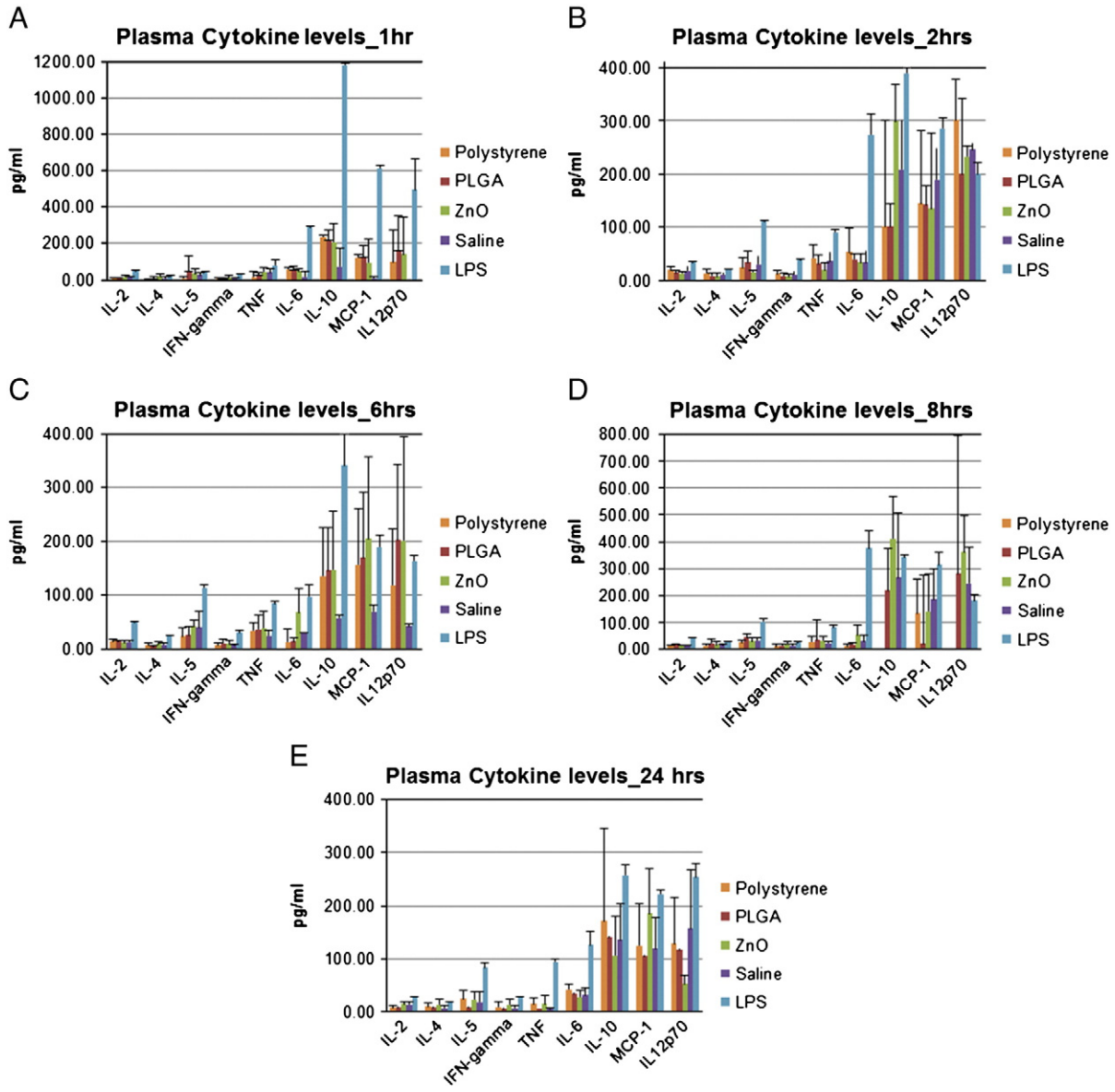

Fig. 7. Cytokine production profile in plasma post oral administration of particles.

we illustrated how oral administration of the particles resulted in biodistribution of these particles to various tissues, thus indicating that these particles migrate from the gastrointestinal tract.

Cytokine production

To determine whether PLGA nanoparticles elicit an acute immunological response during the activation of monocytes to macrophages followed by the uptake of the particles, the secretions of pro-inflammatory cytokines IL-2, IL-6, IL-12 and TNF-α together with anti-inflammatory cytokines IL-10 and chemokines INF-γ, IL-4, IL-5, and MCP-1 were analysed. The mice were treated as described. At the PLGA dose administered, i.e. 4 mg/0.2 ml saline, the expression of pro-inflammatory cytokines was found to be within similar production ranges to that of saline, polystyrene nanoparticles in both plasma and peritoneal lavage as depicted in Figs. 7 and 8 respectively. This observation was maintained over the time frame of analysis, i.e. 24 h. ZnO nanoparticles also presented with the same observation at the dose administered. However, LPS treated mice presented with increased production of these cytokines within the first hour of analysis, typical of an immune active substance. This was most prominent with IL-10: A 6 fold increase in the expression of IL-10 was observed within the first hour of LPS exposure. This may follow from the fact that the mode of administration was oral and IL-10 is a prominent immunoregulator in the intestinal tract. The production of IL-10 decreased with time in plasma, although it was maintained quite high in the peritoneal lavage for a longer period of time.

The concentration of MCP-1 in the polystyrene, ZnO and PLGA nanoparticles was variable compared to saline treated mice in the first hours in both the plasma and lavage, but did not maintain an enduring response over 24 h like LPS induced. The variable response could relate to the monocytes that were transiently activated to macrophages resulting from particle uptake and possibly some chemotaxis of cells such as the neutrophils, known to be attracted to sites where phagocytosis activity occurs. A study by Semete et al. (2010), indicated PLGA particle localisation occurring in various tissues including the liver, thus this variable MCP-1 secretion could be as a function of a localised chemotaxis at the tissues where particles are observed. LPS treated mice consistently presented with much higher

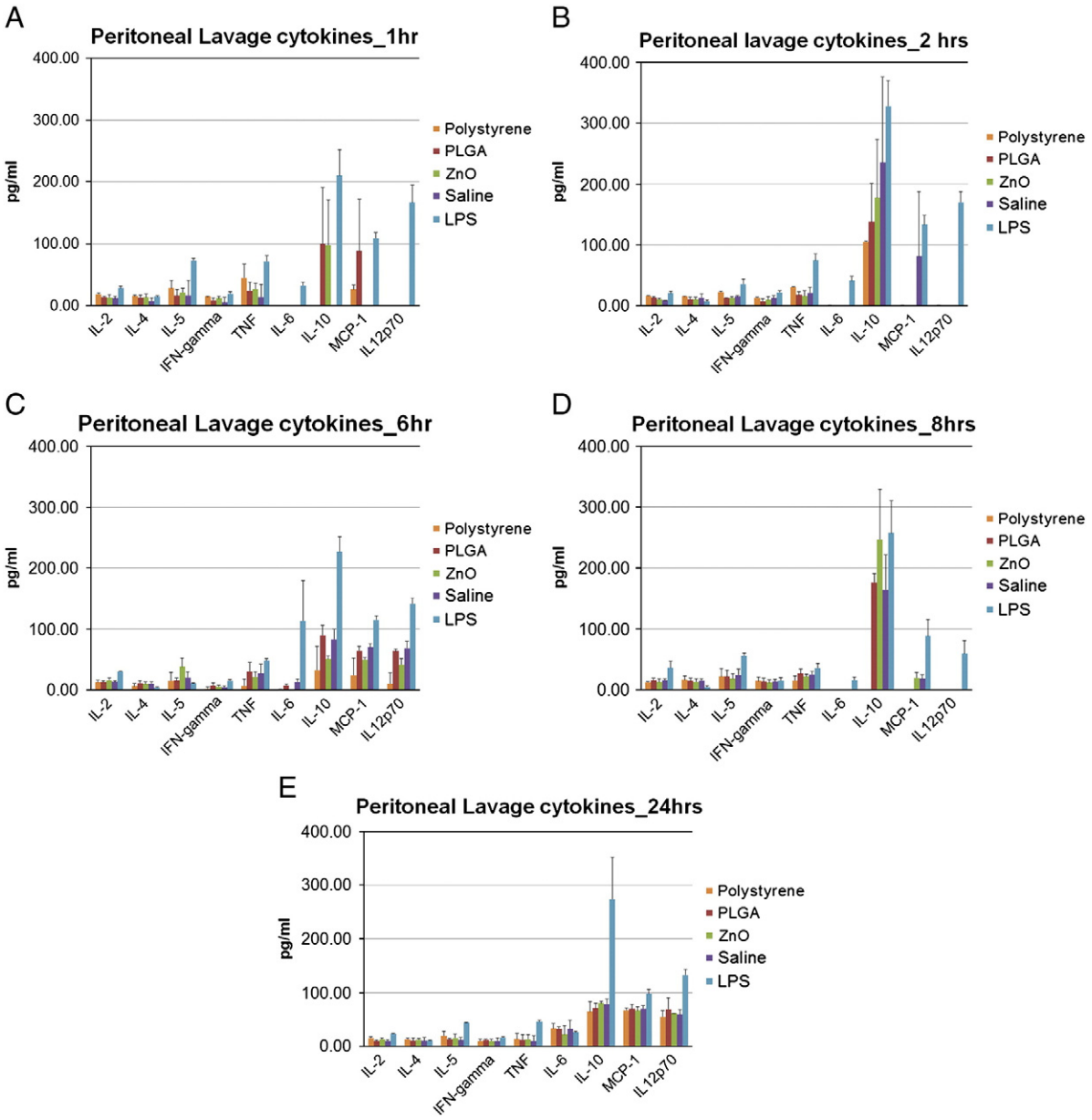

Fig. 8. Cytokine production profile in peritoneal lavage post oral administration of particles.

concentrations of MCP-1 sustained over the full 24 h of observation. IL-12 responded strongly and sustainable to LPS in especially the peritoneal lavage, compared to the PLGA and polystyrene particles. In plasma this effect was less visible. This strong inflammatory cytokine is secreted by all phagocytosing cells, but strongly in the case of inflammatory agents like LPS. The low, transient IL-12 response by the particles confirms the absence of any significant inflammatory activity associated with them.

Low levels of IL-4 were detected in both plasma and lavage throughout the time of analysis in all the treated groups. This argues against an allergic type response by any of the particles as well as LPS. The concentrations of IL-4 observed in the LPS treated mice were not as high as those reported by Lee et al. (2009). However, although Lee et al. (2009) administered LPS at the same concentration as in this study, it was by injection and not oral administration and therefore not strictly comparable.

The expression of TNF-α, IL-6 and IL-5 in LPS treated mice was significantly higher than that of PLGA, polystyrene and saline treated mice, both in the plasma and in the peritoneal lavage. The difference was also noted in nanoparticles treated mice suggesting that at the concentrations used i.e. 4 mg/0.2 ml, even ZnO based nanoparticles do not cause immunological response, thus suggestive of a dose dependent effect. A summary of the cytokines release profile for all the groups is presented in Table 1. Combined, all these results argue against an immunological contra-indication for the oral administration of PLGA particles in mice.

Discussion

At this specific size and composition of the nanoparticles, it can be concluded that chitosan and PEG coated PLGA nanoparticles are efficiently taken up by macrophage cells of the peritoneal exudate cells. Particle uptake by blood monocytes or other cells of the immune systems such as dendritric cells cannot be excluded. This observation indicates that intracellular delivery of compounds against intracellular pathogens will be feasible. The size of the particles, (low negative) zeta potential and their physicochemical properties all facilitated the observed intracellular uptake.

Table 1
Summary of cytokine production profile across the groups.

Cytokine	LPS (20 mg/kg)	ZnO (20 mg/ml)	Polystyrene (20 mg/ml)	PLGA (20 mg/ml)	Saline
IL-2	↑(Small increase)	↔	↔	↔	↔
IL-4	↑(Small increase)	↔	↔	↔	↔
IL-5	↑(Small increase)	↔	↔	↔	↔
INF-γ	↑(Small increase)	↔	↔	↔	↔
TNF-α	↑(Significant increase)	↔	↔	↔	↔
IL-6	↑(Significant increase)	↔	↔	↔	↔
IL-10	↑(Significant increase)	↑	↑	↑	↔
MCP-1	↑(Significant increase)	↑	↑	↑	↔
IL-12p70	↑(Significant increase)	↔	↔	↔	↔

↑ = increase; ↔ = remain at similar levels to saline group.

There are a large number of *in vitro* studies on nanoparticulate cytotoxicity with various types of engineered nanoparticles (Suh et al., 2009). Some reports indicate the possibility of ultrafine particles acting as adjuvants to enhance inflammatory responses and improve release of pro-inflammatory mediators by macrophages. However, more information is needed about the potential effects of biodegradable and biocompatible nanoparticles versus those of metal oxide particles *in vivo* to determine whether the observed *in vitro* cytotoxicity and inflammatory response is physiologically relevant (Cho et al., 2009; Palomäki et al., 2010). The inability to elicit a significant effect of the immune response does not mean that PLGA particles are completely inert from the immunological point of view. As polyesters in nature, PLGA undergoes hydrolysis and enzymatic degradation upon implantation into the body, forming biologically compatible moieties that can be metabolised (lactic acid and glycolic acid) and are eventually removed from the body by the citric acid cycle (Campbell, 1995). These PLGA biodegradation products are formed at a very slow rate, and hence they do not affect the normal cell function.

Olivier et al. (2004) observed some toxicity when polystyrene beads were analysed *in vitro* in J774.2 macrophages and L929 fibroblasts. A composition dependent effect was also observed where, as reported in our previous study, high doses of PLGA did not lead to any tissue lesions as compared to the same high dose of ZnO nanoparticles that led to toxicity in mice. This study illustrates the safety of using PLGA nanoparticles for drug delivery applications and further complements our previous study (Semete et al., 2010) where using various other parameters, the safety of PLGA nanoparticles was illustrated.

Acknowledgments

This research was supported by funding from the South African Department of Science and Technology. We would like to thank Karolina Kuun from BD Bioscience, SA and Dr Chrisna Durandt from Beckman Coulter, SA for their technical assistance with the respective equipment. Thank you to Saloshnee Naidoo and Patrick Nkuna from the CSIR (Polymers and Composites) for assistance with the analysis of the chitosan content in the particles.

References

Ahsan, F., Rivas, I.P., Khan, M.A., Torres Suárez, A.I., 2002. Targeting to macrophages: role of physicochemical properties of particulate carriers–liposomes and microspheres–on the phagocytosis by macrophages. J. Control. Release 79, 29–40.
Anderson, J.M., Rodriguez, A., Chang, D.T., 2008. Foreign body reaction to biomaterials. Semin. Immunol. 20, 86–100.
Bawarski, W.E., Chidlowsky, E., Bharali, D.J., Mousa, S.A., 2008. Emerging nanopharmaceuticals. Nanomed. Nanotechnol. Biol. Med. 4, 273–282.
Brown, D.M., Wilson, M.R., MacNee, W., Stone, V., Donaldson, K., 2001. Size-dependent proinflammatory effects of ultrafine polystyrene particles: a role for surface area and oxidative stress in the enhanced activity of ultrafines. Toxicol. Appl. Pharmacol. 175, 191–199.
Campbell, 1995. Biochemistry. Saunders College Publishing, pp. 365–384.
Chang, C., 2010. The immune effects of naturally occurring and synthetic nanoparticles. J. Autoimmun. 34, J234–J246.
Cho, W.S., Cho, M., Jeong, J., Choi, M., Cho, H.Y., Han, B.S., Kim, S.H., Kim, H.O., Lim, Y.T., Chung, B.H., Jeong, J., 2009. Acute toxicity and pharmacokinetics of 13 nm-sized PEG-coated gold nanoparticles. Toxicol. Appl. Pharmacol. 236, 16–24.
Cui, F., Qian, F., Yin, C., 2006. Preparation and characterization of mucoadhesive polymer-coated nanoparticles. Int. J. Pharm. 316, 154–161.
Duncan, R., 2005. Nanomedicine gets clinical. Mater. Today 8, 16–17.
Farokhzad, O.C., Langer, R., 2006. Nanomedicine: developing smarter therapeutic and diagnostic modalities. Adv. Drug Deliv. Rev. 58, 1456–1459.
Jani, P., 1990. Nanoparticle uptake by the rat gastrointestinal mucosa: quantitation and particle size dependency. J. Pharm. Pharmacol. 42, 821–826.
Jones, A.T., Gumbleton, M., Duncan, R., 2003. Understanding endocytic pathways and intracellular trafficking: a prerequisite for effective design of advanced drug delivery systems. Adv. Drug Deliv. Rev. 55, 1353–1357.
Kim, S.B., Ozawa, T., Tao, H., Umezawa, Y., 2007. A proinflammatory cytokine sensor cell for assaying inflammatory activities of nanoparticles. Anal. Biochem. 362, 148–150.
Kisich, K.O., Gelperina, S., Higgins, M.P., Wilson, S., Shipulo, E., Oganesyan, E., Heifets, L., 2007. Encapsulation of moxifloxacin within poly(butyl cyanoacrylate) nanoparticles enhances efficacy against intracellular *Mycobacterium tuberculosis*. Int. J. Pharm. 345, 154–162.
Lamprecht, A., Ubrich, N., Hombreiro Perez, M., Lehr, C.-M., Hoffman, M., Maincent, P., 1999. Biodegradable monodispersed nanoparticles prepared by pressure homogenization–emulsification. Int. J. Pharm. 184, 97–105.
Langer, R., 2000. Biomaterials in drug delivery and tissue engineering: one laboratory's experience. Acc. Chem. Res. 33, 94–101.
Lee, H.M., Shin, D.M., Song, H.M., Yuk, J.M., Lee, Z.W., Lee, S.H., Hwang, S.M., Kim, J.M., Lee, C.S., Jo, E.K., 2009. Nanoparticles up-regulate tumor necrosis factor-[alpha] and CXCL8 via reactive oxygen species and mitogen-activated protein kinase activation. Toxicol. Appl. Pharmacol. 238, 160–169.
Liversidge, G.G., Cundy, K.C., 1995. Particle size reduction for improvement of oral bioavailability of hydrophobic drugs: I. absolute oral bioavailability of nanocrystalline danazol in beagle dogs. Int. J. Pharm. 125, 91–97.
Morgan, E., Varro, R., Sepulveda, H., Ember, J.A., Apgar, J., Wilson, J., Lowe, L., Chen, R., Shivraj, L., Agadir, A., Campos, R., Ernst, D., Gaur, A., 2004. Cytometric bead array: a multiplexed assay platform with applications in various areas of biology. Clin. Immunol. 110, 252–266.
Noti, J.D., Reinemann, B.C., 1995. The leukocyte integrin gene CD11c is transcriptionally regulated during monocyte differentiation. Mol. Immunol. 32, 361–369.
Olivier, V., Rivière, C., Hindié, M., Duval, J.-L., Bomila-Koradjim, G., Nagel, M.-D., 2004. Uptake of polystyrene beads bearing functional groups by macrophages and fibroblasts. Colloids Surf., B 33, 23–31.
Palomäki, J., Karisola, P., Pylkkänen, L., Savolainen, K., Alenius, H., 2010. Engineered nanomaterials cause cytotoxicity and activation on mouse antigen presenting cells. Toxicology 267, 125–131.
Rihova, B., 2002. Immunomodulating activities of soluble synthetic polymer-bound drugs. Adv. Drug Deliv. Rev. 54, 653–674.
Semete, B., Booysen, L., Lemmer, Y., Kalombo, L., Katata, L., Verschoor, J., Swai, H.S., 2010. In vivo evaluation of the biodistribution and safety of PLGA nanoparticles as drug delivery systems. Nanomedicine: Nanotechnology, Biology and Medicine 6, 662–671.
Suh, W.H., Suslick, K.S., Stucky, G.D., Suh, Y.H., 2009. Nanotechnology, nanotoxicology, and neuroscience. Prog. Neurobiol. 87, 133–170.
Takeuchi, H., Thongborisute, J., Matsui, Y., Sugihara, H., Yamamoto, H., Kawashima, Y., 2005. Novel mucoadhesion tests for polymers and polymer-coated particles to design optimal mucoadhesive drug delivery systems. Adv. Drug Deliv. Rev. 57, 1583–1594.
Torchilin, V.P., Trubetskoy, V.S., 1995. Which polymers can make nanoparticulate drug carriers long-circulating? Adv. Drug Deliv. Rev. 16, 141–155.
Trewyn, B.G., Nieweg, J.A., Zhao, Y., Lin, V.S.Y., 2008. Biocompatible mesoporous silica nanoparticles with different morphologies for animal cell membrane penetration. Chem. Eng. J. 137, 23–29.
Yoshida, A., Matumoto, M., Hshizume, H., Oba, Y., Tomishige, T., Inagawa, H., Kohchi, C., Hino, M., Ito, F., Tomoda, K., Nakajima, T., Makino, K., Terada, H., Hori, H., Soma, G.I., 2006. Selective delivery of rifampicin incorporated into poly(dl-lactic-co-glycolic) acid microspheres after phagocytotic uptake by alveolar macrophages, and the killing effect against intracellular *Mycobacterium bovis* Calmette–Guérin. Microbes Infect. 8, 2484–2491.

BASIC SCIENCE

Nanomedicine: Nanotechnology, Biology, and Medicine 6 (2010) 662–671

nanomedicine

www.nanomedjournal.com

Original Article

In vivo evaluation of the biodistribution and safety of PLGA nanoparticles as drug delivery systems

Boitumelo Semete, PhD[a,*], Laetitia Booysen, MSc[a,b], Yolandy Lemmer, MSc[a,c], Lonji Kalombo, MSc[a], Lebogang Katata, PhD[a], Jan Verschoor, PhD[c], Hulda S. Swai, PhD[a]

[a]*Council of Scientific and Industrial Research, Polymers and Bioceramics, Pretoria, South Africa*
[b]*Department of Pharmaceutics, North-West University, Potchefstroom Campus, Potchefstroom, South Africa*
[c]*Department of Biochemistry, University of Pretoria, Pretoria, South Africa*

Received 14 August 2009; accepted 28 February 2010

Abstract

The remarkable physicochemical properties of particles in the nanometer range have been proven to address many challenges in the field of science. However, the possible toxic effects of these particles have raised some concerns. The aim of this article is to evaluate the effects of poly(lactide-co-glycolide) (PLGA) nanoparticles in vitro and in vivo compared to industrial nanoparticles of a similar size range such as zinc oxide, ferrous oxide, and fumed silica. An in vitro cytotoxicity study was conducted to assess the cell viability following exposure to PLGA nanoparticles. Viability was determined by means of a WST assay, wherein cell viability of greater than 75% was observed for both PLGA and amorphous fumed silica particles and ferrous oxide, but was significantly reduced for zinc oxide particles. In vivo toxicity assays were performed via histopathological evaluation, and no specific anatomical pathological changes or tissue damage was observed in the tissues of Balb/C mice. The extent of tissue distribution and retention following oral administration of PLGA particles was analyzed for 7 days. After 7 days, the particles remained detectable in the brain, heart, kidney, liver, lungs, and spleen. The results show that a mean percentage (40.04%) of the particles were localized in the liver, 25.97% in the kidney, and 12.86% in the brain. The lowest percentage was observed in the spleen. Thus, based on these assays, it can be concluded that the toxic effects observed with various industrial nanoparticles will not be observed with particles made of synthetic polymers such as PLGA when applied in the field of nanomedicine. Furthermore, the biodistribution of the particles warrants surface modification of the particles to avoid higher particle localization in the liver.

From the Clinical Editor: The aim of this study was to evaluate the effects of poly(lactide-co-glycolide) (PLGA) nanoparticles in vitro and in vivo compared to industrial nanoparticles including zinc oxide, ferrous oxide, and fumed silica. The authors concluded that the toxic effects observed with various industrial nanoparticles is unlikely to be observed with particles made of PLGA. The biodistribution of these particles warrants surface modification to avoid particle accumulation in the liver.

Key words: Nanoparticles; Nanomedicine; PLGA; Biodistribution; Toxicity

Nanotechnology has become one of the critical research endeavors of the 21st century; thus, researchers must intensify their efforts to further understand the potential effects of these materials on biological systems. Materials on a nanometer scale have unique physicochemical properties that are due to their small size, surface area, chemical composition, surface structure, solubility, and shape[1]; these properties have thus far been utilized in various fields including drug and gene delivery, imaging, and diagnostics.[2-4]

Much work in elucidating the possible effects of nanomaterial has been conducted on metal nanoparticles. This is primarily due to the rapid increase in the production of these materials, fueled by the growing need for the properties that these materials provide. Particle toxicity has been studied over a fair number of years, particularly in lung injury in the case of metal nanoparticles, ambient ultrafine particles, asbestos fibers, and dust particles.[3,5] Various reports have indicated that these particles induce oxidative injury, inflammation, fibrosis, and cytotoxicity.[3,6,7] It has been reported that smaller particles (aerodynamic diameter <100 nm) have a greater propensity to lead to pulmonary toxicity owing to their small size, larger

No conflict of interest was reported by the authors of this paper.

*Corresponding author: Council for Scientific and Industrial Research, Polymers and Bioceramics, P.O. Box 395, Pretoria 0001, South Africa.
E-mail address: Bsemete@csir.co.za (B. Semete).

1549-9634/$ – see front matter © 2010 Elsevier Inc. All rights reserved.
doi:10.1016/j.nano.2010.02.002

surface area, and deeper penetration into the lungs than bulkier particles of the same material.[3]

However, with regard to nanomedicine, the adverse effects of the particles have not been extensively studied, possibly because in nanomedicine, mainly biodegradable, biocompatible, and U.S. Food and Drug Administration–approved materials are used.[2,8] However, concerns over the effects of the physicochemical properties of nanoparticles such as size, surface area, and molecular weight of the material warrants further investigation.

It has been speculated that the specific surface area of nanoparticles is responsible for the potential adverse effects that nanoparticles could have in drug delivery applications.[3] This is because smaller particle size increases the specific surface area, thus exposing more atoms or molecules (and thus more reactive groups of the material) on the surface to molecules that would not have access to larger particles.[9] This aspect could form the basis of the production of reactive oxygen species, wherein the electron donor or acceptor sites on the nanomaterial interact with molecular oxygen, resulting in the formation of superoxide anion or hydrogen peroxide, which subsequently oxidize other chemical species by an electron transfer mechanism. The production of reactive oxygen species has been reported as the most likely mechanism by which these particles exert a toxic effect.[3] Therefore, the specific surface area is an important parameter to consider when elucidating the possible adverse effects of a nanomaterial. For efficient drug delivery, the nanosize range of particles is the "holy grail", because it can facilitate increased intracellular uptake of the drugs to specific cellular targets—a process that is not very efficient in conventional formulations. This, in turn, improves the bioavailability of therapeutic compounds.[4,10] As suggested by various studies on ultrafine particles,[5,7] this beneficial property of nanoparticles' ability to be taken up intracellularly could also be a source of concern, given that the nanosize range of the particles enables unique interaction with biological materials such as key proteins in the cellular pathways, which could possibly culminate in adverse effects.[6]

With the above-mentioned uncertainties about the potential effects of specific surface area, size, and composition of polymeric nanoparticles in mind, our team focused on elucidating the effect of poly(lactide-co-glycolide) (PLGA) nanoparticles, as well as particles composed of ferrous oxide (Fe_2O_3), zinc oxide (ZnO), and fumed silica (SiO_2) on cell viability. Also studied was the effect of PLGA nanoparticles and ZnO particles on various tissues after oral administration. Various reports have indicated that the oral route of drug delivery is still the preferred route and will dominate the drug delivery market for decades to come.[11] Hence, for the purpose of the study we explored the effect of these particles when administered orally to Balb/C mice.

In addition, the nanosize range of nanoparticles has been reported to facilitate the crossing of various biological barriers such as the blood-brain barrier (BBB), the skin, and the tight junctions of various epithelial layers.[12] Thus, we further explored the tissue distribution of PLGA particles after oral administration to determine to which tissues these particles localize.

Methods

Preparation of PLGA particles

Nanoparticles were prepared with poly(dl-lactide-co-glycolide (PLG) 50:50 (molecular weight 45,000–75,000) (Sigma-Aldrich, Johannesburg, South Africa) using a modified double-emulsion solvent evaporation technique.[13] Aqueous phosphate-buffered saline pH 7.4 was emulsified for a short period with a solution of 100 mg PLGA dissolved in 8 mL of ethyl acetate (EA), by means of a high-speed homogenizer (Silverson L4R, Silverson Machines Limited, Buckinghamshire, United Kingdom) with a speed varying between 3000 and 5000 rpm. The resulting water-in-oil (w/o) emulsion was transferred into a specific volume of an aqueous solution of 1% (wt/vol) polyvinyl alcohol (molecular weight 13,000–23,000 and partially hydrolyzed: 87–89%) used as an emulsion stabilizer, also purchased from Sigma-Aldrich. The mixture was further emulsified for 5 minutes by homogenization at 8000 rpm. The double emulsion (w/o/w) obtained was directly fed into a benchtop Buchi mini-spray dryer (Model B-290, BÜCHI Labortechnik AG, Flawil, Switzerland) and spray-dried at a temperature ranging between 95° and 110°C, with an atomizing pressure varying between 5 and 8 bars.

To prepare fluorescently labeled PLGA nanoparticles, Rhodamine-6G (Sigma-Aldrich) was dissolved in 2.5 mL EA (0.5 mg/mL), which was added to the solution of PLGA in EA. In cases wherein the particles were labeled with coumarin (Sigma-Aldrich), it was also dissolved in 2.5 mL EA at 0.5 mg/mL. For the preparation of these fluorescently labeled particles, the w/o/w emulsion was left overnight to allow evaporation of the solvent. The pellet recovered after centrifugation was then lyophilized using the Virtis Benchtop freeze dryer (SP Industries, Gardiner, New York). Spray-drying was also applied. The results presented in this article are from the spray-dried formulation, because this method proved to be easier to scale up for the application of these nanoparticles.

Particle size, zeta potential, and surface morphology

Particle size and size distribution were measured by dynamic laser scattering or photon correlation spectroscopy using a Malvern Zetasizer Nano ZS (Malvern Instruments, Worcestershire, United Kingdom). For each sample, 1–3 mg of nanoparticles were suspended in distilled water, then vortexed and/or sonicated for a few minutes. Each sample was measured in triplicate. The zeta potential was also determined using the same instrument, in pH 6.8. The morphology of PLGA nanoparticles was analyzed using a scanning electron microscope (LEO 1525 Field Emission scanning electron microscope, Zeiss, Oberkochen, Germany).

Surface area determination

Surface area measurements were carried out according to the conventional BET method,[14] using the Nova 1000e surface area and pore size analyzer (Quantachrome Instruments, Boynton Beach, Florida). The method is based on isothermal adsorption of nitrogen onto the particles at liquid nitrogen temperature and relative pressures (P/Po) ranging from 0.05 to 0.2. Spray-dried

PLGA particles (50 mg), Fe_2O_3, and SiO_2 (obtained from Walter Focke, University of Pretoria, Department of Chemical Engineering) were degassed by heating under vacuum and used for the measurement. The adsorbed nitrogen volume at 77.3 K was calculated by measuring the pressure change resulting from the adsorption of nitrogen gas onto the surface of particles. The area per molecule value for nitrogen was taken at 162 nm^2, and using this value, the total surface area of the sample was determined. The specific surface area was calculated by dividing the surface area by the sample weight.

In vitro cell viability assay

Caco-2 cells (human colorectal carcinoma) and Hela (human epithelial carcinoma) cells were purchased from Highveld Biologicals, Johannesburg, South Africa. The cells were cultured in 25-mL flasks at 37°C in humidified atmosphere (90% humidity), 5% CO_2, Dulbecco's minimal essential medium, 1% (wt/vol) nonessential amino acids, 1% (wt/vol) glutamine, 10% (vol/vol) fetal bovine serum, penicillin, (100 U/mL), and streptomycin (100 μg/mL). Stocks of the cells were prepared in culture medium containing 80% (vol/vol) fetal bovine serum and 10% (vol/vol) dimethyl sulfoxide and kept in liquid nitrogen until further use. The cells were maintained according to routine cell culture procedures. To determine cell viability after exposure of all cell lines to different concentrations of PLGA nanoparticles of an average size of 374 nm incubated for 24 hours, the WST assay (Quick Cell Proliferation Assay Kit II, Mountain view, California) was performed according to manufacturer's instructions. This colorimetric cell proliferation kit allows for easy and reliable colorimetric determination of viable cell numbers with excellent sensitivity and linearity. The kit utilizes the tetrazolium salt WST-1, which is reduced to water-soluble orange formazan by cellular mitochondrial dehydrogenase present in viable cells. The amount of formazan dye, determined by the absorbance at 450 nm with a reference wavelength at 630 nm, is directly proportional to the number of living cells. Fe_2O_3, SiO_2, and ZnO (Sigma) nanoparticles were used as controls.

In vivo studies

Animals

Unchallenged Balb/C female mice weighing between 20 and 25 g were selected and housed under standard-environment conditions at ambient temperature of 25°C. Animals were humanely cared for and supplied with food and water ad libitum. Ethics approval was obtained for this study from the Ethics Committee for Research on Animals (ECRA), Tygerberg, Cape Town, South Africa.

Histopathology assays

Mice were placed into different groups with three mice per group based on the particles they were treated with and the time frame of treatment. The different groups consisted of animals treated separately with 4 mg PLGA particles, 4 mg SiO_2, and 4 mg ZnO nanopowder (purity >99%; Sigma-Aldrich) by mouth. The latter was used as a positive control in this study, as it is known to have toxic effects on tissues.[15] Polystyrene beads (Sigma-Aldrich, 300 nm) were used as negative control. Group 1 was treated for 24 hours, group 2 was treated daily for 5 days, and group 3 was treated daily for 10 days. Mice were euthanized on day 1, 5 and 7 respectively. The study was repeated once, except that the second time mice were overdosed with the particles (i.e., 60 mg of PLGA particles and 60 mg of SiO_2 and polystyrene beads for 24 hours, for 5 days, and for 10 days. Full necropsies were conducted on the mice following humane euthanasia. The brain, heart, kidney, liver, lung, spleen, gonad (female genitalia), large and small intestines, pancreas, stomach, and thymus were collected from each animal. Tissues were fixed with formalin, and tissue sections cut and processed using routine histological methods in an automated system. Sections of 5 μm were prepared after paraffin embedding. The slides obtained were stained with routine hematoxylin and eosin staining method in an automated stainer.

Tissue distribution assays of PLGA nanoparticles

To determine the biodistribution of the nanoparticles, fluorescently labeled particles were orally administered to mice. The mice were grouped with three mice per group, and the study was repeated three times. Group 1 was treated with 4 mg of rhodamine-PLGA nanoparticles in 0.2 mL sterile saline by oral gavage. Group 2 was treated with 4 mg coumarin-labeled PLGA nanoparticles in 0.2 mL sterile saline by oral gavage. The two fluorescent dyes were used to determine if there any differential biodistribution occurred based on the fluorescent dyes. Furthermore, rhodamine and coumarin were spray-dried without encapsulating into PLGA nanoparticles and orally administered to mice.

In addition, 4 mg of fluorescently labeled polystyrene beads were orally administered as a control to group 3. The mice were killed via cervical dislocation. The brain, heart, kidneys, liver, lungs, and spleen as well as plasma were collected. The tissues were homogenized on ice in 2 mL phosphate-buffered saline, and diluted 100 times. The resulting diluted homogenates were analyzed for fluorescent particles on the FLx8000 Biotek plate reader (Biotek, Winooski, Vermont) at excitation and emission wavelengths of 488 nm and 525 nm, respectively. The tissues were further analyzed via confocal microscopy to determine if the fluorescence observed was still in the particulate matter or had been leached out.

Results

Particle size, zeta potential, surface morphology, and specific surface area

Various parameters were optimized to obtain an average particle size ranging between 200 and 350 nm, with an average polydispersity index of 0.1 observed when freeze-drying was used (Figure 1, *A*). However, the polydispersity index of the spray-dried formulation was higher (0.2 as observed in Figure 1, *B*) with a size range of 300 nm to 1 μm. The particles had a zeta potential between −10 and −18 mV. The spray-dried particles were characterized by a very smooth surface, similar to the freeze-dried particles as depicted by scanning electron microscopy (images in Figure 1, *A* and *B*). However, the

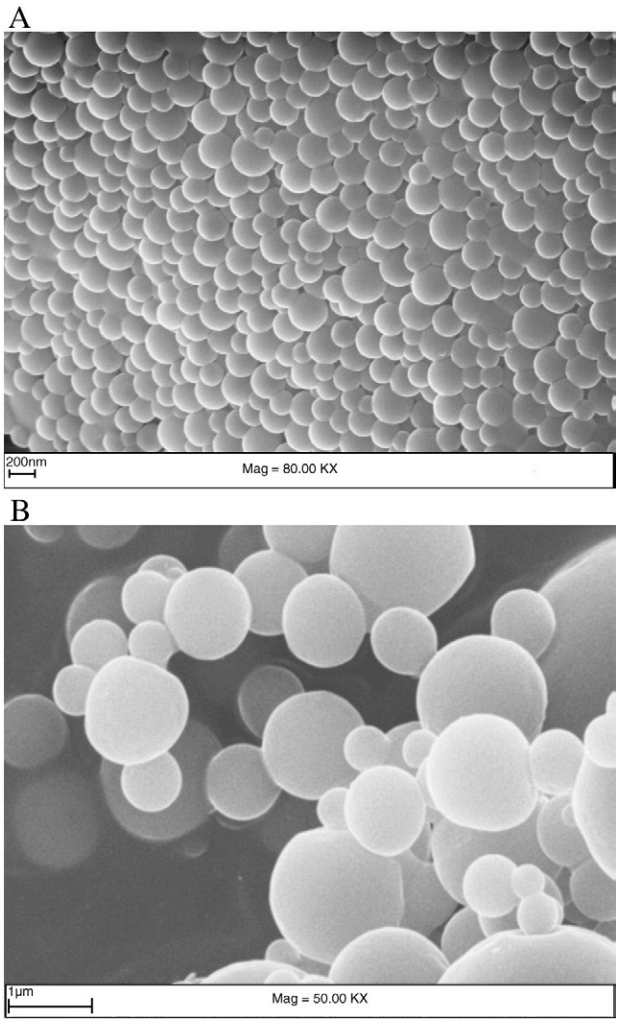

Figure 1. **(A)** SEM picture of freeze-dried formulation (prepared with 40 mL 1% wt/vol polyvinyl alcohol). Bar = 200 nm. **(B)** Spray-dried formulation with the same parameters. Bar = 1 µm.

particles were not equivalent in size. The freeze-dried PLGA nanoparticles had a specific surface area ranging between 3 and 10 m^2/g, whereas a specific surface area ranging between 15 and 25 m^2/g was found for ZnO nanoparticles at a size of 50–150 nm. Fe_2O_3 and SiO_2 had specific surface areas of 11–15 m^2/g and 755–1043 m^2/g, respectively, and a size range of 100–250 nm. The in vitro and in vivo data presented in the manuscript are for the freeze-dried PLGA particles.

In vitro cell viability assays

The in vitro cytotoxicity of PLGA nanoparticles, SiO_2, Fe_2O_3 particles, and ZnO particles was determined at concentrations of 0.1, 0.01 and 0.001 mg/mL, on Caco-2 cells and Hela cells via the WST assay. The results depicted in Figure 2 indicate that, compared with untreated cells (control), the Hela and Caco-2 cell lines retained more than 75% viability when treated with various concentrations of PLGA nanoparticles, SiO_2, and Fe_2O_3. This result supports literature indicating that amorphous silica, as was used in this study, is not toxic to cells.[15] However, ZnO

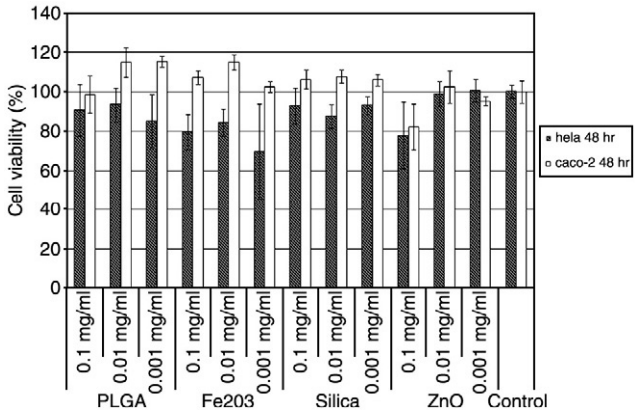

Figure 2. Effects of poly(lactide-co-glycolide), ferrous oxide, and fumed silica particles on percentage viability of Caco-2 and Hela cell lines as shown by a WST assay. The data are representative of two repeats of n = 6; error bars indicate SEM.

nanopowder resulted in a significant reduction in cell viability, as indicated in Figure 2. This result is also in accordance with those of Sharma et al 2009, where it was indicated that ZnO nanoparticles are toxic to cells.

Histopathology assays

Subsequent to oral administration of PLGA particles as well as polystyrene beads for 1, 5, and 10 days, no pathological lesions were detected in the respective groups that could be suggestive of toxicity. (Images of the polystyrene-treated group are not included, as they are similar to those of PLGA particles.) The data were in accordance with those of the saline control group. None of the analyzed tissues exhibited any lesions, even at 60 mg PLGA, as depicted in Table 1. The group treated with amorphous SiO_2 particles showed no noticeable lesion (images not included). The group of mice that were treated with 4 mg ZnO for 24 hours died, and a subset of the mice showed weight loss. Based on these observations, the positive control was not continued for the 5- and 10-day studies. Thus, it can be suggested from these data that PLGA particles at the various concentrations administered do not exhibit any toxicity in mice based on histopathological assays.

Tissue distribution assays

The fluorescently labeled particles were initially not detected in the 5-µm tissue sections via fluorescent microscopy, as a result of the intense autofluorescence of the tissues. Thus, a fluorometer was used to detect fluorescence in the tissue homogenates. The data were normalized with the negative control, which was tissue from mice treated with only saline. The background fluorescence from these tissues was subtracted from the experimental tissue fluorescence readings to exclude the effect of autofluorescence. The percentage particles detected was expressed as the ratio of the fluorescence unit of each tissue relative to the sum of fluorescence units of all tissues analyzed and graphically illustrated in Figure 3 and listed in Table 2 for each tissue. From these data it is evident that most of the particles were detected in the liver at 40.04% ± 8.42%), followed by the

Table 1
Histopathology and confocal images of different mouse tissues after oral administration of fluorescently labeled PLGA or fumed silica

Tissue	Tissues treated with PLGA nanoparticles (fumed SiO_2 gave results similar to the PLGA particles)	Confocal microscope images (62× magnification) of tissue sections, 1 day after administration of rhodamine-labeled particles
Liver	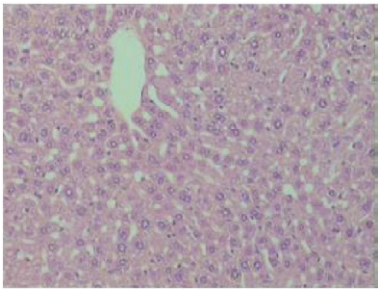	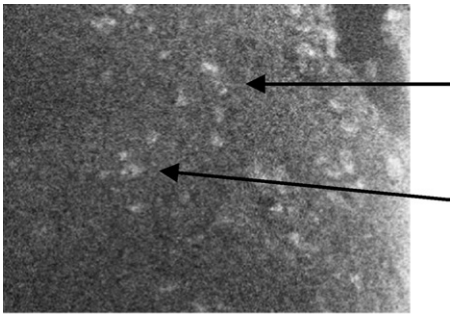
Spleen red pulp	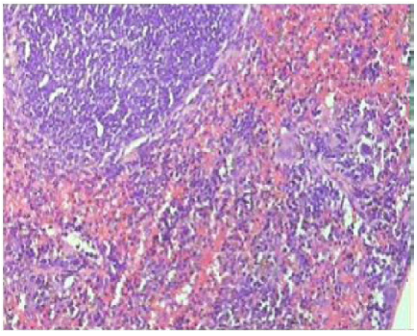	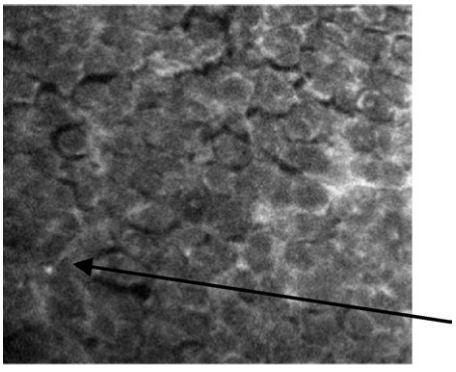
Kidney	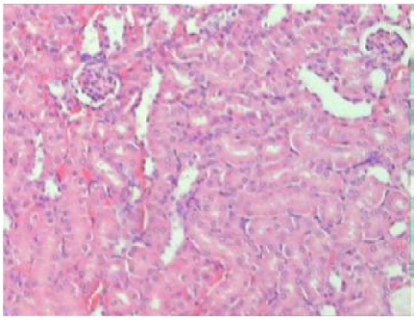	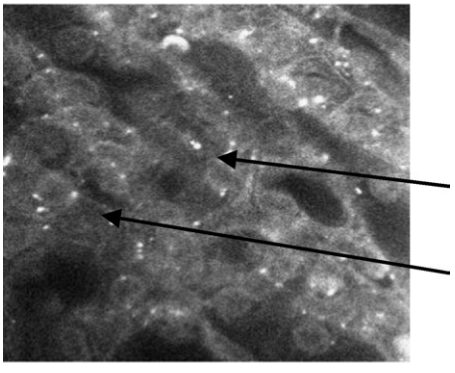
Hippocampus in the cerebrum	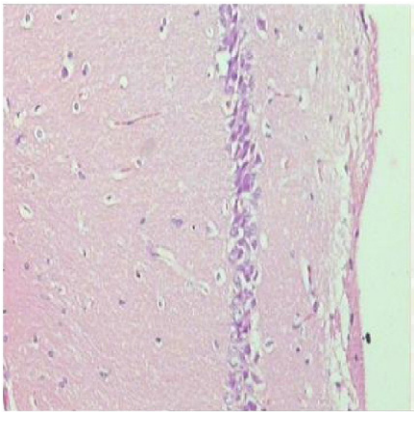	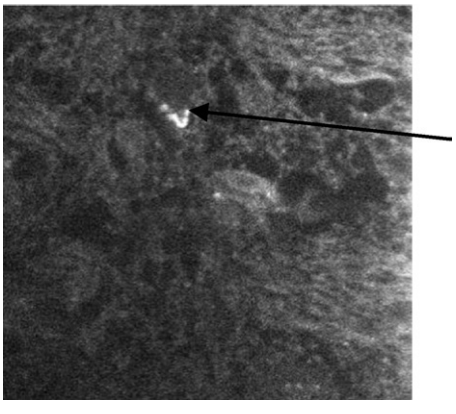

Table 1 (*continued*)

Tissue	Tissues treated with PLGA nanoparticles (fumed SiO_2 gave results similar to the PLGA particles)	Confocal microscope images (62× magnification) of tissue sections, 1 day after administration of rhodamine-labeled particles
myocardium	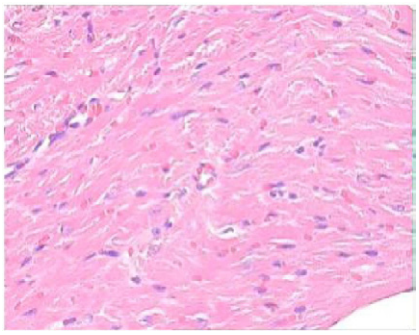	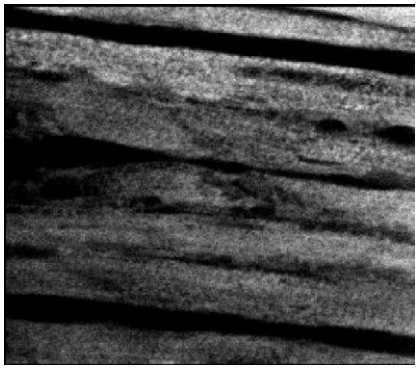
Terminal bronchiolus and lung	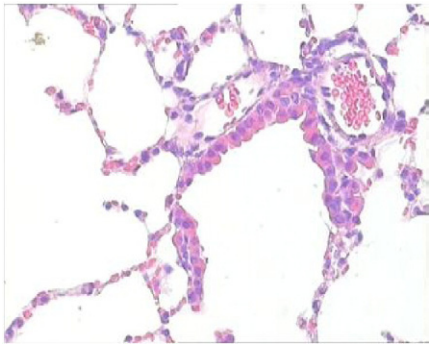	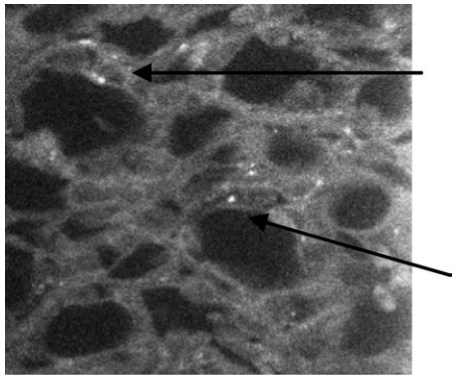
Large intestines	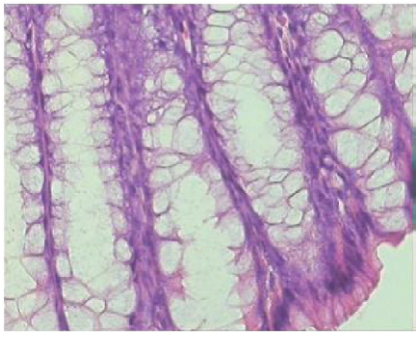	Not analyzed via confocal microscope
Ovarian follicles and corpus luteum	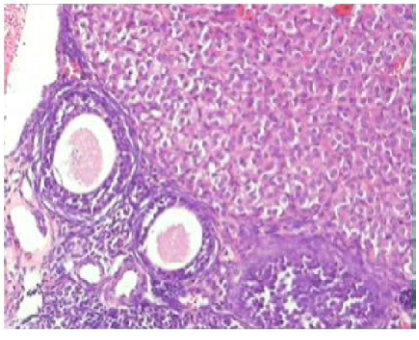	Not analyzed via confocal microscope

(*continued on next page*)

Table 1 (*continued*)

Tissue	Tissues treated with PLGA nanoparticles (fumed SiO_2 gave results similar to the PLGA particles)	Confocal microscope images (62× magnification) of tissue sections, 1 day after administration of rhodamine-labeled particles
Fallopian duct	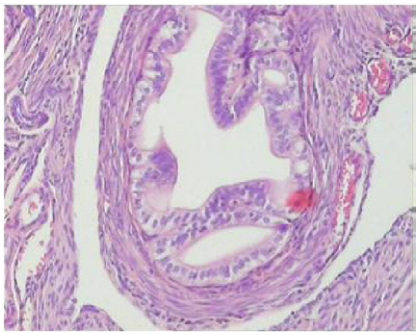	Not analyzed via confocal microscope
Glandular gastric mucosa	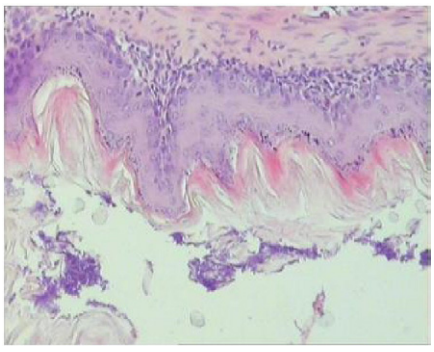	Not analyzed via confocal microscope
Endometrium of uterine mucosa	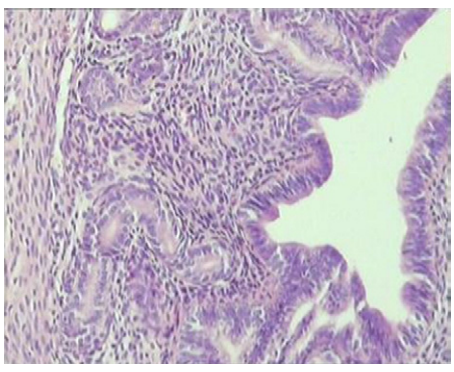	Not analyzed via confocal microscope
Thymus lymphoid tissues	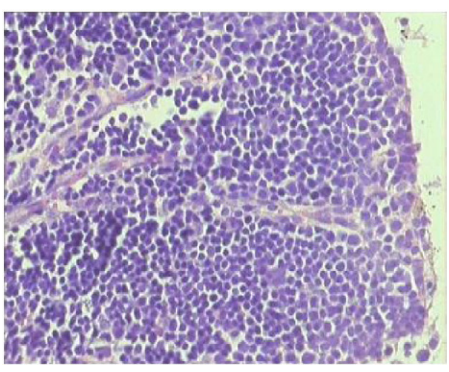	Not analyzed via confocal microscope

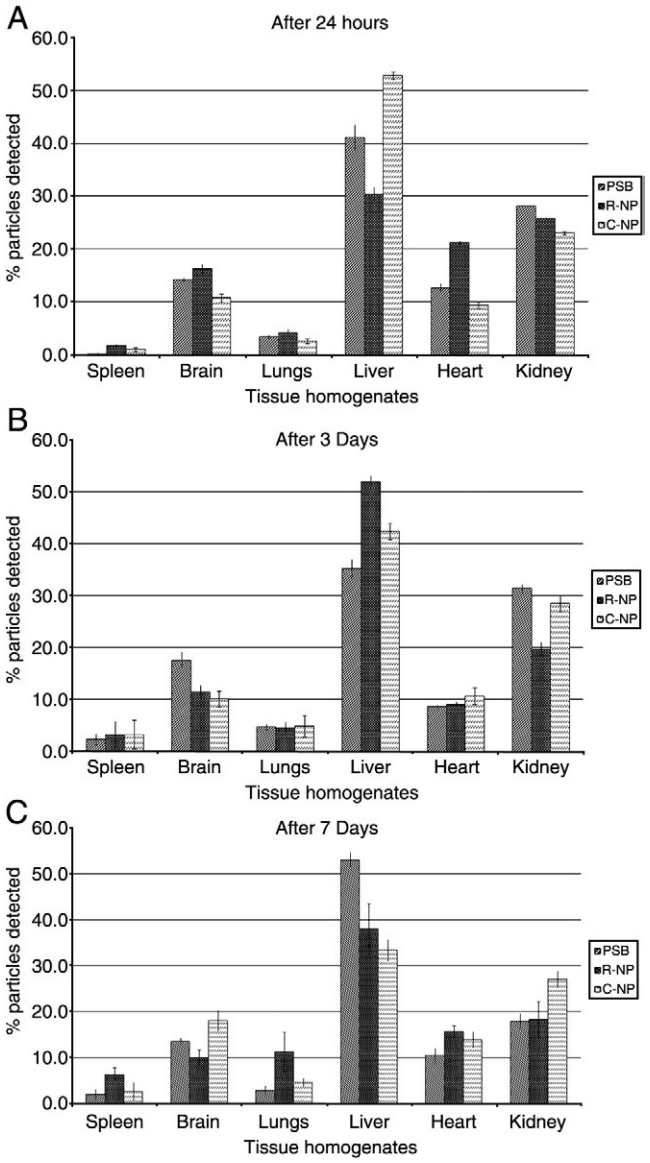

Figure 3. Tissue distribution graphically represented as a measure of percentage of particles detected of the total particles. The data represent three repeats of n = 6; error bars indicate SEM. **(A)** 24 hours; **(B)** 3 days; **(C)** 7 days. PSB, polystyrene beads; R-NP, rhodamine nanoparticles; C-NP, coumarin nanoparticles.

kidney (25.97% ± 7.09%), heart (11.92% ± 3.16%), and brain (12.86% ± 2.82%) throughout all 7 days in which the tissues were analyzed. Plasma was also analyzed from day 3 as indicated in Figure 4, but only very small amounts of the particles were detected. Confocal images of the tissues after 1 day of administration of the rhodamine-labeled particles are presented in Table 1, where we have shown, using unstained tissues for comparison, that the fluorescent particles can be detected within the various tissues. It has been reported that rhodamine release from nanoparticles is very slow, and therefore, the detection of fluorescence in the different tissues can be considered to be that of the rhodamine associated with the PLGA nanoparticles.[16,17] It must be emphasized that the confocal images do not correlate to

Table 2
Percentage particles detected, calculated as a function of total particles

Organ	% Particles detected								
	1 day			3 days			7 days		
	PSB	R-NP	C-NP	PSB	R-NP	C-NP	PSB	R-NP	C-NP
Brain	14.3	16.4	10.8	17.6	11.5	10.2	13.6	10.1	18.1
Heart	12.8	21.3	9.4	8.7	9.1	10.7	10.5	15.7	14
Kidney	28.2	25.9	23.1	31.5	19.7	28.6	18	18.3	27.1
Lung	3.4	4.2	2.7	4.8	4.5	4.9	2.9	11.4	4.7
Liver	41.3	30.5	52.9	35.2	51.9	42.4	53	38.1	33.4
Spleen	0.2	1.7	1.1	2.3	3.3	3.3	2	6.4	2.7

PSB, polystyrene beads; R-NP, rhodamine nanoparticles; C-NP, coumarine nanoparticles.
Data are expressed as a representation of percentage particles detected of total particles; n = 6.

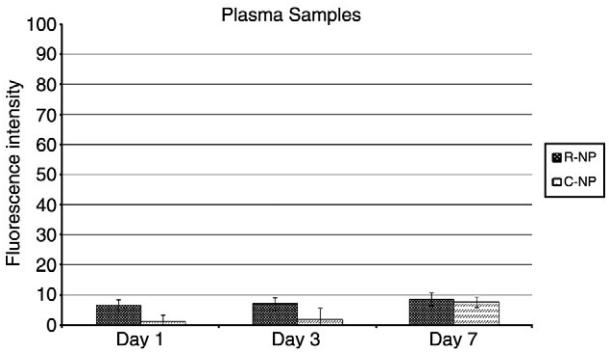

Figure 4. Fluorescence detection in plasma represented as a function of fluorescence intensity. R-NP, rhodamine nanoparticles; C-NP, coumarin nanoparticles.

the quantity of the particles in the tissues, but only indicate the presence of the particles in the respective tissues and also indicate the particulate nature of the fluorescence, suggesting that the observed fluorescence is that of rhodamine in the nanoparticles and not leached rhodamine.

Discussion

The toxicity of nanoparticles involves physiological, physicochemical, and molecular considerations. Extensive studies on industrial nanoparticles investigating these parameters have been conducted, but not much is known about nanoparticles that are used for therapeutic purposes. At present, PLGA is used extensively for drug delivery applications.[4,18] It is with this in mind that this study focused on elucidating the effect of PLGA nanoparticles in vitro and in vivo. Much controversy still exists regarding the potential adverse effects, so there is a need for reports indicating the safety of these materials. The particles analyzed had specific surface areas within a similar range, except for the amorphous silica, which had a higher specific surface area. Thus, although these PLGA particles had a surface area similar to that of ZnO, which served as a positive control, no toxic effect as presented in the viability

Table 3
Fluorescence units of tissues after oral administration of fluorescently labelled particles or spray dried fluorophores

	Brain	Heart	Kidney	Liver	Lungs	Spleen
RH-NPs day 1	35.9	47.8	53.9	67.1	8.9	3.8
RH day 1	2.5	1	11.8	4	1	1
RH-NPs day 3	36.3	28.4	170.4	63.4	14.4	10.5
RH day 3	4.8	1	4.2	6	1	1
RH NPs day 7	40.3	64.8	156.8	93.2	43.2	29.5
RH day 7	5	1	2	2	1	1
C-NPs day 1	35.4	31.4	75.6	176.3	8.4	3.5
C day 1	1.3	1	4.8	1	14.3	1
C-NPs day 3	50.7	54	171	214.3	27.7	24
C day 3	1	1	5.8	50.3	10.1	1
C-NPs day 7	66.9	53	110.9	140.7	18.9	9.9
C day 7	−0.2	1	8.8	73.3	1	1

RH, Rhodamine; NPs, nanoparticles, C, Coumarin. n = 3.

assays was observed. This suggests that the biodegradability and biocompatibility of PLGA nanoparticles facilitates their safe use in medical applications.

In vitro cytotoxicity of the respective particles was tested in two different cell lines. The PLGA nanoparticles were shown to have no cytotoxic effects on the cells. Although specific surface area has been reported to be causal in some of the observed toxicities in metal nanoparticles,[6] it is clear from the viability assay that the surface area of PLGA particles did not significantly affect the viability of the cells analyzed. Second, it can be suggested that the chemical composition of the PLGA nanoparticles did not contribute to toxicity. As polyesters in nature, PLGA undergoes hydrolysis and enzymatic degradation upon implantation into the body, forming biologically compatible moieties that can be metabolized (lactic acid and glycolic acid) and are eventually removed from the body by the citric acid cycle.[19] These PLGA biodegradation products are formed at a very slow rate and hence do not affect normal cell function. Although SiO_2 nanopowder and Fe_2O_3 particles had larger specific surface areas as compared with PLGA particles, they did not exhibit any toxicity, thus supporting the observation that surface area is not the main determinant of toxicity in nanoparticulate structures.

Subsequent to oral administration of polystyrene beads, rhodamine-labeled PLGA particles, as well as coumarin-labeled PLGA particles in the respective groups, particles were detected in all tissues evaluated. The highest percentage of particles was detected in the liver, followed by the kidney, the brain, and the heart, as shown in Table 2. To confirm that the fluorescence detected is from the encapsulated fluorophores, Table 3 illustrates the fluorescence measured of the encapsulated fluorophores versus the unencapsulated but spray-dried fluorophores. Thus, from these data it is evident that rhodamine and coumarin are cleared from the tissues within 1 day, and thus low concentrations are detected in comparison with when these fluorophores are encapsulated in PLGA nanoparticles. This result also confirms that these nanoparticles are able to cross cellular barriers such as the BBB and reach hard-to-target tissues—in accordance with work published elsewhere.[12,20] However, we have also shown that although these particles are detected in various tissues within a 7-day period, these particles do not cause any morphological pathology in the respective tissues even at high doses (i.e., 60 mg per 25g mice). As demonstrated by the histopathology assays conducted, no lesions or inflammation was observed in the brain. The lowest concentrations were observed in the spleen and lungs. This result could indicate that for oral administration of PLGA particles for drug delivery purposes, these particles will have to be surface-modified with hydrophilic molecules such as polyethylene glycol to minimize opsonization of the particles, thus increasing the circulation time in the blood with the eventual effect of minimizing the amount of particles that reach the liver. Thus far, various hydrophilic surfactants have been used to minimize opsonization.[21] Poloxamers, poloxamines, and other polymers such as chitosan can also be used for this purpose.[22] This will, in turn, minimize first-pass metabolism of the encapsulated drugs. Various groups have also reported modification of the particles with peptides or proteins.[16]

Drug delivery systems such as PLGA nanoparticles will provide an ideal carrier system to various tissues that are generally hard to target even with oral administration, as presented in this study as well as other studies.[18,20] Because of its ability to cross the BBB, this system will present a means of effectively treating neurological and psychiatric disorders,[16] as well as other disseminated diseases such as tuberculosis, by administering the nanoencapsulated drugs orally or via any other noninvasive modes. Furthermore, according to this study, PLGA nanoparticles are safe to use as a drug delivery system, although many concerns still exist regarding the safety of nanomaterials in general.

From this study conducted with biodegradable and biocompatible PLGA nanoparticles, it is clear that these particles are not toxic in cell culture and when orally administered at the mentioned doses to Balb/c mice. More studies need to be conducted with other polymeric nanoscale drug delivery systems, to evaluate their safety. It is clear from the biodistribution data that nanoscale drug delivery systems will be suitable to improve the permeability, and thus the bioavailability of therapeutic compounds. With this approach, delivery of drugs that have poor permeability and solubility can be greatly enhanced with safe and effective drug delivery systems.

Acknowledgments

We thank Kobus Venter at the Medical Research Council for assisting with the mice studies, Robyn Brackin at the Council of Scientific and Industrial Research for assistance with the confocal images, and Dr. Willem Botha of Vetpath Laboratories for assisting with the histopathology assays.

References

1. Magenheim B, Benita S. Nanoparticle characterization:a comprehensive physicochemical approach. S T P Pharm Sci 1991;1:221-41.
2. Duncan R. Nanomedicine gets clinical. Materials Today 2005;8:16-7.
3. Nel A, Xia T, Madler L, Li N. Toxic potential of materials at the nanolevel. Science 2006;311:622-7.
4. Panyam J, Labhasetwar V. Biodegradable nanoparticles for drug and gene delivery to cells and tissue. Adv Drug Deliv Rev 2003;55:329-47.
5. Stone V, Donaldson K. Nanotoxicology: signs of stress. Nat Nanotechnol 2006;1:23-4.

6. Li N, Xia T, Nel AE. The role of oxidative stress in ambient particulate matter-induced lung diseases and its implications in the toxicity of engineered nanoparticles. Free Radic Biol Med 2008;44:1689-99.
7. Oberdorster G, Maynard A, Donaldson K, Castranova V, Fitzpatrick J, Ausman K, et al. Principles for characterizing the potential human health effects from exposure to nanomaterials: elements of a screening strategy. Particle Fibre Toxicol 2005;2:8-43.
8. McNeil SE. Nanotechnology for the biologist. J Leukocyte Biol 2005; 78:585-94.
9. Liversidge GG, Cundy KC. Particle size reduction for improvement of oral bioavailability of hydrophobic drugs: I. Absolute oral bioavailability of nanocrystalline danazol in beagle dogs. Int J Pharm 1995;125: 91-7.
10. Desai MP, Labhasetwar V, Amidon GL, Levy RJ. Gastrointestinal uptake of biodegradable microparticles: effect of particle size. Pharm Res 1996;13:1838-45.
11. Wilkinson JM. Roadmapping medical devices. Medical Device Link 2006;6:1-0090 Ref Type: Electronic Citation. Available at: http://www.devicelink.com/mdt/archive/06/06/014.html.
12. Koziara JM, Lockman PR, Allen DD, Mumper RJ. In situ blood brain barrier transport of nanoparticles. Pharm Res 2003;20:1772-8.
13. Lamprecht A, Ubrich N, Hombreiro Perez M, Lehr CM, Hoffman M, Maincent P. Biodegradable monodispersed nanoparticles prepared by pressure homogenization-emulsification. Int J Pharm 1999;184: 97-105.
14. Brunauer S, Emmett PH, Teller E. Adsorption of gases in multimolecular layers. J Am Chem Soc 1938;60:309-19.
15. Merget R, Bauer T, Küpper H, Philippou S, Bauer H, Breitstadt R, et al. Health hazards due to the inhalation of amorphous silica. Arch Toxicol 2002;75:625-34.
16. Vergoni AV, Tosi G, Tacchi R, Vandelli MA, Bertolini A, Costantino L. Nanoparticles as drug delivery agents specific for CNS: in vivo biodistribution. Nanomed Nanotechnol Biol Med 2009;5:369-77.
17. Tosi G, Costantino L, Rivasi F, Ruozi B, Leo E, Vergoni AV, et al. Targeting the central nervous system: in vivo experiments with peptide-derivatized nanoparticles loaded with Loperamide and Rhodamine-123. J Control Release 2007;122:1-9.
18. Jain RA. The manufacturing techniques of various drug loaded biodegradable poly(lactide-co-glycolide) (PLGA) devices. Biomaterials 2000;21:2475-90.
19. Campbell MK. Biochemistry. Philadelphia: Saunders College Publishing; 1995. p. 365-84.
20. Lockman PR, Mumper RJ, Khan A, Allen DD. Nanoparticle technology for drug delivery across the blood-brain barrier. Drug Dev Ind Pharm 2002;28:1-13.
21. Storm G, Belliot SO, Daemen T, Lasic DD. Surface modification of nanoparticles to oppose uptake by the mononuclear phagocyte system. Adv Drug Deliv Rev 1995;17:31-48.
22. Torchilin VP, Trubetskoy VS. Which polymers can make nanoparticulate drug carriers long-circulating? Adv Drug Deliv Rev 1995;16:141-55.

International Journal of Pharmaceutics xx (2012) xxx–xxx

Contents lists available at SciVerse ScienceDirect

International Journal of Pharmaceutics

journal homepage: www.elsevier.com/locate/ijpharm

Graphical Abstract

International Journal of Pharmaceutics xx (2012) xxx–xxx

Effects of protein binding on the biodistribution of PEGylated PLGA nanoparticles post oral administration

Boitumelo Semete, Laetitia Booysen, Lonji Kalombo, Bathabile Ramalapa, Rose Hayeshi*, Hulda S. Swai

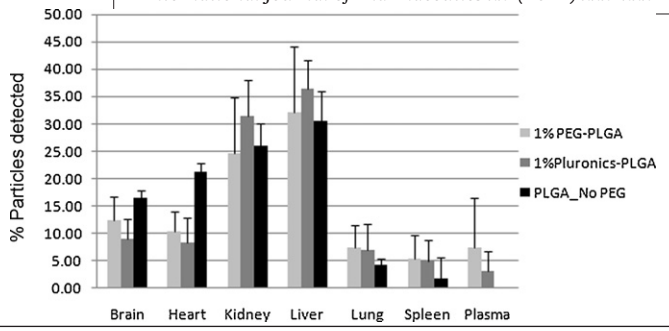

International Journal of Pharmaceutics xxx (2012) xxx–xxx

Contents lists available at SciVerse ScienceDirect

International Journal of Pharmaceutics

journal homepage: www.elsevier.com/locate/ijpharm

Pharmaceutical Nanotechnology

Effects of protein binding on the biodistribution of PEGylated PLGA nanoparticles post oral administration

Boitumelo Semete[a], Laetitia Booysen[a,b], Lonji Kalombo[a], Bathabile Ramalapa[a], Rose Hayeshi[a,*], Hulda S. Swai[a]

[a] Council for Scientific and Industrial Research, Pretoria 0001, South Africa
[b] Department of Pharmaceutics, North West University, Potchefstroom Campus, Potchefstroom 2520, South Africa

ARTICLE INFO

Article history:
Received 8 September 2011
Received in revised form
21 December 2011
Accepted 22 December 2011
Available online xxx

Keywords:
Nanoparticles
PEGylation
Protein binding
Biodistribution

ABSTRACT

The surface of nanoparticles is often functionalised with polymeric surfactants, in order to increase systemic circulation time. This has been investigated mainly for intravenously administered nanoparticles. This study aims to elucidate the effect of surface coating with various concentrations of polymeric surfactants (PEG and Pluronics F127) on the *in vitro* protein binding as well as the tissue biodistribution, post oral administration, of PLGA nanoparticles. The *in vitro* protein binding varied depending on the polymeric surfactant used. However, *in vivo*, 1% PEG and 1% Pluronics F127 coated particles presented similar biodistribution profiles in various tissues over seven days. Furthermore, the percentage of PEG and Pluronics coated particles detected in plasma was higher than that of uncoated PLGA particles, indicating that systemic circulation time can also be increased with oral formulations. The difference in the *in vitro* protein binding as a result of the different poloxamers used *versus* similar *in vivo* profiles of these particles indicates that *in vitro* observations for nanoparticles cannot represent or be correlated to the *in vivo* behaviour of the nanoparticles. Our results therefore suggest that more studies have to be conducted for oral formulations to give a better understanding of the kinetics of the particles.

1. Introduction

The application of nanotechnology based drug delivery systems has been on the increase in the past two decades. It has been reported that by encapsulating drugs into nanoparticles, the bioavailability, tissue distribution and half-life can be improved and that toxicity of the drugs can be minimised (Bawarski et al., 2008; Li and Huang, 2008). Despite significant progress with nanoparticle-based drug delivery, shortcomings have been experienced, with rapid clearance of the particles from the blood in intravenously (iv) administered formulations (Moghimi and Szebeni, 2003; Owens and Peppas, 2006). This occurrence has been reported to be as a result of the adsorption of plasma proteins including opsonins on the surface of particles triggering recognition and uptake of the particles by the mononuclear phagocytic system (MPS) (Moghimi and Szebeni, 2003). This phenomenon has lead to the exploration of surface modification of the particles with non-ionic polymeric surfactants, to make these particles 'stealth'. Some of the extensively researched surfactants are poloxamers and poly-ethyleneglycol (PEG) (Moghimi and Szebeni, 2003; Stolnik et al., 1995). When particles are coated with these polymers, the recognition by plasma proteins is minimised, thus reducing the rate of MPS uptake. It is postulated that the presence of surfactants on the surface of the particles reduces the interparticulate attractive Van der Waals forces and increases the repulsive barrier between the particles (Owens and Peppas, 2006).

Much of the research conducted with stealth particles focuses on intravenously administered particles, however very little is known regarding the protein binding and thus tissue distribution of PEGylated particles when orally administered. Semete et al. (2010) evaluated the biodistribution of poly(DL-Lactic-*co*-Glycolic Acid) (PLGA) nanoparticles post oral administration into mice. Due to the preferential uptake of non-stealth particles by macrophages of the liver, *i.e.* the Kupffer cells, a greater proportion of particles were detected in the liver (Semete et al., 2010). Based on Semete et al. (2010) and other reports (Li and Huang, 2008; Owens and Peppas, 2006), it is well accepted that nanoparticles will generally be taken up by tissues with leaky endothelial walls such as the liver, spleen, bone marrow and tumours. It is postulated that when protein binding (primarily opsonisation) of the particles is minimised, this preferential uptake by macrophages and tissues will be reduced, however a balance needs to be obtained in that intracellular uptake of the particles is not compromised. In addition not much is known about the effect that minimised opsonisation will have on the biodistribution of orally administered stealth

* Corresponding author at: CSIR Materials Science and Manufacturing, PO Box 395, Pretoria 0001, South Africa. Tel.: +27 12 841 4697; fax: +27 12 841 3553.
E-mail address: RHayeshi@csir.co.za (R. Hayeshi).

0378-5173/$ – see front matter © 2011 Published by Elsevier B.V.
doi:10.1016/j.ijpharm.2011.12.043

Table 1
Summary of nanoparticle characterisation.

Formulation	Ave size (nm)	Polydispersity index	Zeta potential (mV[a])
PLGA–Rhd[b]	296.8	0.229	+35.2
PLGA–Rhd (1% PEG)	313.3	0.303	+30.1
PLGA–Rhd (1% Pluronics F127)	442.7	0.293	+28.6
PLGA–Rhd (0.5% PEG)	340.2	0.145	+33.5
PLGA–Rhd (0.5% Pluronics F127)	442.7	0.293	+29.7

[a] mV: millivolts.
[b] Rhd: Rhodamine.

particles. Thus, in this study, we explore the effect of PEGylation on the biodistribution of PLGA particles, and furthermore ask to what extent the observed difference with the *in vitro* protein binding of nanoparticles can represent the *in vivo* observation.

2. Methods

2.1. Nanoparticle preparation

Nanoparticles were prepared with PLGA 50:50 (M_w: 45,000–75,000 Da) using a modified double emulsion solvent evaporation spray-drying technique. Briefly, aqueous phosphate buffered saline (PBS) pH 7.4 was emulsified for a short period with a solution of 100 mg PLGA dissolved in 8 ml of ethyl acetate (EA), by means of a high speed homogeniser (Silverson L4R) with a speed varying between 3000 and 5000 rpm. The resulting water-in-oil (w/o) emulsion was transferred into a specific volume of an aqueous solution of 1% w/v of the polyvinyl alcohol (PVA, M_w: 13,000–23,000 partially hydrolysed (87–89%)), 0.3% weight/volume (w/v) of chitosan and 5% (w/v) lactose to stabilise the emulsion. The mixture was further emulsified for 5 min by homogenisation at 8000 rpm. The double emulsion, *i.e.* water-in-oil-in-water (w/o/w) obtained was directly fed into a bench top Buchi mini-spray dryer (Model B-290) and spray dried at a temperature ranging between 95 and 110 °C, with an atomising pressure varying between 6 and 7 bar. PEG (M_w: 9000 Da) or Pluronics F127 (poly-ethylene oxide (PEO) and poly-propylene oxide (PPO) triblock, M_w: 10,000 Da. PEO is the hydrophilic polymer and PPO the hydrophobic polymer) were introduced in the formulations as excipients to increase the *in vivo* residence time of nanoparticles in the blood circulation (Torchilin and Trubetskoy, 1995). Rhodamine-6G labelled nanoparticles coated with either 0.5 or 1% volume/volume (v/v) PEG/Pluronics F127 were prepared for the biodistribution assays. These nanoparticles were prepared as described above by including Rhodamine-6G together with PLGA in the oil phase of the first w/o emulsion.

2.2. In vitro protein binding assays

The nanoparticle protein binding was analysed using an adapted method as described previously for protein adsorption to polymer nanoparticles (Stolnik et al., 2001). Pooled human plasma was donated by the Department of Pharmacology at the University of Pretoria and was stored at −20 °C until use. Briefly, samples were prepared in varying ratios of plasma to nanoparticle suspension (10:90; 20:80; 40:60 (v/v)) to a total volume of 600 μl. The plasma/nanoparticle suspension was incubated for 2 h at room temperature and then centrifuged at 14,000 rpm for 45 min to obtain a nanoparticle pellet. The pellet was washed once with 600 μl McIllvaine's buffer (91.7 ml 0.1 M Na_2HPO_4 + 8.3 ml 0.2 M citric acid) at pH 7.5 to remove any additional unbound protein and centrifuged again at the same parameters. The resulting supernatants from the washes and the original supernatant were combined for protein analysis using the Bradford assay to determine the concentration of protein that did not bind to the nanoparticles.

2.3. In vivo studies

2.3.1. Animals

Female Balb/C mice weighing between 20 and 25 g were selected and housed under standard environment conditions at ambient temperature of 25 °C. Animals were humanely cared for and supplied with food and water *ad libitum*. Ethics approval was obtained for this study from the Ethics Committee for Research on Animals (ECRA), Tygerberg, Cape Town, South Africa.

2.3.2. Tissue distribution assays of PLGA nanoparticles

In order to determine the biodistribution of surface functionalised PLGA nanoparticles with different concentrations of PEG or Pluronics F127, these formulations were fluorescently labelled with Rhodamine 6G and orally administered to mice at 4 ml particles in 0.2 ml sterile saline by oral gavage. The mice were grouped with three mice per group and the study was repeated three times. Group 1 was treated with PLGA-nanoparticles. Group 2 was treated with 0.5% PEG–PLGA nanoparticles; Group 3: 0.5% Pluronics F127–PLGA-nanoparticles, Group 4: 1% PEG–PLGA nanoparticles and Group 5: 1% Pluronics F127–PLGA–nanoparticles. Oral administration was performed on the same day and the mice were euthanised 1, 3 or 7 days post administration.

The mice were sacrificed by cervical dislocation. The brain, heart, kidney, liver, lung and spleen as well as plasma were collected and processed immediately for analysis. Briefly, the tissues were homogenised on ice in 2 ml PBS, and diluted 100 times. The resulting diluted homogenates were analysed for fluorescent particles on the FLx8000 Biotek plate reader at an excitation and emission wavelength of 488 nm and 525 nm, respectively.

3. Results

3.1. Nanoparticle formulation

Particles of sizes ranging between 250 and 440 nm with a polydispersity index less than 0.3 were prepared. It was observed that the zeta potential as indicated in Table 1 was not significantly affected by the presence or absence of poloxamer coating. Lactose was included in the formulation as drying aid agent together with

Table 2
Protein binding values of various nanoparticle formulations with varying ratios of plasma: nanoparticle suspension.

Plasma:nanoparticle ratio	Protein binding (%)		
	PLGA	1% Pluronics	1% PEG
10:90	25.02 (4.58)	22.78 (6.49)	31.41 (13.80)
20:80	22.03 (4.81)	21.23 (6.62)	20.57 (6.60)
40:60	20.91 (4.44)	31.30 (9.76)	14.32 (7.40)

% protein bound was calculated as 100 minus % unbound. Standard deviation is shown in parentheses.

Please cite this article in press as: Semete, B., et al., Effects of protein binding on the biodistribution of PEGylated PLGA nanoparticles post oral administration. Int J Pharmaceut (2012), doi:10.1016/j.ijpharm.2011.12.043

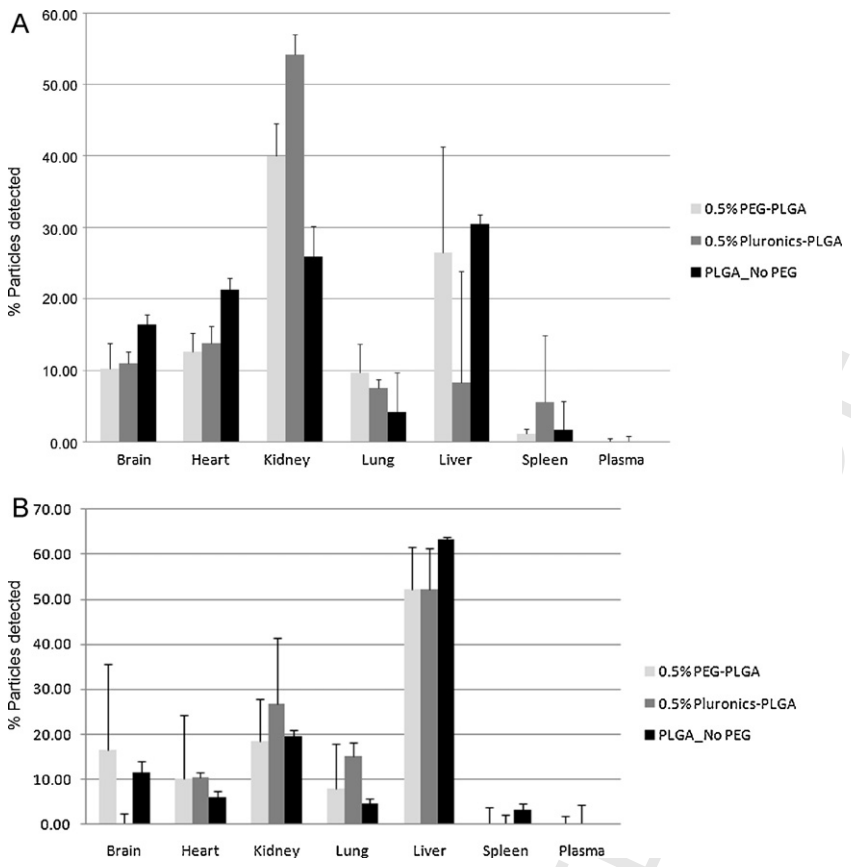

Fig. 1. Biodistribution of Rhodamine labelled PLGA nanoparticles coated with 0.5% PEG or Pluronics F127. (A) After 1 day oral administration, (B) after 3 days oral administration.

the mucoadhesive polysaccharide chitosan for surface charge modification. The inclusion of chitosan, a positively charged ligand, has been recommended in previous reports to enhance uptake through the gastrointestinal tract (Cui et al., 2006; Takeuchi et al., 2005). 0.5% and 1% w/w coated particles were prepared. When the concentration of the polymeric surfactants, *i.e.* PEG and Pluronics were increased beyond 1%, this led to an increase in the size of the particles (data not shown), possibly due to polymer chain entanglement.

3.2. In vitro protein binding of PLGA nanoparticles

Various concentrations of plasma: nanoparticle suspensions were included to evaluate the Vroman effect. This refers to a plasma protein concentration and exposure time dependent effect on the competitive adsorption of proteins for a finite number of surface sites on the particles (Moghimi and Szebeni, 2003). At a 10% plasma volume, PLGA formulations demonstrated an average protein binding of 25.02 ± 4.58%. A comparison between this formulation and a similar formulation coated with 1% Pluronics F127 as depicted in Table 2, illustrated no significant difference in plasma protein binding ($p > 0.01$, 95% confidence level (CI)). However, the formulation coated with 1% PEG resulted in a percentage protein binding of 31.4 ± 13.8% which was found to be significantly different when compared to the uncoated formulation ($p < 0.01$). Similarly, the percentage protein binding of the two coated formulations also differed significantly as indicated in Table 2. The increased protein binding for PEG formulations observed at 10% plasma volume was an unexpected result since surface modification with PEG has been well documented to reduce protein adsorption (Gref et al., 2000; Tan et al., 1993). At the 20% v/v plasma concentration, no significant difference was observed between the three formulations ($p > 0.01$). Interestingly, at 40% v/v plasma concentration, the 1% Pluronics F127–PLGA formulation resulted in a higher protein binding compared to both the uncoated PLGA and 1%PEG–PLGA formulations.

Comparisons of the same formulation at different plasma protein concentration revealed that for the uncoated PLGA formulations, no significant difference ($p > 0.01$) was observed between the plasma protein concentration, *i.e.* 10, 20 and 40%. Therefore this result suggests that the affinity of these formulations for plasma proteins was not dependent on plasma concentration. However, a significant increase ($p < 0.01$) in protein binding was observed for formulations coated with 1% Pluronics F127 at 40% v/v plasma concentration compared to the 10 and 20%. In contrast, the formulations coated with 1% PEG presented a significant decrease in protein binding from 31.41 ± 13.8% at 10% to 14.32 ± 7.4% for 40% v/v plasma concentration.

3.3. Biodistribution of PLGA nanoparticles

When the fluorescently labelled particles were orally administered to mice and the tissues analysed, the particles were initially not detected in the tissues (5 μm tissue sections) *via* fluorescent microscopy, as a result of the intense auto-fluorescence of the tissues. Thus, a fluorometer was used to detect fluorescence in the tissue homogenates. The data was normalised with the negative control, which was tissue from mice treated with saline only. The background fluorescence from these tissues was deducted from the control tissue fluorescent readings to exclude the effect of auto-fluorescence. The percentage particles detected was expressed as the concentration of the fluorescence unit (FU) of each tissue

Please cite this article in press as: Semete, B., et al., Effects of protein binding on the biodistribution of PEGylated PLGA nanoparticles post oral administration. Int J Pharmaceut (2012), doi:10.1016/j.ijpharm.2011.12.043

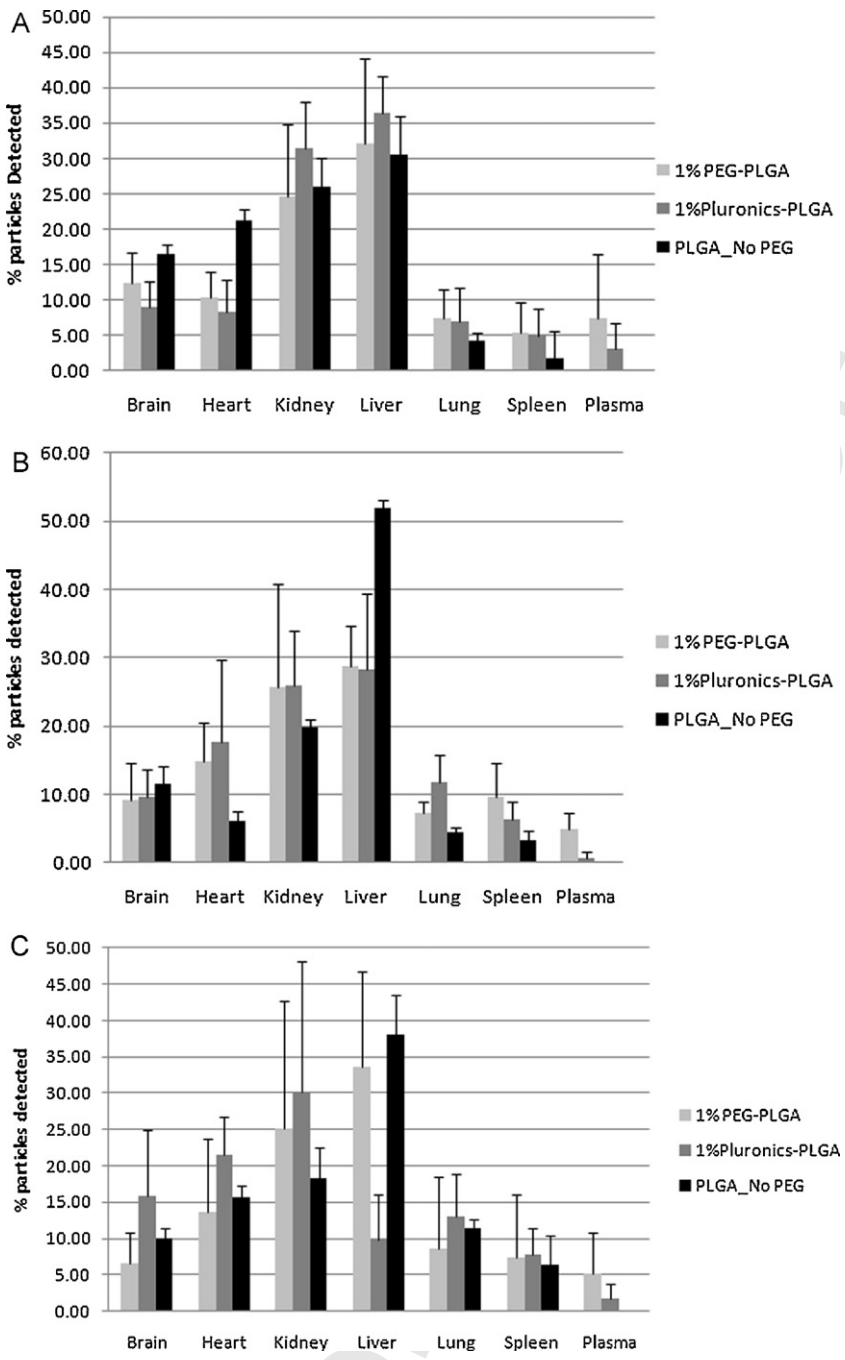

Fig. 2. Biodistribution of Rhodamine labelled PLGA nanoparticles coated with 1% PEG or Pluronics F127. (A) 1 day oral administration, (B) Day 3 after oral administration, (C) Day 7 after oral administration.

relative to the sum of fluorescence units of all tissues analysed and graphically illustrated.

As illustrated in our previous study (Semete et al., 2010) PLGA particles with no poloxamer coating were detected in the liver, spleen, lungs, kidneys, heart and the brain over a period of 7 days. However, very low concentrations or no particles were observed in the plasma over the same period. It was confirmed in Semete et al. (2010), *via* confocal imaging that the fluorescence detected in these tissues is of Rhodamine in the nanoparticles and not leached Rhodamine.

At 0.5% PEG and Pluronics F127 coating of the particles, no particles were detected in plasma over the 3 days as depicted in Fig. 1A and B. Furthermore, no significant difference between the three formulations ($p > 0.01$) was observed for the liver, heart, brain, spleen and lungs. Interestingly though, a significantly higher concentration of coated particles was detected in the kidneys compared to the uncoated formulation on day 1. This could indicate a possible renal clearance of the particles at this time point. These results indicate that at this specific surface coverage with 0.5% poloxamer coating, no significant difference in the biodistribution of PLGA nanoparticles is observed.

When 1% PEG or Pluronics F127 coated particles were orally administered, the biodistribution profile indicated in Fig. 2 was observed. The presence of 1% PEG–PLGA nanoparticles in the brain decreased over the 7 days, whereas in the heart, kidney, liver and lungs the % detected remained relatively constant. A slight

Please cite this article in press as: Semete, B., et al., Effects of protein binding on the biodistribution of PEGylated PLGA nanoparticles post oral administration. Int J Pharmaceut (2012), doi:10.1016/j.ijpharm.2011.12.043

accumulation of 1% PEG–PLGA nanoparticles was detected in the spleen, indicating uptake by the M cells of the Peyer's patches. Furthermore, these particles were detected in the plasma over the 7 days. An accumulation of 1% Pluronics F127–PLGA particles was observed in the brain over the 7 days as indicated in Fig. 2. A similar profile to that of 1% PEG–PLGA nanoparticles was observed in the rest of the tissues including the spleen and plasma. Plasma concentrations were significantly higher than those for uncoated PLGA particles. This increase in the residence time in plasma is in agreement to that of Stolnik et al. (1995).

4. Discussion

PEG and Pluronics have been extensively used in drug delivery to increase the circulation time of particles in blood. Much work has focused on intravenously administered particles, primarily liposomes, where stealth particles have been shown to circulate for prolonged periods of time with half-lives as long as 45 h (Moghimi and Szebeni, 2003). This study however focused on the effect of PEGylation and coating with Pluronics F127 on the *in vitro* protein binding as well as the biodistribution of PLGA particles post oral administration.

The *in vitro* protein binding of the different formulations indicated that when PLGA particles are made stealth, the protein binding varies depending on the polymeric surfactant used. In this case, 1% Pluronics F127–PLGA particles did not display the Vroman effect nor reduce the protein binding of the particles. However, for 1% PEG–PLGA particles, the plasma protein concentration had a significant effect on protein binding, with a lower protein binding at higher plasma protein concentration. This data is more physiologically relevant than the data at low plasma protein concentration because *in vivo*, the ratio of plasma protein will be high. The reduction of protein binding in 1% PEG coated nanoparticles could be attributed to the higher surface coverage which is obtained as a result of the conformation of the PEG chains in a 'brush-like' configuration as schematically illustrated in Fig. 3A. This conformation has been reported to result in a more efficient repulsion of protein (Owens and Peppas, 2006). On the other hand, the conformation of Pluronics on the surface of the particles as depicted in Fig. 3B would result in less surface coverage and thus a less efficient repulsion. The quantification of PEG and Pluronics in the formulation could not be carried out since PEG and Pluronics have similar composition to PVA which is also in the formulation, thus characterisation of the quantity of these poloxamers on the surface of the particles would not be accurate.

Particles were detected in all tissues over the 7 days and the plasma concentration of coated particles was higher than that of uncoated PLGA particles, indicating that the long residence time can also be achieved with oral formulations. Although accumulation of the particles was detected in the spleen and the brain, Semete et al. (2010) reported the safety of these particles in these tissues at high doses of PLGA particles. Furthermore, detection of the particles in the liver and the spleen irrespective of these particles being made stealth indicates that although opsonisation or protein binding is minimised, particle uptake/recognition by macrophages will still occur to some extent. In addition, the lower percentage of particles detected in plasma as opposed to the higher proportion in the liver, kidney and the lungs could be attributed to surface heterogeneity in the population of PEG or Pluronics coated PLGA particles. This surface heterogeneity and the hydrophobic nature of PLGA could further explain the presence of nanoparticles in the spleen (representing particles that are taken up by the M cells of the Peyer's patches *via* opsonisation) and the liver (representing particles that are taken up by the Kupffer cells of the liver).

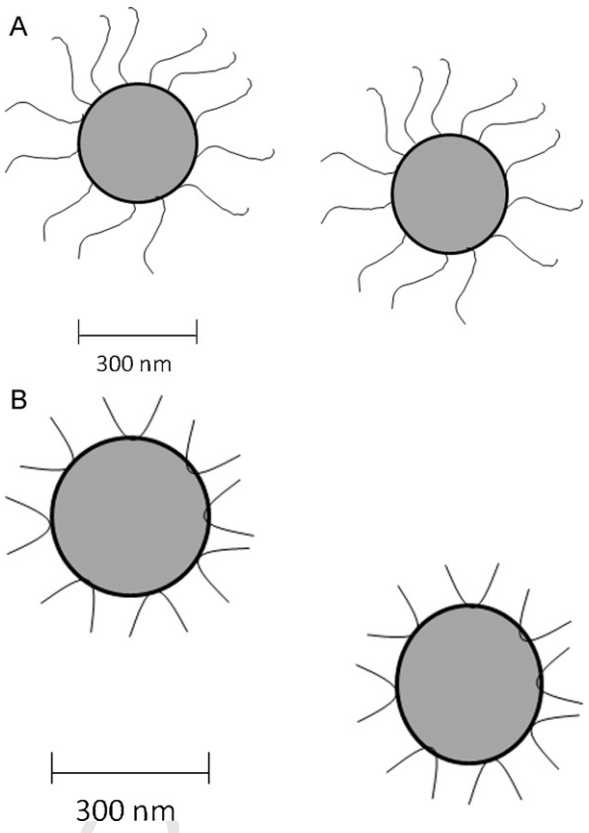

Fig. 3. Schematic illustration of the configuration of the poloxamers on PLGA nanoparticles. (A) Pluronics F127 and (B) PEG.

Although the 1% PEG–PLGA formulation resulted in reduced protein binding as per various reports (Owens and Peppas, 2006; Stolnik et al., 1995), when the same particles are administered orally, as much as there is a significant increase in the percentage detected in plasma, the distribution to various tissues is not significantly different to the non-stealth particles. Furthermore, these results indicate that for nanoparticle formulations *in vitro* observations cannot represent or be correlated to the *in vivo* behaviour of the nanoparticles. Our results therefore suggest that more studies have to be conducted for oral formulations to give a better understanding of the kinetics of the particles since they vary to that of intravenous formulations.

Conflict of interest

No conflict on interest exists.

Acknowledgements

We thank Mr Kobus Venter, at the Medical Research Council for assisting with the mice studies.

This study was funded by the South African Department of Science and Technology.

References

Bawarski, W.E., Chidlowsky, E., Bharali, D.J., Mousa, S.A., 2008. Emerging nanopharmaceuticals. Nanomedicine 4, 273–282.
Cui, G., Wang, L., Davis, P.J., Kara, M., Liu, H., 2006. Preparation and physical characterization of a novel marine oil emulsion as a potential new formulation vehicle for lipid soluble drugs. Int. J. Pharm. 325, 180–185.
Gref, R., Luck, M., Quellec, P., Marchand, M., Dellacherie, E., Harnisch, S., Blunk, T., Muller, R.H., 2000. 'Stealth' corona-core nanoparticles surface modified by polyethylene glycol (PEG): influences of the corona (PEG chain length and

surface density) and of the core composition on phagocytic uptake and plasma protein adsorption. Colloids Surf. B: Biointerfaces 18, 301–313.
Li, S.D., Huang, L., 2008. Pharmacokinetics and biodistribution of nanoparticles. Mol. Pharm. 5, 496–504.
Moghimi, S.M., Szebeni, J., 2003. Stealth liposomes and long circulating nanoparticles: critical issues in pharmacokinetics, opsonization and protein-binding properties. Prog. Lipid Res. 42, 463–478.
Owens 3rd, D.E., Peppas, N.A., 2006. Opsonization, biodistribution, and pharmacokinetics of polymeric nanoparticles. Int. J. Pharm. 307, 93–102.
Semete, B., Booysen, L., Lemmer, Y., Kalombo, L., Katata, L., Verschoor, J., Swai, H., 2010. In vivo evaluation of the biodistribution and safety of PLGA nanoparticles as drug delivery systems. Nanomedicine 6, 662–671.
Stolnik, S., Daudali, B., Arien, A., Whetstone, J., Heald, C.R., Garnett, M.C., Davis, S.S., Illum, L., 2001. The effect of surface coverage and conformation of poly(ethylene oxide) (PEO) chains of poloxamer 407 on the biological fate of model colloidal drug carriers. Biochim. Biophys. Acta 1514, 261–279.
Stolnik, S., Illum, L., Davis, S.S., 1995. Long circulating microparticulate drug carriers. Adv. Drug Deliv. Rev. 16, 195–214.
Takeuchi, H., Thongborisute, J., Matsui, Y., Sugihara, H., Yamamoto, H., Kawashima, Y., 2005. Novel mucoadhesion tests for polymers and polymer-coated particles to design optimal mucoadhesive drug delivery systems. Adv. Drug Deliv. Rev. 57, 1583–1594.
Tan, J.S., Butterfield, D.E., Voycheck, C.L., Caldwell, K.D., Li, J.T., 1993. Surface modification of nanoparticles by PEO/PPO block copolymers to minimize interactions with blood components and prolong blood circulation in rats. Biomaterials 14, 823–833.
Torchilin, V.P., Trubetskoy, V.S., 1995. Which polymers can make nanoparticulate drug carriers long-circulating. Adv. Drug Deliv. Rev. 16, 141–155.

Please cite this article in press as: Semete, B., et al., Effects of protein binding on the biodistribution of PEGylated PLGA nanoparticles post oral administration. Int J Pharmaceut (2012), doi:10.1016/j.ijpharm.2011.12.043

In vitro characterisation of PLGA nanoparticles encapsulating rifampicin and isoniazid - Towards IVIVC

L BOOYSEN[1,2], B SEMETE-MAKOKOTLELA[1], L.KALOMBO[1], H SWAI[2], AF KOTZÉ[1]
[1]CSIR, PO Box 395, Pretoria, 0001, South Africa
[2]Department of Pharmaceutics, North-West University, Potchefstroom Campus, Potchefstroom, 2531, South Africa
lbooysen@csir.co.za - www.csir.co.za

INTRODUCTION

It has been postulated that antituberculosis drugs encapsulated in polymeric nanoparticles are able to control the release of these drugs *in vivo*. These biodegradable polymers facilitate sustained/controlled release by means of degradation of the polymer or by diffusion through the polymer matrix. For oral drug delivery, one of the most important parameters to be elucidated is the absorption of not only the drugs, but also of the nanoparticles. These nanoparticles are postulated to be absorbed in tact and be transported through the lymphatic system.

Once in the systemic circulation, the biodistribution of the particles is highly dependent on its response to the biological environment, mainly binding to plasma proteins. Nanoparticle characteristics such as surface hydrophobicity, size and polymer composition determine the extent of adsorption of blood components, mainly proteins such as albumin and glycoproteins[1]. For drugs with a high degree of protein binding, protein adsorption effects on volume of distribution are observed[2].

Another class of proteins that plays an important role in protein binding are opsonins. Binding of these proteins promotes the activation of the complement system and facilitates phagocytotic uptake by macrophages[3]. To minimise opsonisation, the surfaces of nanoparticles can be modified with biodegradable copolymers with hydrophilic segments such as polyethylene glycol (PEG), including poloxamines and polysorbate 80 which will eventually prolong the duration of systemic circulation of the nanoparticles[4].

The objective of the current study was to determine the effect that PLGA (coated/uncoated with PEG/Pluronic F127) nanoencapsulation of rifampicin (RIF) and isoniazid (INH) has on plasma protein binding of these drugs *in vitro*. Furthermore, the biodistribution of Rhodamine 6G labelled PEG-coated and Pluronic F127-coated nanoparticles was evaluated.

METHODS

Nanoparticle formulations

Poly-lactic-glycolic-acid (PLGA) nanoparticles were prepared by the double emulsion spray drying technique developed by the CSIR. Various formulations of PLGA nanoparticles were prepared and the results are summarised in **Table 1**. PEG (Mw 10 000) and Pluronic-F127 (Mw 9 000) were used to coat the formulations. RIF and INH were gifts from North-West University, Potchefstroom campus, South Africa. Also prepared for biodistribution assays were Rhodamine-6G labelled uncoated nanoparticles and Rhodamine-6G labelled nanoparticles coated with 1% PEG. These nanoparticles were prepared by including Rhodamine-6G in the aqueous phase of the first water-in-oil (w/o) emulsion. .

Protein binding assays

The nanoparticle protein binding was analysed using an adapted method as described previously for protein adsorption to polymer nanoparticles[5]. *In vitro* protein binding of polymeric nanoparticles was determined by preparing varying ratios of plasma to nanoparticles (10: 90; 20:80; 40:60 volume/volume (v/v)) to a total volume of 600 μl. The plasma/nanoparticle suspension was incubated for two hours at room temperature and then centrifuged at 14 000 rpm for 45 minutes to obtain a nanoparticle pellet, following a two-hour incubation in human plasma. The Bradford assay was used for the quantitative analysis of the pellet (bound protein) and the supernatant (unbound protein). Sodium dodecyl sulfate polyacrylamide gel electrophoresis (SDS-PAGE) gels were used for qualitative analysis of the proteins in the pellet suspension. Protein binding of unencapsulated drug controls was analysed by equilibrium dialysis.

Biodistribution assays

To determine the biodistribution of PLGA nanoparticles of 1% PEG or 1% Pluronics-F127, these formulations were fluorescently labelled with Rhodamine 6G and orally administered to mice at 4 mg particles in 0.2 ml sterile saline by oral gavage. The biodistribution of uncoated PLGA nanoparticles illustrated in **Figure 1** was reported previously[6]. The mice were grouped. Each group had three mice and the study was repeated three times. Group one was treated with drug-free PLGA-nanoparticles; group two with 1% PEG-PLGA nanoparticles and group three with 1% Pluronics F127-PLGA-nanoparticles. Oral administration was performed on the same day and the mice were euthanized at one, three or seven days post administration. The percentage detected was expressed as the ratio of the fluorescence unit of each tissue relative to the sum of fluorescence units of all tissues analysed.

Table 1: Summary of nanoparticle characterization

Formulation	Size (nm)	PdI	Encapsulation efficiency (%)	Drug loading (%)	Zeta potential
1. PLGA-DF	296.8	0.229	N/A	N/A	35.2
2. 1% PEG-DF	304.4	0.465	N/A	N/A	39.9
3. 1% Pluronic-DF	310.5	0.417	N/A	N/A	38.6
4. PLGA-RIF	399.2	0.325	69.2	7.64	14.4
5. 1% PEG-RIF	337.8	0.435	65.2	8.4	19.1
6. 1%Pluronic-RIF	260.1	0.355	67.34	8.53	16
7. PLGA-INH	253.4	0.12	73.5	23.43	15.8
8. 1% PEG-INH	281.1	0.35	67.65	24.8	8.52
9.1%Pluronic-INH	319.5	0.347	69	27.6	13.7
PLGA-Rhd(1% PEG)	313.3	0.303	N/A	N/A	N/A
PLGA-Rhd(1% PLU)	442.7	0.293	N/A	N/A	N/A

PLGA-poly-(lactic-co-glycolic) acid; PEG-poly ethylene glycol; DF-drug-free; RIF-rifampicin; INH- isoniazid; Rhd-Rhodamine; PLU- Pluronic

RESULTS

Protein binding

Table 2 illustrates the results observed for the different formulations. At a 10% plasma volume, PLGA-DF formulations demonstrated an average protein binding of 25.02% ± 4.58. A comparison between this formulation and a similar formulation coated with 1% Pluronic F127 illustrated no significant difference in plasma protein binding ($p > 0.01$, 95% confidence level, (CI)). However, the formulation coated with 1% PEG resulted in a percentage protein binding of 31.41% ± 13.8. This result was found to be significantly different when compared to the uncoated formulation ($p < 0.01$).

Comparison of 10%, 20% and 40% v/v ratio of whole plasma to nanoparticle suspension demonstrated no significant difference for the uncoated drug free formulations. A significant increase was observed for Pluronic-F127 coated formulations whereas PEG coated drug free formulation demonstrated a significant decrease in protein binding with an increase in plasma volume. Therefore, the affinity of PEG coated nanoparticles for plasma proteins are dependent on plasma content. For nanoparticles (coated/uncoated) encapsulating RIF, a significant decrease in protein binding is observed when compared to unencapsulated (free) drug.

A 57% decrease in protein binding was observed when PLGA-RIF nanoparticles were coated with 1% PEG (10.16% ± 4.32 protein binding). For formulations encapsulating INH, no significant difference in protein binding was seen for the different formulations. However, nanoencapsulation facilitated decreased protein binding compared to free INH.

Table 2: Data summary of protein binding studies for various nanoparticle formulations with varying ratios of Plasma: Nanoparticle suspension

Nanoparticle formulations										
PLGA-DF	1% PLURONIC	1% PEG	PLGA-RIF	1%PEG-RIF	1% PLURONIC RIF	PLGA-INH	1% PLURONIC INH	1% PEG-INH	Control RIF *	Control INH *
Average percentage 10/90										
25.02 (4.58)	22.78 (6.49)	31.41 (13.80)	23.95 (8.60)	10.16 (4.32)	17.31 (6.78)	19.80 (4.30)	18.46 (3.88)	18.94 (3.7)	71.12 (0.78	43.37 (6.6)
Average percentage 20/80										
22.03 (4.81)	21.23 (6.62)	20.57 (6.60)	18.83 (7.50)	16.87 (2.11)	17.58 (2.86)	13.15 (5.81)	15.51 (6.34)	14.40 (4.60)	79.47 (1.60)	29.96 (10.90)
Average percentage 40/60										
20.91 (4.44)	31.30 (9.76)	14.32 (7.40)	15.40 (5.50)	12.92 (2.15)	16.57 (5.18)	15.07 (3.40)	12.77 (5.41)	15.80 (2.00)	90.00 (1.38)	23.00 (5.2)

* % protein bound was calculated as 100 minus % unbound. Standard deviations shown in parentheses. Experiments were repeated three time (n=3)

BIODISTRIBUTION

From this data illustrated in **Figure 1**, it is evident that most of the particles were detected in the liver at 40.04% ± 8.42%), followed by the kidney (25.97% ± 7.09%), heart (11.92% ± 3.16%), and brain (12.86% ± 2.82%) throughout all seven days in which the tissues were analysed. However, very low concentrations or no particles were observed in the plasma over the same period when plasma collected on day one, three and seven was analysed. The biodistribution for the uncoated nanoparticles warranted surface modification to minimise particle localisation in the liver.

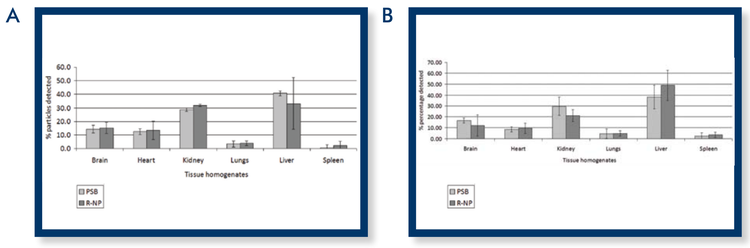

Figure 1:
A = biodistribution of coated PLGA nanoparticles after one day oral administration,
B = day three after oral administration,
C = day seven after oral administration. R-NP= rhodamine nanoparticles; PSB= polystyrene beads

Figure 2:
A = biodistribution of coated PLGA nanoparticles after one day oral administration,
B = day three after oral administration,
C = day seven after oral administration.

Determining the effect of protein binding of nanoencapsulated drugs and its uptake in different organs.

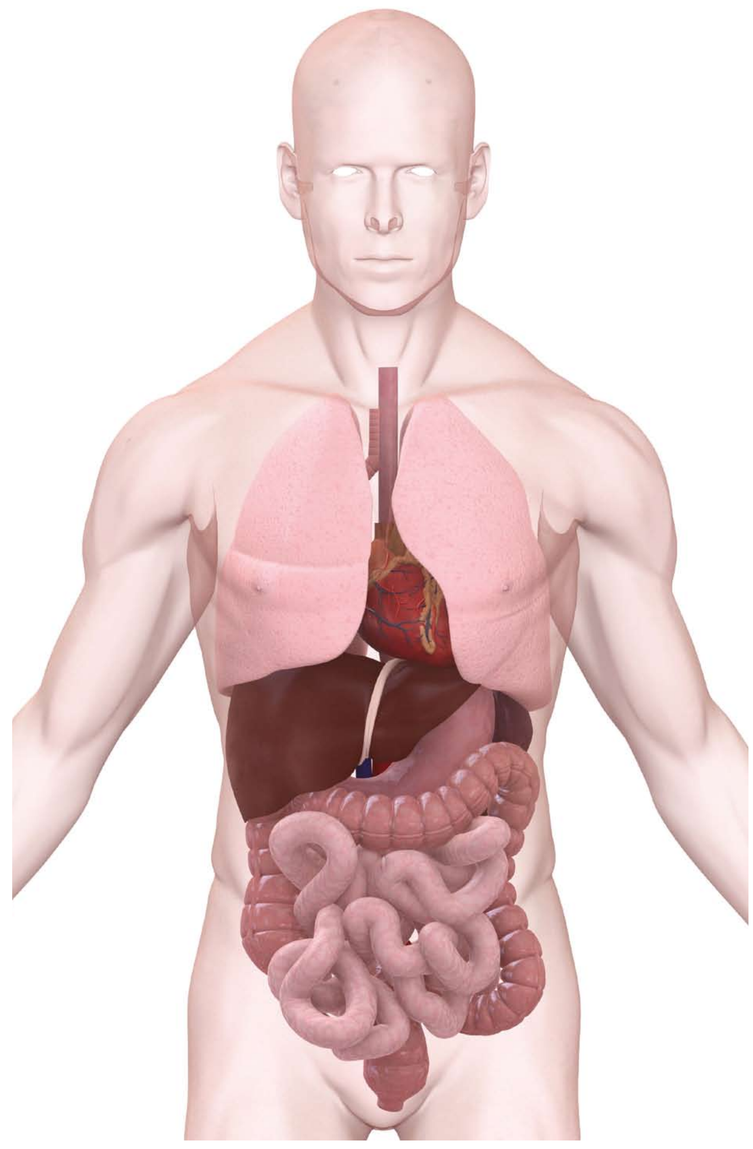

Therefore, 1% PEGylated or pluronic F127 coated particles were orally administered and the biodistribution profile is indicated in Figure 2. The presence of PEG coated particles in the brain decreased over the seven days whereas the presence of particles in the heart, kidney and liver remained relatively constant. Increased accumulations in the lungs were observed. A slight accumulation of particles was detected in the spleen, indicating uptake by the M cells of the payers patches. However, Pluronic F127 coated particles resulted in an accumulation in the brain over the seven days. A similar profile to that of PEG coated particles was observed in the rest of the tissues. In both cases, plasma concentrations were significantly higher than those reported in Semete et al., 2010 for uncoated PLGA particles[6].

CONCLUSION

The decrease in protein binding of RIF observed in this study due to nanoencapsulation would result in higher drug concentrations being available to exert a therapeutic effect. Whether or not *in vivo* protein binding kinetics can be predicted using *in vitro* assays has been a subject of much debate. The *in vitro* data demonstrate decreased protein binding of polymeric nanoparticles coated with a poloxamer may facilitate minimum exposure to protein of highly protein bound drugs such as RIF as well as improve the biodistribution of nanoparticles. This study concludes that poloxamer coating of polymer nanoparticles presents a longer circulation time due to decreased protein binding with a subsequent increase of nanoparticles accumulation in tissues, primarily plasma and spleen.

ACKNOWLEDGEMENTS

Department of Science and Technology for funding
TB Nano Drug Delivery Project, Polymers and Composites, MSM

REFERENCES

1. W. E. Lindup & M. C. L. 'E. Orme,. *Plasma protein binding of drugs*, 282 BRITISH MEDICAL JOURNAL.212, 212-214 (1981).
2. M. A HEDAYA,. BASIC PHARMACOKINETICS 1-300. (CRC Press 2007)
3. Jeffrey Kingsley et al. *Nanotechnology: A Focus on Nanoparticles as a Drug Delivery System*, 1 JOURNAL OF NEUROIMMUNE PHARMACOLOGY.340, 340-350 (2006).
4. V. J. Mohanraj & Y. Chen,. *Nanoparticles-A review*, 5 TROPICAL JOURNAL OF PHARMACEUTICAL RESEARCH.561, 561-573 (2006).
5. S. Stolnik et al. *The effect of surface coverage and conformation of poly(ethylene oxide) (PEO) chains of poloxamer 407 on the biological fate of model colloidal drug carriers*, 1514 BIOCHIMICA ET BIOPHYSICA ACTA (BBA) - BIOMEMBRANES.261, 261-279 (2001).
6. B. Semete et al. *In vivo evaluation of the biodistribution and safety of PLGA nanoparticles as drug delivery systems*, Article in press NANOMEDICINE: NANOTECHNOLOGY, BIOLOGY AND MEDICINE. (2010).

Appendix C: Supporting data

Fluorescence intensities of rhodamine labelled PLGA nanoparticles compared to rhodamine-only nanoparticles detected in the organs evaluated on day 1, 3 and 7 described in chapter 4.

	Brain	Heart	Kidney	Liver	Lungs	Spleen
R-NP day 1	35.9	47.8	53.9	67.1	8.9	3.8
R day 1	2.4	1	11.8	4	1	1
R-NP day 3	36.3	28.4	170.4	63.4	14.4	10.5
R day 3	4.8	1	4.2	6	1	1
R-NP day 7	40.3	64.8	156.8	93.2	43.2	29.5
R day 7	5	1	2	2	1	1

R-NP- rhodamine nanoparticles; R- rhodamine only. Values presented as mean (n=3).

Raw data for bioavailability assays described in chapter 5. Numbering depicts reading for each serum sample per mouse for different time points (three mice per time point) for the different test groups, i.e. RIF and INH nanoparticles versus unencapsulated drugs.

Plate 1: RIF nanoparticles, @ 2hrs., 8hrs., and 1 day

	2 hrs.			8 hrs.			1 day		
Dilutions	**1.1**	**1.2**	**1.3**	**1.4**	**1.5**	**1.6**	**1.7**	**1.8**	**1.9**
1/10	0.083	0.092	0.089	0.134	0.134	0.173	0.098	0.07	0.056
1/20	0.087	0.066	0.069	0.068	0.078	0.106	0.103	0.072	0.103
1/40	0.066	0.062	0.065	0.068	0.077	0.08	0.246	0.103	0.307
1/80	0.072	0.069	0.067	0.067	0.074	0.076	0.24	0.173	0.279
1/160	0.066	0.065	0.071	0.072	0.075	0.097	0.36	0.282	0.318
1/320	0.07	0.072	0.072	0.09	0.076	0.123	0.273	0.34	0.291

Plate 2: RIF nanoparticles, @ 2 days, 3 days, and 7 days

	2 days			3 days			7 days		
Dilutions	**1.10**	**1.11**	**1.12**	**1.13**	**1.14**	**1.15**	**1.16**	**1.17**	**1.18**
1/10	0.236	0.329	0.156	0.167	0.187	0.263	N/A*	0.283	N/A*
1/20	0.34	0.402	0.381	0.407	0.395	0.362	0.385	0.311	0.343
1/40	0.403	0.424	0.405	0.422	0.395	0.409	0.46	0.411	0.443
1/80	0.537	0.408	0.41	0.46	0.41	0.474	0.456	0.418	0.462
1/160	0.402	0.411	0.429	0.393	0.375	0.477	0.392	0.406	0.479
1/320	0.356	0.446	0.451	0.45	0.455	0.505	0.512	0.421	0.555

Plate 3: INH nanoparticles, @ 2hr, 8hr, and 1 day

	2 hr			8 hr			1 day		
Dilutions	**2.1**	**2.2**	**2.3**	**2.4**	**2.5**	**2.6**	**2.7**	**2.8**	**2.9**
1/10	0.088	0.081	0.119	0.108	0.061	0.112	0.414	0.509	0.633
1/20	0.073	0.067	0.077	N/A*	0.062	0.066	0.343	0.429	0.481
1/40	0.067	0.062	0.065	0.063	0.065	0.068	0.411	0.433	0.529
1/80	0.068	0.065	0.066	0.285	0.389	0.077	0.448	0.448	0.503
1/160	0.069	0.064	0.067	0.444	0.406	0.358	0.49	0.353	0.527
1/320	0.073	0.067	0.07	0.484	0.464	0.484	0.509	0.529	0.512

Plate 4: INH nanoparticles, @ 2 days, 3 days, and 7 days

	2 days			3 days			7 days		
Dilutions	**2.10**	**2.11**	**2.12**	**2.13**	**2.14**	**2.15**	**2.16**	**2.17**	**2.18**
1/10	0.608	0.108	0.501	N/A*	0.202	0.248	0.254	N/A*	0.321
1/20	0.651	0.253	0.519	0.514	0.506	0.469	0.527	0.462	0.507
1/40	0.509	0.264	0.469	0.445	0.467	0.471	0.406	0.344	0.394
1/80	0.574	0.271	0.502	0.448	0.344	0.479	0.399	0.364	0.415
1/160	0.507	0.329	0.389	0.474	0.323	0.427	0.449	0.439	0.397
1/320	0.431	0.354	0.496	0.473	0.445	0.39	0.416	0.45	0.4

Plate 5: RIF free drug @ 2hr, 8hr, and 1 day

	2 hr			8 hr			1 day		
Dilutions	**3.1**	**3.2**	**3.3**	**3.4**	**3.5**	**3.6**	**3.7**	**3.8**	**3.9**
1/10	0.255	0.101	0.077	0.123	0.189	0.23	0.232	N/A*	0.082
1/20	0.086	0.08	0.072	0.076	0.071	0.067	0.128	0.168	0.076
1/40	0.074	0.08	0.066	0.071	0.073	0.066	0.096	0.145	0.067
1/80	0.071	0.069	0.073	0.072	0.071	0.065	0.082	0.132	0.067
1/160	0.071	0.078	0.068	0.071	0.074	0.062	0.075	0.096	0.067
1/320	0.074	0.073	0.07	0.068	0.067	0.065	0.093	0.083	0.079

Plate 6: RIF free drug @ 2 days; Controls with and without serum

	2 days			Drugs Without Serum		Drugs With Serum	
	3.10	**3.11**	**3.12**				
1/10	0.084	0.083	0.069	0.046	0.09	0.102	0.146
1/20	0.19	0.168	0.154	0.043	0.208	0.077	0.365
1/40	0.377	0.254	0.54	0.042	0.43	0.068	0.317
1/80	0.521	0.343	0.382	0.044	0.386	0.065	0.384
1/160	0.416	0.279	0.371	0.043	0.287	0.071	0.438
1/320	0.271	0.321	0.377	0.053	0.366	0.068	0.559

Plate 7: INH free drug @ 2hr, 8hr, and 1 day

	2 hr			8 hr			1 day		
	4.1	**4.2**	**4.3**	**4.4**	**4.5**	**4.6**	**4.7**	**4.8**	**4.9**
1/10	0.075	0.06	0.069	0.107	0.574	0.093	0.489	0.409	0.406
1/20	0.064	0.069	0.084	0.091	0.508	0.516	0.463	0.363	0.328
1/40	0.067	0.065	0.068	0.392	0.444	0.482	0.441	0.344	0.4
1/80	0.069	0.067	0.072	0.424	0.412	0.343	0.399	0.402	0.459
1/160	0.074	0.071	0.076	0.469	0.42	0.325	0.404	0.455	0.378
1/320	0.073	0.07	0.069	0.469	0.301	0.382	0.415	0.432	0.437

Plate 8: INH free drug @ 2 days; Controls with and without serum

	2 days			Drugs Without Serum		Drugs With Serum	
	4.10	**4.11**	**4.12**				
1/10	0.363	0.654	0.312	0.042	0.055	0.071	0.07
1/20	0.469	0.695	0.568	0.053	0.402	0.069	0.541
1/40	0.479	0.51	0.477	0.051	0.201	0.068	0.445
1/80	0.524	0.493	0.56	0.053	0.531	0.067	0.497
1/160	0.545	1.23	0.502	0.053	0.46	0.063	0.393
1/320	0.479	0.593	0.485	0.051	0.518	0.069	0.455

*N/A due to possible contaminated well.

Raw data for MIC studies described in chapter 5

Average OD_{600} reading of free INH over 18 days								
µg/ml	**Day 1**	**Day 4**	**Day 6**	**Day 8**	**Day 11**	**Day 13**	**Day 15**	**Day 18**
Untreated control	0.057	0.209	0.396	0.636	0.508	0.923	0.884	0.806
INH-FREE 0.48	0.053	0.076	0.078	0.073	0.068	0.064	0.067	0.120
INH-FREE 0.24	0.054	0.122	0.162	0.271	0.361	0.708	0.542	0.367
INH-FREE 0.12	0.050	0.075	0.082	0.078	0.072	0.070	0.070	0.423
INH-FREE 0.06	0.051	0.110	0.168	0.184	0.163	0.427	0.469	0.465
INH-FREE 0.03	0.053	0.126	0.156	0.172	0.187	0.239	0.245	0.772
INH-FREE 0.015	0.057	0.224	0.335	0.453	0.625	0.424	0.687	0.663
INH-FREE 0.0075	0.051	0.228	0.410	0.470	0.625	0.668	0.970	0.646
INH-FREE 0.00375	0.054	0.257	0.478	0.514	0.674	1.050	0.948	0.803
INH-FREE 0.001875	0.053	0.221	0.519	0.518	0.576	1.090	0.786	1.225
Standard deviation								
µg/ml	**Day 1**	**Day 4**	**Day 6**	**Day 8**	**Day 11**	**Day 13**	**Day 15**	**Day 18**
Untreated control	0.005	0.043	0.153	0.108	0.338	0.195	0.277	0.227
INH-FREE 0.48	0.006	0.003	0.002	0.003	0.003	0.003	0.003	0.002
INH-FREE 0.24	0.005	0.064	0.123	0.313	0.448	0.563	0.496	0.134
INH-FREE 0.12	0.003	0.003	0.003	0.003	0.005	0.001	0.002	0.088
INH-FREE 0.06	0.003	0.074	0.202	0.247	0.205	0.600	0.661	0.183
INH-FREE 0.03	0.003	0.065	0.112	0.160	0.218	0.234	0.240	0.233
INH-FREE 0.015	0.005	0.024	0.058	0.037	0.148	0.136	0.338	0.353
INH-FREE 0.0075	0.004	0.033	0.118	0.153	0.281	0.100	0.238	0.298
INH-FREE 0.00375	0.004	0.020	0.140	0.188	0.296	0.189	0.346	0.230
INH-FREE 0.001875	0.004	0.027	0.076	0.288	0.124	0.100	0.298	0.060

Average OD_{600} reading of nanoencapsulated INH over 18 days								
µg/ml	**Day 1**	**Day 4**	**Day 6**	**Day 8**	**Day 11**	**Day 13**	**Day 15**	**Day 18**
Untreated control	0.054	0.175	0.454	0.334	0.456	0.735	0.985	0.884
INH-NP 32	0.091	0.279	0.299	0.256	0.291	0.117	0.125	0.124
INH-NP 16	0.067	0.096	0.153	0.162	0.195	0.328	0.361	0.434
INH-NP 8	0.057	0.164	0.309	0.352	0.395	0.629	0.502	0.547
INH-NP 4	0.055	0.237	0.440	0.622	0.483	0.676	0.891	0.548
INH-NP 2	0.053	0.232	0.441	0.521	0.796	0.843	0.857	0.987
INH-NP 1	0.052	0.235	0.486	0.642	0.648	0.991	0.983	0.978
INH-NP 0.5	0.051	0.223	0.519	0.559	0.795	0.788	0.746	0.661
INH-NP 0.25	0.050	0.199	0.447	0.583	0.806	0.765	0.689	0.803
INH-NP 0.125	0.053	0.215	0.390	0.519	0.628	0.811	0.881	0.901
Standard deviation								
µg/ml	**Day 1**	**Day 4**	**Day 6**	**Day 8**	**Day 11**	**Day 13**	**Day 15**	**Day 18**
Untreated control	0.001	0.029	0.085	0.212	0.208	0.189	0.271	0.191
Untreated control	0.012	0.400	0.431	0.328	0.430	0.012	0.011	0.011
INH-NP 32	0.010	0.008	0.118	0.150	0.231	0.387	0.434	0.492
INH-NP 16	0.005	0.024	0.070	0.107	0.138	0.081	0.236	0.113
INH-NP 8	0.004	0.023	0.075	0.130	0.227	0.059	0.211	0.272
INH-NP 4	0.003	0.035	0.165	0.289	0.295	0.174	0.159	0.142
INH-NP 2	0.003	0.012	0.040	0.127	0.219	0.044	0.118	0.429
INH-NP 1	0.003	0.035	0.048	0.140	0.202	0.272	0.102	0.209
INH-NP 0.5	0.004	0.039	0.041	0.136	0.160	0.175	0.129	0.211
INH-NP 0.25	0.002	0.024	0.058	0.209	0.307	0.294	0.132	0.387

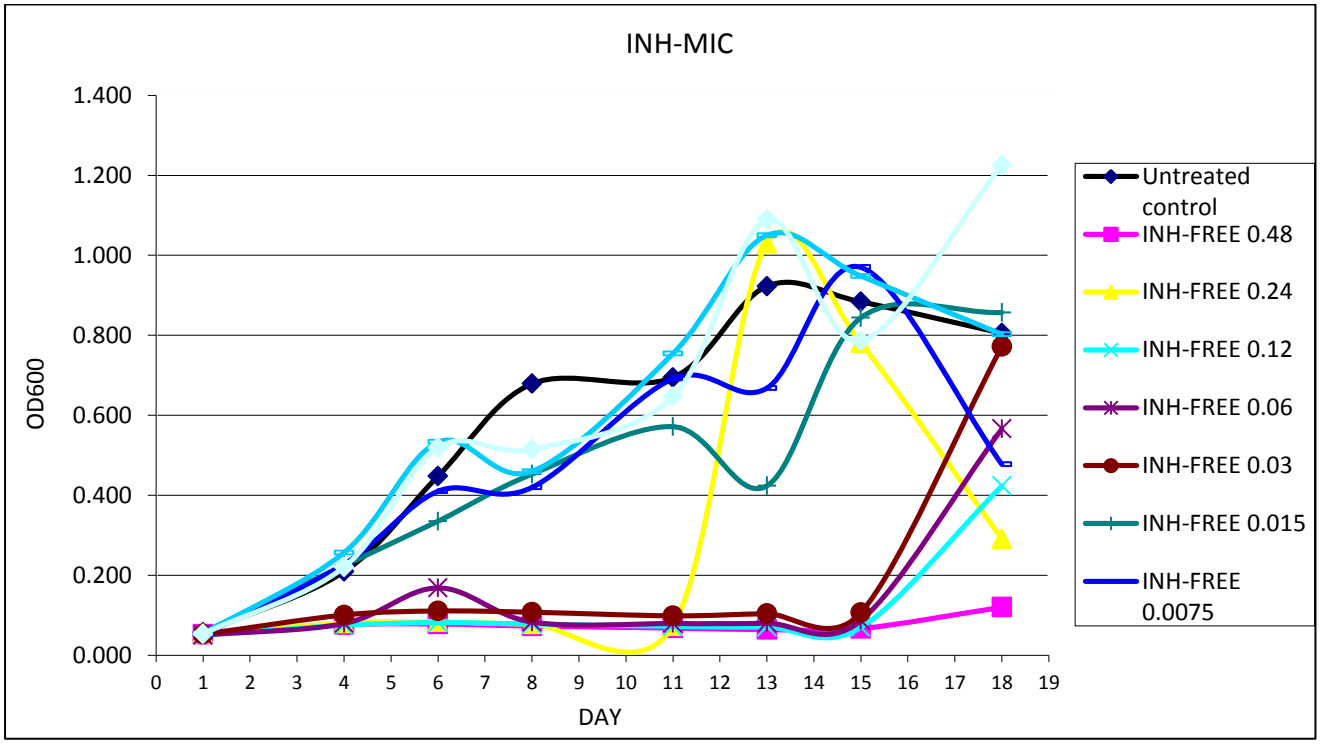

MIC summary graph for free INH.

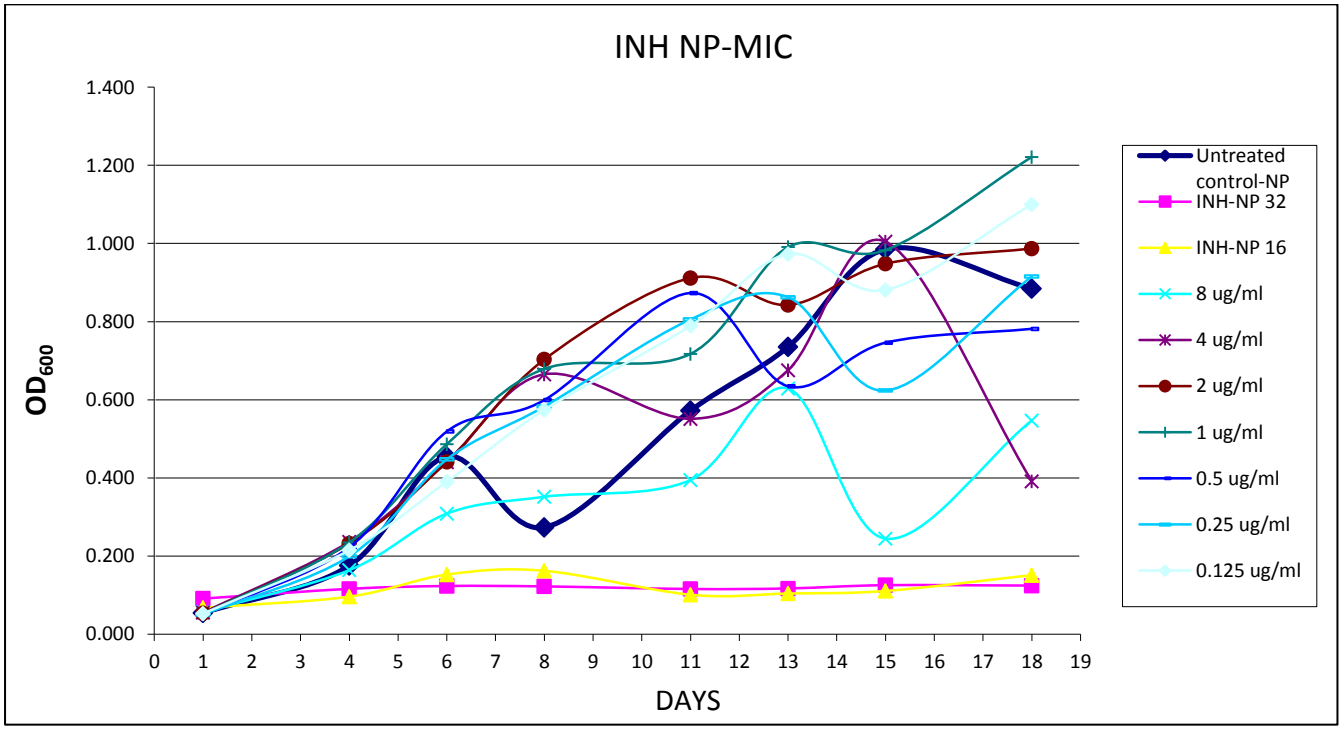

MIC summary graph for nanoencapsulated INH.

Average OD_{600} reading of free RIF over 18 days								
µg/ml	**Day 1**	**Day 4**	**Day 6**	**Day 8**	**Day 11**	**Day 13**	**Day 15**	**Day 18**
Untreated control	0.053	0.227	0.460	0.606	0.702	0.522	0.635	0.808
RIF FREE 0.96	0.054	0.066	0.062	0.057	0.059	0.044	0.057	0.056
RIF FREE 0.48	0.053	0.065	0.063	0.059	0.063	0.046	0.074	0.085
RIF FREE 0.24	0.050	0.072	0.084	0.092	0.116	0.158	0.259	0.411
RIF FREE 0.12	0.053	0.070	0.072	0.074	0.090	0.089	0.122	0.157
RIF FREE 0.06	0.053	0.101	0.140	0.178	0.239	0.290	0.337	0.456
RIF FREE 0.03	0.051	0.114	0.178	0.244	0.361	0.477	0.720	0.462
RIF FREE 0.015	0.050	0.130	0.248	0.368	0.524	0.589	0.800	1.004
RIF FREE 0.0075	0.053	0.144	0.248	0.416	0.578	0.731	0.673	0.900
RIF FREE 0.00375	0.052	0.148	0.300	0.460	0.665	0.773	0.789	0.681
Standard deviation								
µg/ml	**Day 1**	**Day 4**	**Day 6**	**Day 8**	**Day 11**	**Day 13**	**Day 15**	**Day 18**
Untreated control	0.003	0.016	0.081	0.281	0.399	0.208	0.241	0.238
RIF FREE 0.96	0.003	0.002	0.002	0.001	0.002	0.004	0.003	0.002
RIF FREE 0.48	0.002	0.003	0.004	0.005	0.010	0.002	0.029	0.048
RIF FREE 0.24	0.002	0.014	0.033	0.051	0.079	0.101	0.142	0.168
RIF FREE 0.12	0.004	0.002	0.003	0.007	0.010	0.013	0.026	0.034
RIF FREE 0.06	0.002	0.004	0.013	0.022	0.042	0.048	0.021	0.100
RIF FREE 0.03	0.004	0.011	0.018	0.035	0.073	0.096	0.218	0.105
RIF FREE 0.015	0.006	0.012	0.038	0.035	0.063	0.122	0.126	0.392
RIF FREE 0.0075	0.005	0.006	0.033	0.060	0.158	0.213	0.202	0.267
RIF FREE 0.00375	0.003	0.011	0.024	0.045	0.084	0.132	0.051	0.262

Average OD_{600} reading of nanoencapsulated INH over 18 days								
µg/ml	**Day 1**	**Day 4**	**Day 6**	**Day 8**	**Day 11**	**Day 13**	**Day 15**	**Day 18**
Untreated control	0.054	0.178	0.454	0.581	0.801	0.843	1.117	0.806
RIF-NP 32	0.102	0.140	0.131	0.133	0.133	0.126	0.121	0.120
RIF-NP 16	0.071	0.104	0.140	0.172	0.126	0.471	0.590	0.291
RIF-NP 8	0.060	0.100	0.143	0.178	0.250	0.328	0.409	0.423
RIF-NP 4	0.055	0.128	0.217	0.292	0.436	0.605	0.724	0.566
RIF-NP 2	0.053	0.140	0.261	0.357	0.578	0.529	0.396	0.639
RIF-NP 1	0.050	0.162	0.354	0.459	0.600	0.707	0.906	0.857
RIF-NP 0.5	0.054	0.180	0.431	0.470	0.266	0.458	0.583	0.478
RIF-NP 0.25	0.052	0.204	0.438	0.440	0.743	0.343	0.890	0.803
RIF-NP 0.125	0.049	0.200	0.459	0.589	0.833	1.127	0.991	1.225
Standard deviation								
µg/ml	**Day 1**	**Day 4**	**Day 6**	**Day 8**	**Day 11**	**Day 13**	**Day 15**	**Day 18**
Untreated control	0.006	0.040	0.111	0.199	0.283	0.319	0.340	0.227
RIF-NP **32**	0.013	0.008	0.009	0.006	0.008	0.004	0.002	0.002
RIF-NP **16**	0.012	0.014	0.054	0.100	0.131	0.175	0.274	0.134
RIF-NP **8**	0.004	0.005	0.011	0.020	0.037	0.059	0.047	0.088
RIF-NP **4**	0.004	0.011	0.029	0.042	0.086	0.103	0.105	0.183
RIF-NP **2**	0.002	0.009	0.115	0.190	0.185	0.281	0.367	0.233
RIF-NP **1**	0.001	0.008	0.042	0.069	0.072	0.114	0.255	0.353
RIF-NP **0.5**	0.004	0.019	0.037	0.096	0.343	0.310	0.229	0.298
RIF-NP **0.25**	0.005	0.022	0.077	0.265	0.269	0.090	0.104	0.230
RIF-NP **0.125**	0.003	0.023	0.047	0.170	0.189	0.311	0.242	0.060

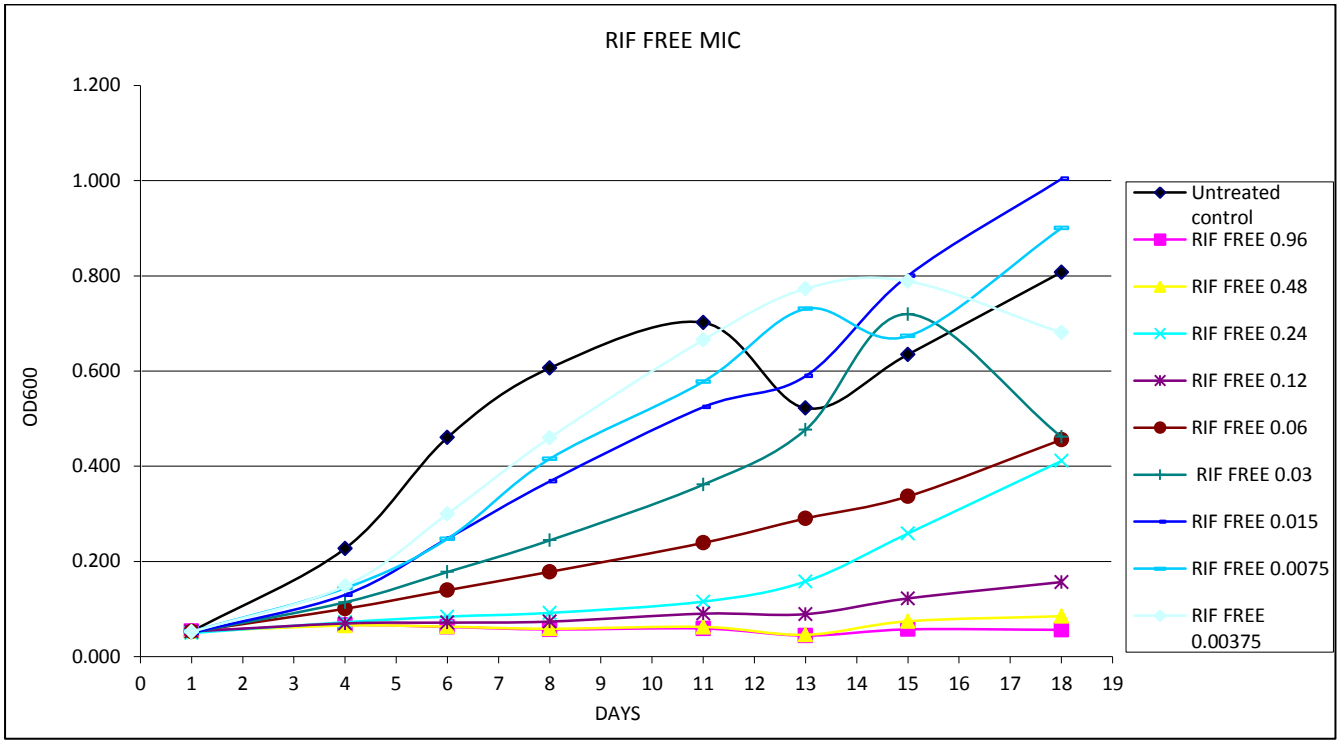

MIC summary graph for free RIF.

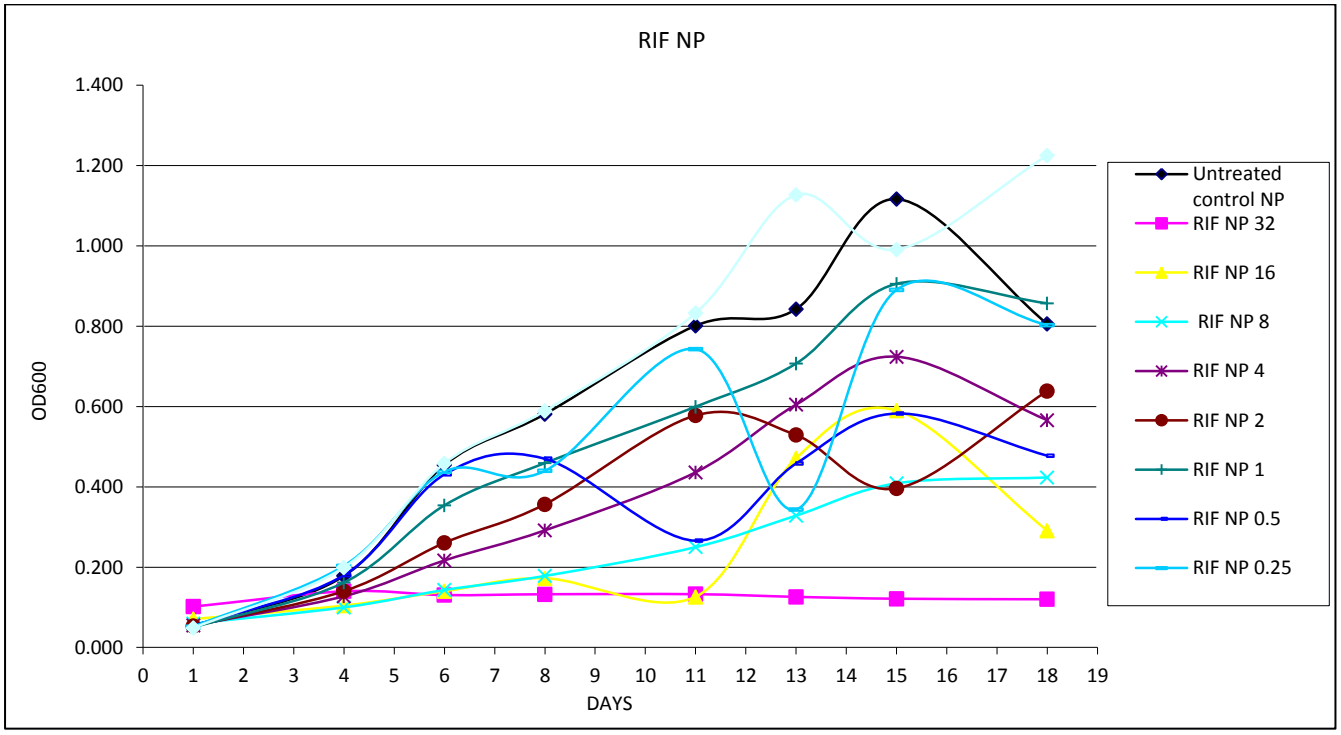

MIC summary graph for nanoencapsulated RIF.

Average OD_{600} reading of free ETB over 18 days								
µg/ml	**Day 1**	**Day 4**	**Day 6**	**Day 8**	**Day 11**	**Day 13**	**Day 15**	**Day 18**
Untreated control	0.057	0.243	0.472	0.570	0.768	1.062	0.937	0.793
ETB FREE 16	0.053	0.090	0.096	0.095	0.065	0.066	0.078	0.069
ETB FREE 8	0.054	0.106	0.088	0.088	0.070	0.067	0.076	0.051
ETB FREE 4	0.054	0.090	0.090	0.087	0.071	0.074	0.081	0.077
ETB FREE 2	0.053	0.091	0.091	0.088	0.075	0.074	0.082	0.078
ETB FREE 1	0.051	0.143	0.158	0.198	0.318	0.595	0.576	0.644
ETB FREE 0.5	0.051	0.181	0.325	0.359	0.525	1.256	1.077	1.042
ETB FREE 0.25	0.053	0.210	0.467	0.493	0.686	0.750	0.970	0.495
ETB FREE 0.125	0.054	0.242	0.466	0.461	0.645	0.875	0.832	0.958
ETB FREE 0.0625	0.054	0.243	0.408	0.598	0.859	0.496	1.068	0.884
Standard deviation								
µg/ml	**Day 1**	**Day 4**	**Day 6**	**Day 8**	**Day 11**	**Day 13**	**Day 15**	**Day 18**
Untreated control	0.003	0.025	0.108	0.162	0.299	0.292	0.378	0.205
ETB FREE 16	0.003	0.004	0.005	0.003	0.013	0.005	0.002	0.005
ETB FREE 8	0.002	0.046	0.173	0.058	0.186	0.540	0.671	0.477
ETB FREE 4	0.004	0.005	0.006	0.007	0.007	0.005	0.005	0.010
ETB FREE 2	0.004	0.006	0.002	0.003	0.008	0.005	0.003	0.005
ETB FREE 1	0.004	0.049	0.159	0.220	0.343	0.272	0.106	0.348
ETB FREE 0.5	0.002	0.038	0.125	0.110	0.118	0.403	0.191	0.209
ETB FREE 0.25	0.004	0.022	0.060	0.127	0.193	0.159	0.350	0.196
ETB FREE 0.125	0.006	0.009	0.074	0.179	0.255	0.283	0.108	0.252
ETB FREE 0.0625	0.004	0.026	0.099	0.240	0.415	0.155	0.439	0.416

Average OD_{600} reading of nanoencapsulated ETB over 18 days								
µg/ml	**Day 1**	**Day 4**	**Day 6**	**Day 8**	**Day 11**	**Day 13**	**Day 15**	**Day 18**
Untreated control NP	0.050	0.205	0.499	0.532	0.368	0.777	0.904	0.798
ETB NP 32	0.086	0.282	0.460	0.519	0.712	0.843	0.953	0.766
ETB NP 16	0.059	0.221	0.439	0.530	0.665	1.066	0.884	0.936
ETB NP 8	0.056	0.230	0.464	0.594	0.598	0.917	0.739	0.898
ETB NP 4	0.054	0.246	0.456	0.498	0.587	0.952	0.712	0.718
ETB NP 2	0.054	0.234	0.421	0.317	0.473	0.745	1.078	1.030
ETB NP 1	0.053	0.270	0.411	0.545	0.554	1.044	0.682	1.239
ETB NP 0.5	0.056	0.248	0.299	0.478	0.562	0.658	0.824	0.971
ETB NP 0.25	0.049	0.266	0.417	0.591	0.450	0.738	1.022	0.818
ETB NP 0.125	0.049	0.258	0.405	0.610	0.724	0.696	0.650	0.627
Standard deviation								
µg/ml	**Day 1**	**Day 4**	**Day 6**	**Day 8**	**Day 11**	**Day 13**	**Day 15**	**Day 18**
Untreated control	0.0027	0.0478	0.0762	0.1816	0.1549	0.2076	0.2025	0.3935
ETB NP 32	0.0226	0.0720	0.0407	0.1897	0.3943	0.2454	0.1146	0.3580
ETB NP 16	0.0064	0.0303	0.0932	0.2068	0.3724	0.1397	0.0765	0.5071
ETB NP 8	0.0033	0.0321	0.0874	0.2211	0.3341	0.1023	0.1424	0.4800
ETB NP 4	0.0044	0.0410	0.0815	0.2535	0.2381	0.1350	0.3177	0.2425
ETB NP 2	0.0032	0.0383	0.1394	0.2067	0.1184	0.3439	0.3307	0.6011
ETB NP 1	0.0026	0.0154	0.1131	0.1484	0.2525	0.2985	0.5230	0.1268
ETB NP 0.5	0.0033	0.0421	0.1137	0.2916	0.2237	0.4855	0.3866	0.1141
ETB NP 0.25	0.0044	0.0182	0.0833	0.1713	0.2544	0.3516	0.1144	0.5355
ETB NP 0.125	0.0024	0.0077	0.1400	0.0877	0.2070	0.1542	0.2011	0.4157

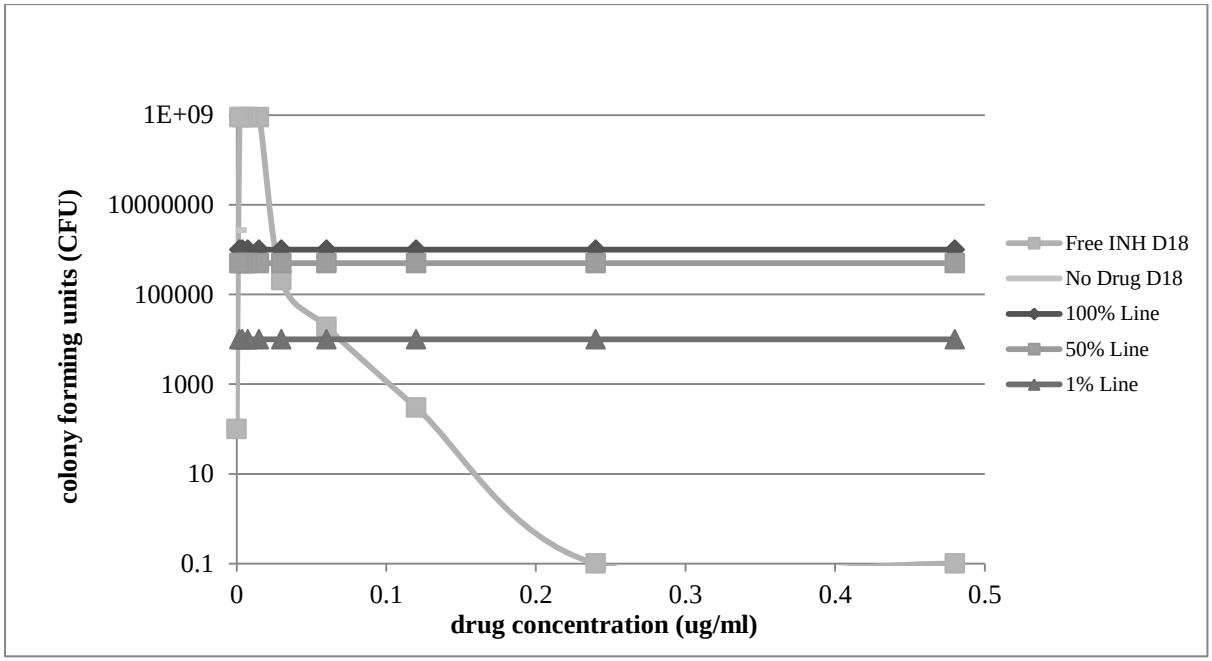

A

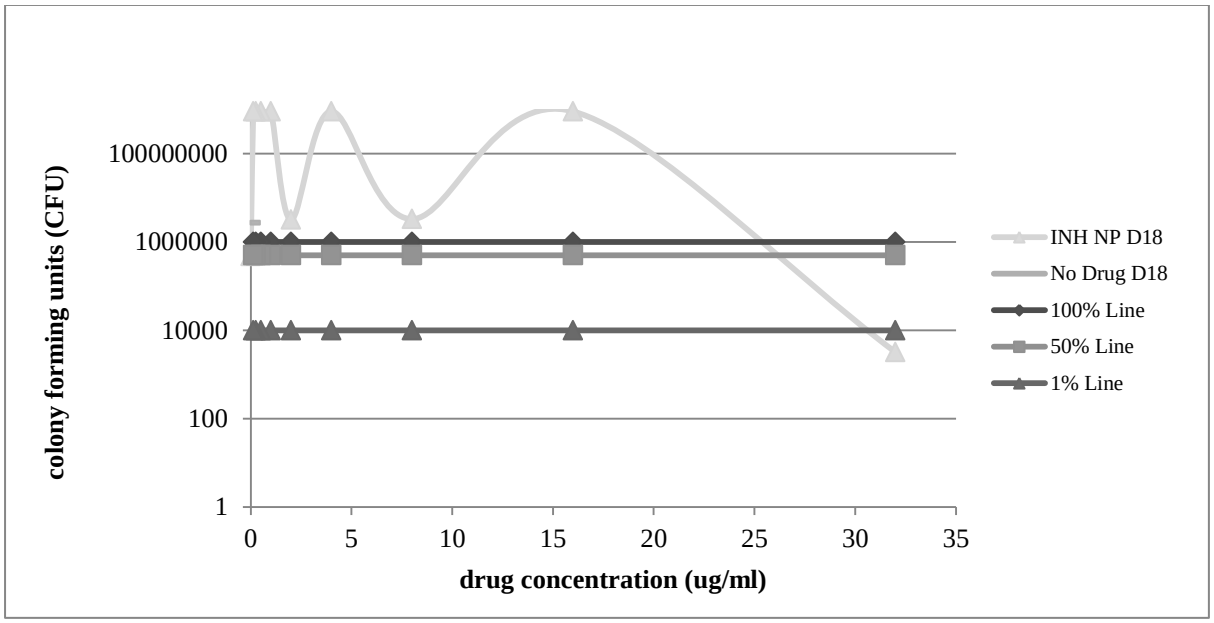

B

Figure 4 (A) MBC profile for free-INH and (B) MBC profile for nanoencapsulated INH at day 18 of MBC analysis. The decrease in colony forming units (cfu) are depicted as the 100 % line (no bacterial killing), 50 % line (50 % killing) and 1 % line (99 % killing).

Similarly to the INH assay, Figure 5 A and B summarizes the MBC for RIF following plating of MIC samples over 18 days. The untreated controls (no drug), indicates where 100% bacterial growth was still present. The figures are illustrated as cfu versus drug concentrations. Figure 5 A demonstrates

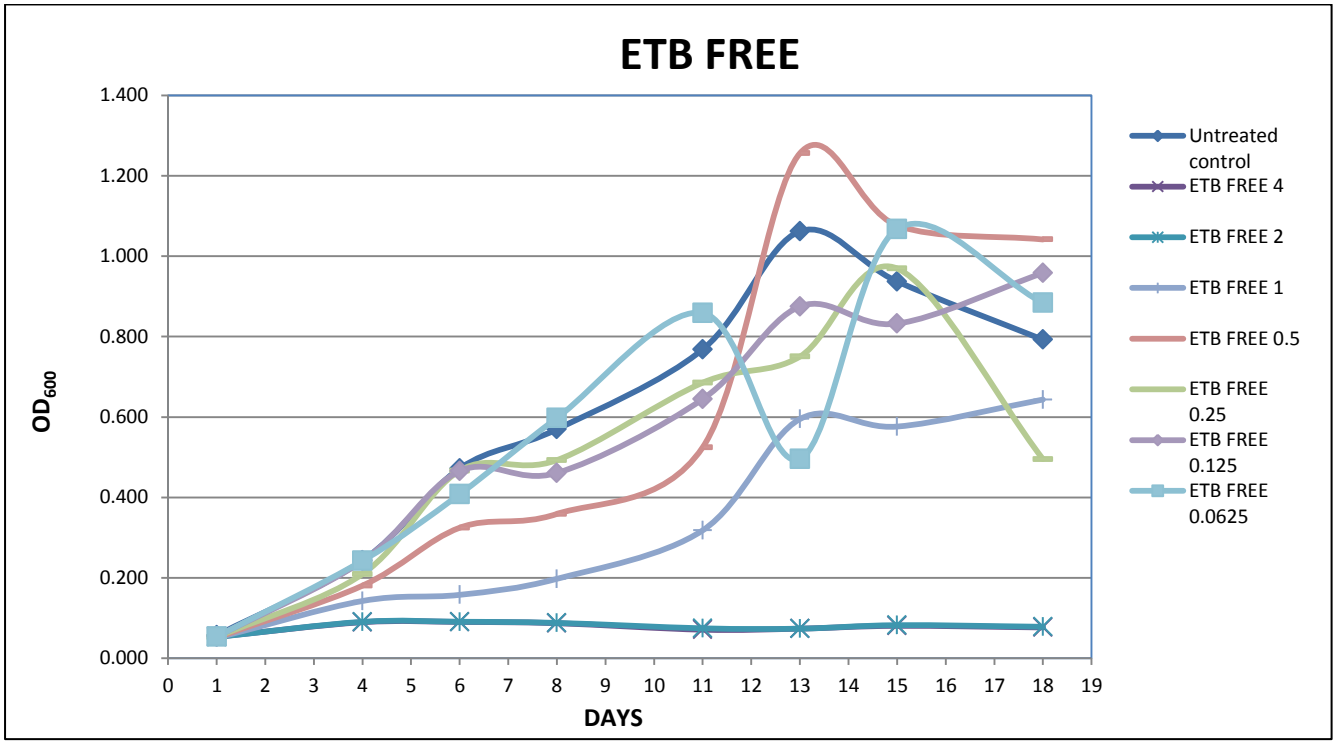

MIC summary graph for free ETB.

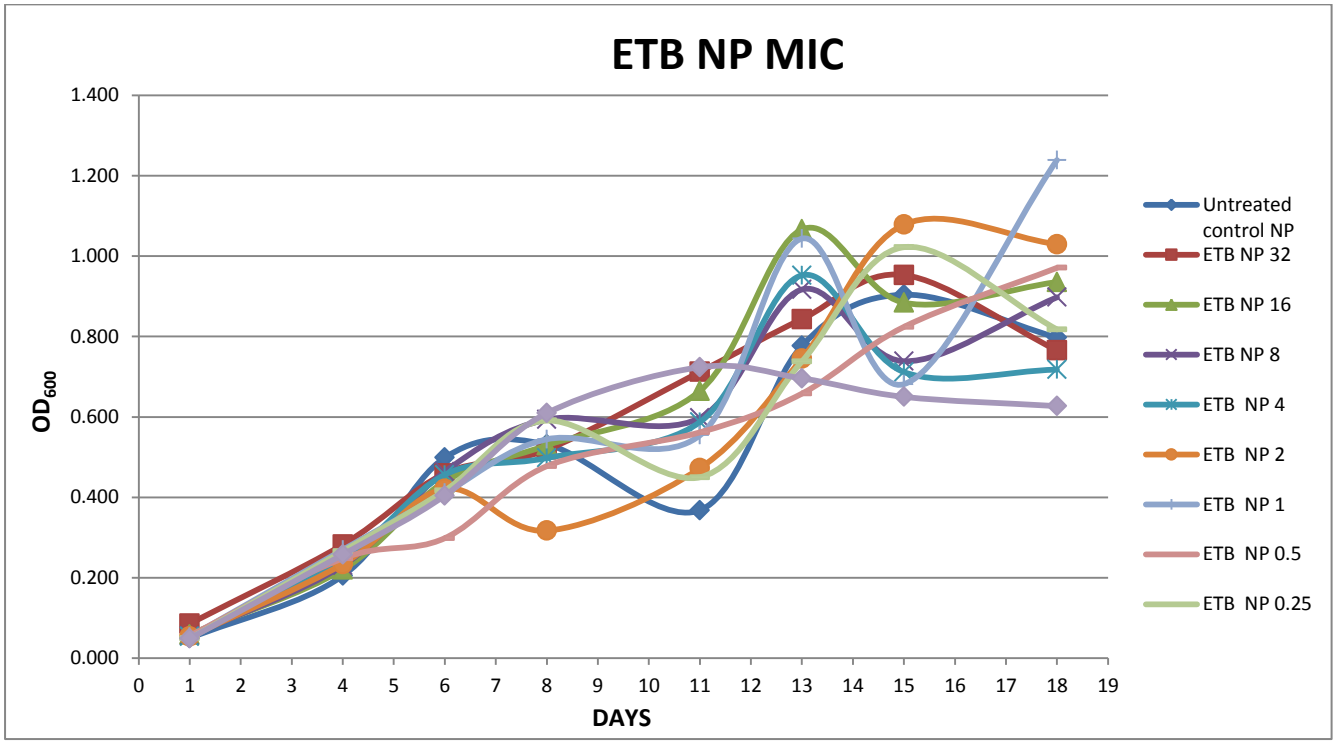

MIC summary graph for nanoencapsulated ETB.

MIC/MBC combination study data for INH and RIF presented in chapter 5

		CFU	CFU	CFU	CFU
Sample	**ug/mL**	**Day 1**	**Day 7**	**Day 14***	**Day 18***
Free INH	0.48	1600000	200	0.1	0.1
Free INH	0.24	2000000	300	800	0.1
Free INH	0.12	800000	200	9000	300
Free INH	0.06	5200000	400	22000	19000
Free INH	0.03	1900000	10000	80000	210000
Free INH	0.015	2200000	900000000	900000000	900000000
Free INH	0.0075	3700000	900000000	900000000	900000000
Free INH	0.00375	8000000	900000000	900000000	900000000
Free INH	0.001875	7900000	900000000	900000000	900000000
Free INH	0	8800000	900000000	11000	100
INH NP	32	1500000	6000	5000	3200
INH NP	16	2900000	70000	900000000	900000000
INH NP	8	2900000	80000	900000000	3300000
INH NP	4	5100000	700000	900000000	900000000
INH NP	2	2100000	900000000	900000000	3200000
INH NP	1	1500000	900000000	900000000	900000000
INH NP	0.5	1300000	900000000	900000000	900000000
INH NP	0.25	1400000	900000000	900000000	900000000
INH NP	0.125	2500000	900000000	900000000	900000000
INH NP	0	4000000	900000000	5200000	480000
No Drug	0	900000	450000000	330000000	2700000

*Less than 50 uL left in wells at these time points. CFU-colony forming unit

		OD_{600} Day	OD_{600} Day	OD_{600} Day	OD_{600} Day			OD_{600} StDev	OD_{600} StDev	OD_{600} StDev	OD_{600} StDev
Sample	**ug/mL**	**1**	**7**	**14**	**18**	**Sample**	**ug/mL**	**1**	**7**	**14**	**18**
Free INH	0.48	0.0595	0.2925	0.3685	0.32	Free INH	0.48	0.01	0.02	0.03	0
Free INH	0.24	0.055	0.296	0.4084	0.339	Free INH	0.24	0	0.03	0.01	0
Free INH	0.12	0.051	0.2105	0.378	0.338	Free INH	0.12	0	0.01	0.05	0
Free INH	0.06	0.0605	0.2245	0.379	0.454	Free INH	0.06	0	0.04	0.11	0
Free INH	0.03	0.0605	0.5635	1.088	1.406	Free INH	0.03	0	0.28	0.24	0
Free INH	0.015	0.0615	1.147	1.393	1.303	Free INH	0.015	0	0.49	0.08	0
Free INH	0.0075	0.0565	1.4455	1.439	1.201	Free INH	0.0075	0.01	0.07	0.19	0
Free INH	0.00375	0.0596	1.518	1.2265	1.143	Free INH	0.00375	0	0.05	0.58	0
Free INH	0.001875	0.058	1.5265	1.356	0.993	Free INH	0.001875	0.01	0.01	0.02	0
Free INH	0	0.063	1.457	1.1415	0.974	Free INH	0	0.01	0.05	0.38	0
INH NP	32	0.0595	0.39	0.3855	0.434	INH NP	32	0	0.27	0	0
INH NP	16	0.0585	1.258	1.5575	1.489	INH NP	16	0	0.03	0.08	0
INH NP	8	0.0575	1.4175	1.58	1.569	INH NP	8	0.01	0.02	0.1	0
INH NP	4	0.062	1.3765	1.564	1.435	INH NP	4	0.01	0.06	0.05	0
INH NP	2	0.0625	1.387	1.62	1.736	INH NP	2	0	0.04	0.04	0
INH NP	1	0.0595	1.349	1.5965	1.421	INH NP	1	0	0.03	0.02	0
INH NP	0.5	0.0745	1.341	1.5845	1.523	INH NP	0.5	0.01	0.01	0.04	0
INH NP	0.25	0.0645	1.3815	1.6225	1.322	INH NP	0.25	0	0.04	0.03	0
INH NP	0.125	0.063	1.45	1.435	0.925	INH NP	0.125	0	0.02	0.25	0
INH NP	0	0.0585	1.5105	1.105	1.203	INH NP	0	0	0.05	0.55	0
No Drug	0	0.0676	1.4326	1.386	1.279	No Drug	0	0.02	0.06	0.31	0.24

StDev- standard deviation

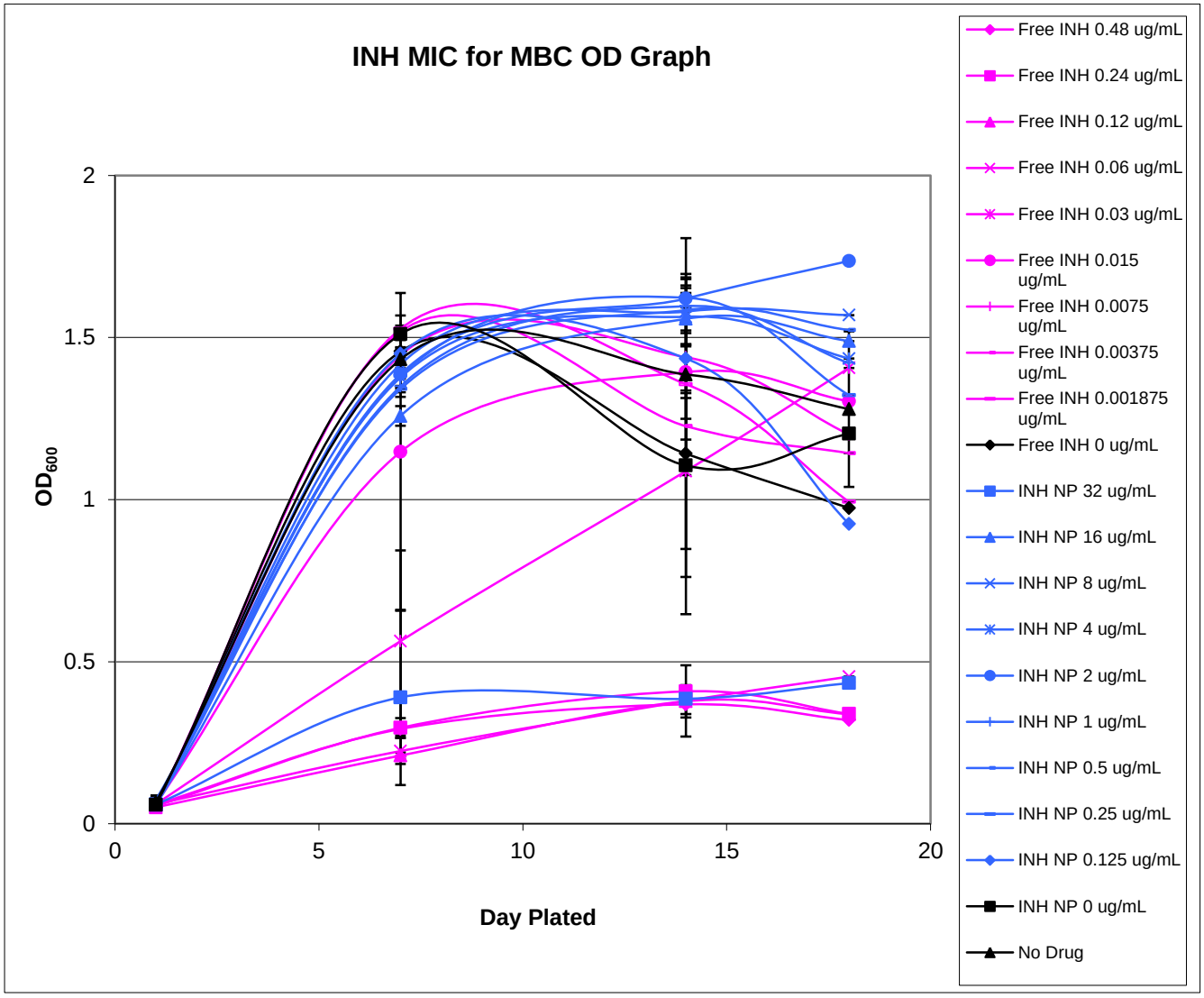

MIC data for MBC studies

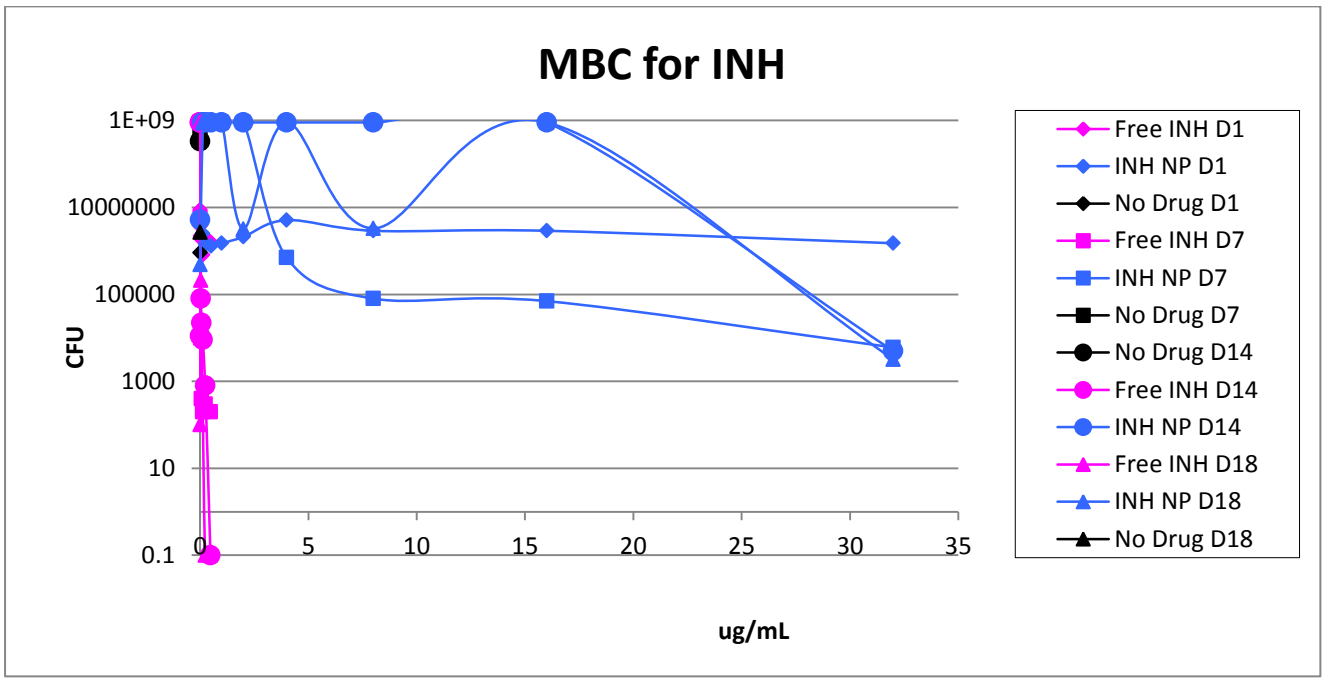

MBC for INH at highest drug concentrations

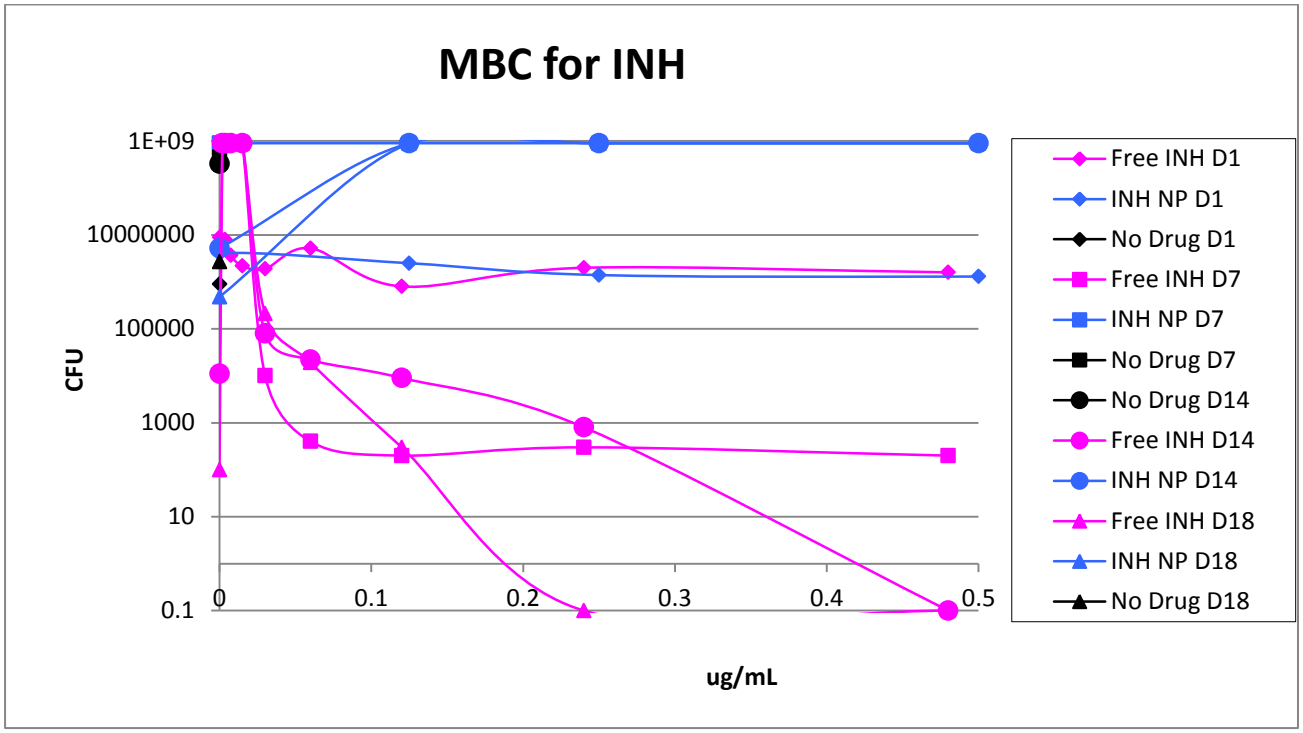

MBC for INH at lower drug concentrations

		CFU	CFU	CFU	CFU
Sample	**ug/mL**	**Day 1**	**Day 7**	**Day 14**	**Day 18**
Free RIF	0.48	300000	100000	11000	10000
Free RIF	0.24	130000	40000	10000	20000
Free RIF	0.12	140000	30000	20000	900000000
Free RIF	0.06	170000	20000	10000	8000
Free RIF	0.03	230000	70000	10000	40000
Free RIF	0.015	300000	100000	1000	26000
Free RIF	0.0075	550000	900000000	900000000	900000000
Free RIF	0.00375	570000	900000000	900000000	900000000
Free RIF	0.001875	770000	900000000	900000000	900000000
Free RIF	0	530000	900000000	900000000	900000000
RIF NP	32	170000	50000	40000	10000
RIF NP	16	330000	60000	30000	20000
RIF NP	8	340000	120000	10000	900000000
RIF NP	4	370000	70000	20000	20000
RIF NP	2	350000	100000	10000	10000
RIF NP	1	480000	170000	900000000	20000
RIF NP	0.5	500000	900000000	900000000	900000000
RIF NP	0.25	530000	900000000	900000000	900000000
RIF NP	0.125	550000	900000000	900000000	900000000
RIF NP	0	590000	900000000	900000000	900000000
No Drug	0	490000	220000000	520000000	130000000

CFU-colony forming units

		OD_{600} Day	OD_{600} Day	OD_{600} Day	OD_{600} Day			OD_{600} StDev	OD_{600} StDev	OD_{600} StDev	OD_{600} StDev
Sample	**ug/mL**	**1**	**7**	**14**	**18**	**Sample**	**ug/mL**	**Day1 n=3**	**Day7 n=3**	**Day14 n=2**	**Day18 n=1**
Free RIF	0.48	0.219	0.261	0.246	0.26	Free RIF	0.48	0.025	0.007	0.01	0
Free RIF	0.24	0.194	0.239	0.226	0.234	Free RIF	0.24	0.005	0.005	0.003	0
Free RIF	0.12	0.189	0.234	0.209	0.311	Free RIF	0.12	0.007	0.022	0.03	0
Free RIF	0.06	0.171	0.256	0.204	0.203	Free RIF	0.06	0.002	0.003	0.004	0
Free RIF	0.03	0.163	0.328	0.223	0.225	Free RIF	0.03	0.004	0.016	0.01	0
Free RIF	0.015	0.157	0.501	0.306	0.297	Free RIF	0.015	0.009	0.003	0.001	0
Free RIF	0.0075	0.144	0.769	0.834	1.003	Free RIF	0.0075	0.014	0.045	0.08	0
Free RIF	0.00375	0.15	0.92	0.953	1.066	Free RIF	0.00375	0.004	0.029	0.146	0
Free RIF	0.001875	0.153	0.796	0.948	1.167	Free RIF	0.001875	0.035	0.054	0.141	0
Free RIF	0	0.137	0.739	1.29	1.454	Free RIF	0	0.013	0.047	0.03	0
RIF NP	32	0.194	0.221	0.226	0.232	RIF NP	32	0.003	0.002	0.03	0
RIF NP	16	0.182	0.189	0.22	0.195	RIF NP	16	0.009	0.009	0	0
RIF NP	8	0.191	0.215	0.229		RIF NP	8	0.008	0.005	0.03	0
RIF NP	4	0.197	0.233	0.217	0.22	0.209	4	0.007	0.012	0.008	0
RIF NP	2	0.172	0.22	0.191	0.188	RIF NP	2	0.003	0.007	0.0007	0
RIF NP	1	0.164	0.274	0.225	0.209	RIF NP	1	0.007	0.035	0.03	0
RIF NP	0.5	0.154	0.464	0.665	0.822	RIF NP	0.5	0.009	0.03	0.06	0
RIF NP	0.25	0.142	0.857	0.84	0.98	RIF NP	0.25	0.008	0.03	0.04	0
RIF NP	0.125	0.14	0.777	0.815	1.073	RIF NP	0.125	0.008	0.035	0.02	0
RIF NP	0	0.152	0.721	1.05	1.39	RIF NP	0	0.009	0.059	0.06	0
No Drug	0	0.147	0.843	1.29	1.523	No Drug	0	0.01	0.136	0.09	0.08

StDev- standard deviation

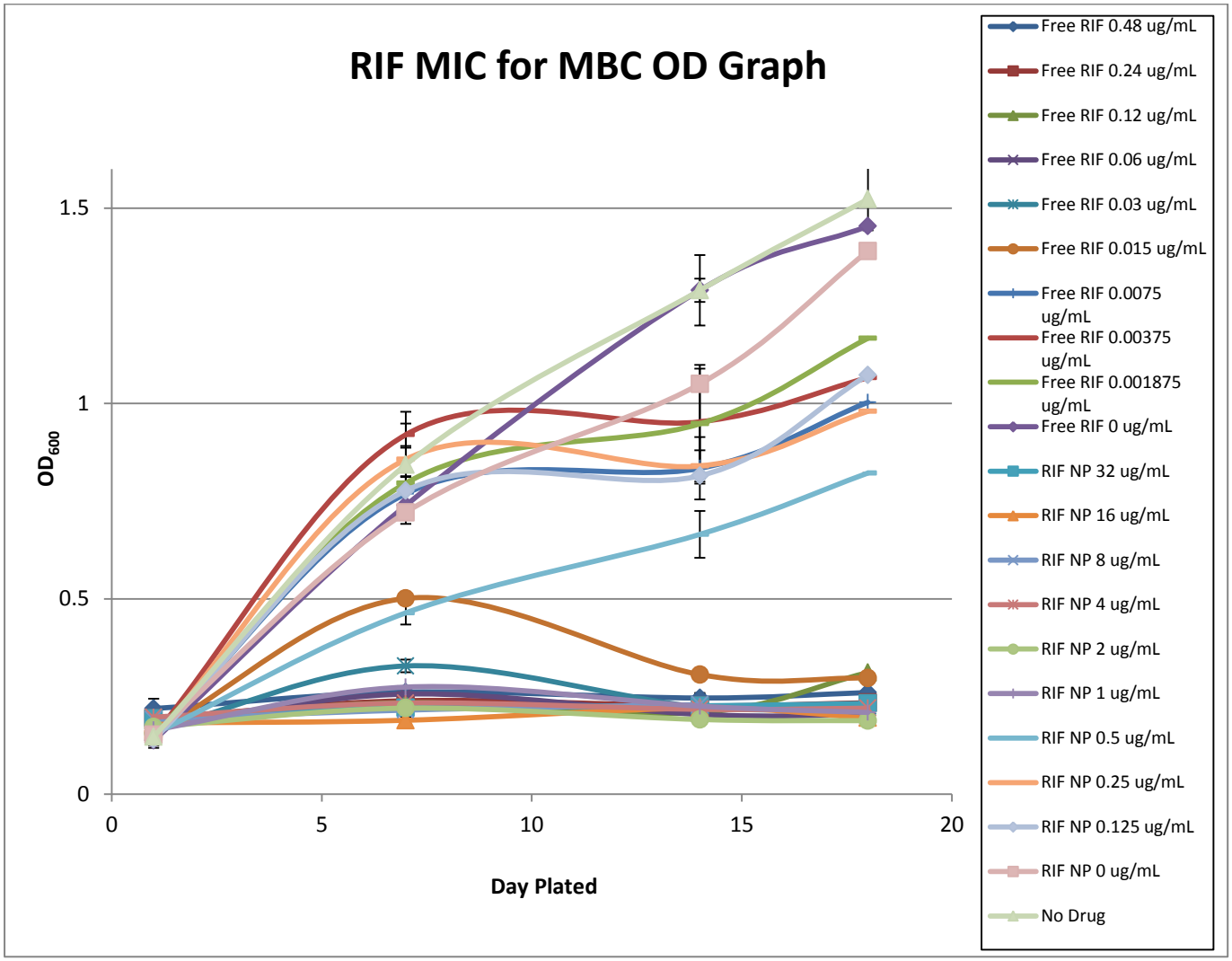

MIC data for MBC studies

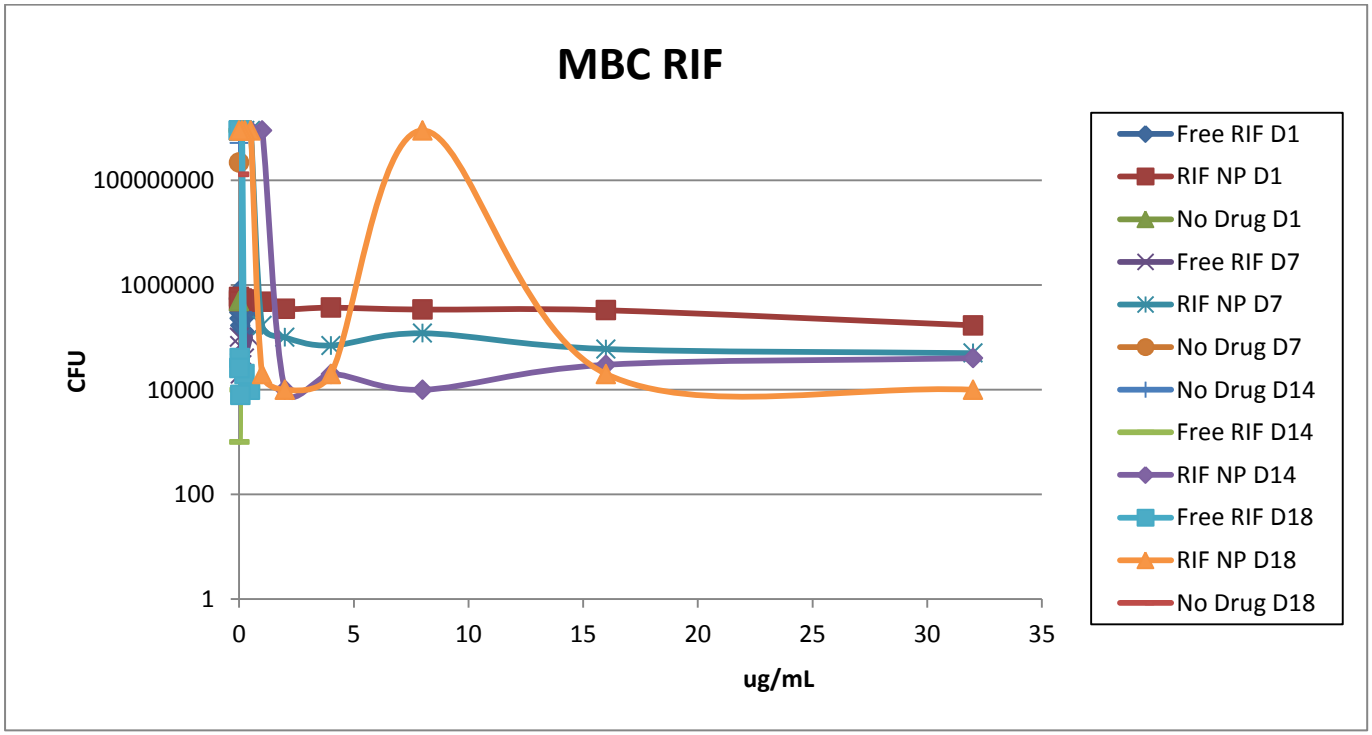

MBC for RIF at highest drug concentrations

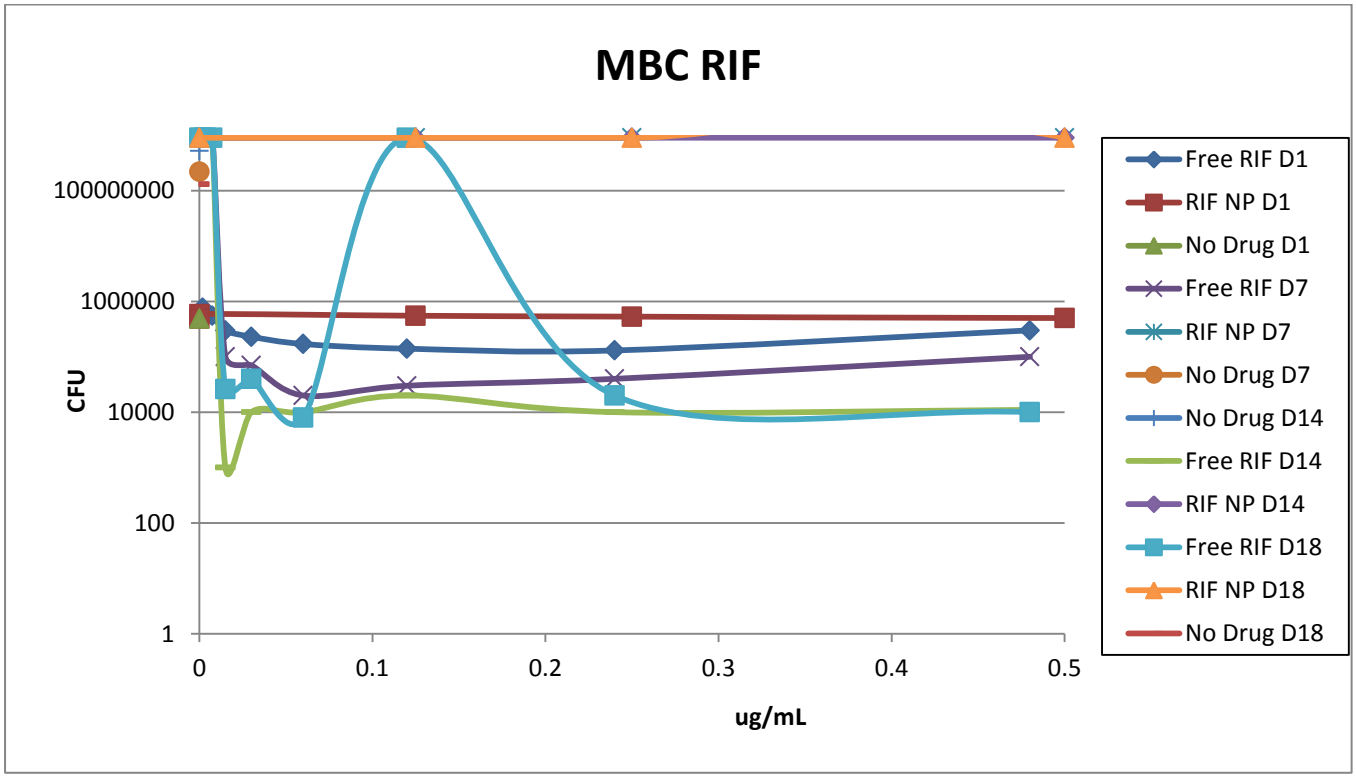

MBC for RIF at lower drug concentrations